Trehalose Transport in *Corynebacterium glutamicum* and its Significance for Cell Envelope Synthesis

I n a u g u r a l – D i s s e r t a t i o n

zur

Erlangung des Doktorgrades

der Mathematisch-Naturwissenschaftlichen Fakultät

der Universität zu Köln

vorgelegt von

Alexander Werner Eck

aus Speyer

Köln, 2014

Berichterstatter/in: Prof. Dr. Reinhard Krämer
Prof. Dr. Karin Schnetz

Tag der mündlichen Prüfung: 21.05.2014

Kurzzusammenfassung

Corynebacterium glutamicum ist ein Gram-positives, apathogenes Bodenbakterium. Es ist ein wichtiger industriell genutzter Aminosäureproduzent und dient als Modellorganismus für die Synthese der Zellhülle in verwandten pathogenen Arten wie *Mycobacterium tuberculosis*, dem Tuberkuloseerreger. Ein auffälliges Merkmal der Zellhülle dieser Bakterien ist das Vorhandensein einer zweiten Permeabilitätsbarriere ähnlich der äußeren Membran Gram-negativer Bakterien. Wichtige Bestandteile sind Trehalosemono- (TMM) und dimycolat (TDM), langkettige Fettsäuren, die mit einem Molekül des Disaccharids Trehalose verestert sind. Frühere Versuche mit *C. glutamicum* zeigten, dass die Verknüpfung im Periplasma erfolgt, wofür der Export beider Moleküle notwendig ist. Dieses Modell wurde durch neue Studien in Frage gestellt, welche MmpL-Transporter mit dem Export von TMM aus dem Cytosol in Verbindung brachten. Um das beschriebene Modell der TMM-Synthese zu überprüfen, wurde daher in dieser Arbeit der Export von Trehalose untersucht.

In einem *C. glutamicum* Teststamm konnten die cytosolische Umwandlung zuvor aufgenommener Maltose in Trehalose und dessen Exkretion nachgewiesen werden, wobei eine extrazelluläre Umwandlung ausgeschlossen wurde. Die bestimmte Exportrate von 0.19 nmol × mg^{-1} cdw × min^{-1} ist für die TMM-Synthese während des Wachstums ausreichend und war unabhängig von der Aktivität mechanosensitiver Kanäle, welche Trehalose in anderen Organismen freisetzen, und von der TMM-Synthese. Zusammen mit mechanistischen Analysen der Exkretion deutet dies auf das Vorhandensein eines Trehalosetransporters hin, der diese für die TMM-Synthese im Periplasma bereitstellt. TMM und TDM wurde nur in Zellen nachgewiesen, in denen einer von zwei redundanten MmpL-Transportern aktiv war. Es wird daher ein Modell vorgeschlagen, das eine periplasmatische Synthese von TMM aus zuvor exportierten Substraten und einem MmpL-vermittelten Transport von TMM aus der äußeren Schicht der Plasmamembran zur Mycolatschicht vereint.

Da ein rationaler Ansatz nicht zur Identifizierung eines Trehaloseexporters führte, wurde ein genetisch kodierter Trehalosesensor entwickelt und optimiert, welcher für das Screening einer Mutantenbibliothek eingesetzt werden sollte. Die Affinität dieses Sensors konnte jedoch durch gerichtete Mutagenese nicht ausreichend reduziert werden, um eine *in vivo*-Applikation zu ermöglichen. Der Trehaloseexporter von *C. glutamicum* ist daher weiterhin unbekannt.

Abstract

Corynebacterium glutamicum is a Gram-positive, non-pathogenic soil bacterium. It is one of the main industrial producers for amino acids and also serves as a model organism for cell envelope synthesis in related pathogenic species like *Mycobacterium tuberculosis*, the causative agent of tuberculosis. A common feature of their cell envelope is the presence of a second permeability barrier similar to the outer membrane of Gram-negative bacteria. Important constituents of this lipid bilayer are the glycolipids trehalose monomycolate (TMM) and trehalose dimycolate (TDM), long chain fatty acids esterified to the disaccharide trehalose. Previous experiments with *C. glutamicum* indicated that the linkage of trehalose and a mycolic acid precursor takes place in the periplasm, necessitating the export of both substrates. This model was challenged by the recently described connection of MmpL transporters to TMM transport from the cytosol to the periplasm. To validate the current model of TMM synthesis, the export of trehalose was investigated in this work.

In a *C. glutamicum* test strain, the cytosolic conversion of imported maltose to trehalose and the excretion of the latter could be shown. The extracellular conversion of substrate to trehalose could be excluded. Trehalose accumulation in the supernatant occurred with a specific rate of 0.19 nmol × mg^{-1} cdw × min^{-1}, which is sufficient to maintain mycolic acid synthesis during growth. The rate of trehalose excretion was independent of mechanosensitive channels, which mediate trehalose excretion in other bacteria, and of TMM synthesis. Together with mechanistic analyses, this indicates the presence of a carrier dedicated to provide trehalose for TMM synthesis in the periplasm.

Confirming the results published by other groups, the detection of TMM and TDM in whole cell extracts was dependent on the activity of either of two MmpL proteins. Nevertheless, a model is presented in this work that allows the periplasmic synthesis of TMM after precursor export and that assumes the MmpL-catalysed transport of TMM from the outer leaflet of the plasma membrane across the periplasm to the outer membrane.

A trehalose export carrier could not be identified in a rational approach. Thus, a genetically encoded trehalose sensor was constructed and optimised to allow the screening of a mutant library. Although functional *in vitro*, the affinity of this sensor for trehalose is still too high and could not be reduced sufficiently by site-directed mutagenesis to allow its application in *C. glutamicum*. Thus, the trehalose export system of *C. glutamicum* remains unknown.

Abbreviations

ABC	ATP Binding Cassette
APS	Ammonium Persulfate
ATCC	American Type Culture Collection
ATP	Adenosine Triphosphate
BCIP	5-Bromo-4-chloro-3-indolyl Phosphate
BHI	Brain Heart Infusion
BLAST	Basic Local Alignment Search Tool
bp	Base Pairs
CAPS	N-cyclohexyl-3-aminopropanesulfonic Acid
cDNA	Copy Desoxyribonucleic Acid
cdw	Cellular Dry Weight
CTAB	Cetyltrimethyl Ammoniumbromide
DIG-11-UTP	Digoxigenin Deoxyuridine Triphosphate
DNA	Desoxyribonucleic Acid
EDTA	Ethylenediaminetetraacetic Acid
FRET	Förster Resonance Energy Transfer
g	Gravitational Force
HPLC	High Pressure Liquid Chromatography
IM	Integration Mutant
IMAC	Ion Metal Affinity Chromatography
IPTG	Isopropyl-β-D-thiogalactoside
LB	Luria Bertani
MES	2-(*N*-Morpholino)ethanesulfonic Acid
MFS	Major Facilitator Superfamily
MOPS	3-Morpholinopropane-1-sulfonic Acid
NBT	Nitro Blue Tetrazolium Chloride
OD_{600}	Optical Density at 600 nm
PAGE	Polyacrylamide Gel Electrophoresis
PBP	Periplasmic Binding Protein
PCR	Polymerase Chain Reaction
PIPES	1,4-Piperazinediethanesulfonic Acid
RNA	Ribonucleic Acid
RND	Restriction, Nodulation, Cell Division
rpm	Rounds per Minute
SDS	Sodiumdodecyl Sulfate
SEC	Size Exclusion Chromatography
SOB	Super Optimal Broth
TAE	Tris-Acetate-EDTA Buffer
TB	Terrific Broth
TDM	Trehalose Dimycolate
TE	Tris EDTA Buffer
TEMED	Tetramethylethylenediamine
TLC	Thin Layer Chromatography
TMM	Trehalose Monomycolate
Tris	Tris(hydroxymethyl)aminomethane
2TY	Tryptone Yeast Extract Medium
WT	Wild Type
$Y_{P/s}$	Yield Coefficient Product/Substrate

1 Introduction

1.1 *Corynebacterium glutamicum* is an industrial producer and a model organism

Corynebacterium glutamicum is a Gram-positive soil bacterium belonging to the Corynebacterineae suborder of the Actinobacteria phylum (Liebl, 2005). *C. glutamicum* has been known since the 1950s for its ability to excrete L-glutamate into the culture supernatant (Kinoshita *et al.*, 1957) and today it is the main industrially applied producer of L-glutamate and other amino acids. 2.5 million tons of L-glutamate, which is mainly used as a flavour enhancer, and 1.5 million tons of L-lysine, which is mainly used for animal nutrition, are produced in fermentation processes with *C. glutamicum* per year (Becker & Wittmann, 2012). Besides amino acids, nucleoside monophosphates, which also serve as flavour enhancers, are produced with *C. glutamicum* (Demain *et al.*, 1966; Kazarinova *et al.*, 2002). The continuous optimisation of production strains demands a profound understanding of metabolic and regulatory pathways to increase product yields, to reduce the formation of byproducts, or to allow the use of alternative carbon sources. Substrate import and product export are also important targets to further boost production (Burkovski & Krämer, 2002). *C. glutamicum* has been studied for several decades, which has led to the development of a variety of techniques to construct genetically engineered *C. glutamicum* strains. The production of multiple bulk and high-value compounds like vitamins, solvents, diamines, ethanol, and organic acids in genetically modified *C. glutamicum* strains has been achieved in the laboratory scale, showing potential future applications for this bacterium (Sahm & Eggeling, 1999; Smith *et al.*, 2010; Blombach *et al.*, 2011; Mimitsuka *et al.*, 2007; Kind *et al.*, 2011; Inui *et al.*, 2004; Okino *et al.*, 2005).

The Corynebacterineae suborder also comprises pathogenic species like *Mycobacterium leprae*, *Corynebacterium diphtheriae*, and *Mycobacterium tuberculosis*, the causative agents of leprosy, diphtheria, and tuberculosis, respectively. The latter causes about 2 million deaths per year, which is more than any other infectious disease (Dye, 2006). *C. glutamicum* serves as a model organism for cell envelope synthesis within the Corynebacterineae suborder. The cell envelope of Corynebacterineae shows a complex structure compared to other Gram-positive bacteria. While the envelope of *C. glutamicum* resembles that of mycobacteria and other related bacteria in structure and function, its composition is

comparatively simple (Puech *et al.*, 2001). In addition, *C. glutamicum* is non-pathogenic, grows rapidly on different carbon sources, its genome has been sequenced completely (Kalinowski *et al.*, 2003), and it has been used successfully for the expression of mycobacterial genes (Puech *et al.*, 2001).

1.2 Cell envelope architecture in *C. glutamicum*

A common feature of the cell envelope of Corynebacterineae (Figure 1) is the presence of a second lipid membrane similar to the outer membrane of Gram-negative bacteria, which can be seen as a fracture plane in freeze-fractured cells (Puech *et al.*, 2001). This bilayer mainly consists of mycolic acids, long chain α-alkyl, β-hydroxy fatty acids with 22 to 36 carbon atoms in *C. glutamicum*, that are covalently linked to the disaccharide trehalose as trehalose monomycolate (TMM) and trehalose dimycolate (TDM) as well as to the arabinogalactan layer, forming an approximately 42 Å thick hydrophobic permeability barrier in *C. glutamicum* (Bansal-Mutalik & Nikaido, 2011; Rath *et al.*, 2013). The arabinogalactan layer is covalently attached to both the peptidoglycan layer and the mycolic acid layer, constituting a mycolyl-arabinogalactan-peptidoglycan complex on top of the plasma membrane. The cell envelope is completed by an outer layer mainly consisting of carbohydrates and a minor share of free fatty acids (Puech *et al.*, 2001). In some but not all species, an additional surface layer consisting of proteins can be found (Chami *et al.*, 1995; Soual-Hoebeke *et al.*, 1999). Mycolic acids found in corynebacteria have a simple structure in comparison to their mycobacterial equivalents. In general, the latter are longer (C_{70} – C_{90}) and carry modifications like desaturations, cyclopropane rings, methoxy groups, and keto groups. Besides TMM and TDM, a multitude of other lipid compounds is present in the mycolic acid layer of mycobacteria like phthiocerol dimycocerosates, glycopeptidolipids, polyacyltrehaloses, and sulfolipids (Brennan & Nikaido, 1995).

The mycolic acid layer is a major determinant of the low permeability of the cell envelope for antibiotics and other noxious compounds (Liu *et al.*, 1996; Jackson *et al.*, 1999). Mycolic acid synthesis is essential in mycobacteria and thus of high medical interest as a drug target for the treatment of tuberculosis. This extends to the synthesis of trehalose, a non-reducing disaccharide, which forms the polar head groups of TMM and TDM (De Smet *et al.*, 2000; Kalscheuer *et al.*, 2010).

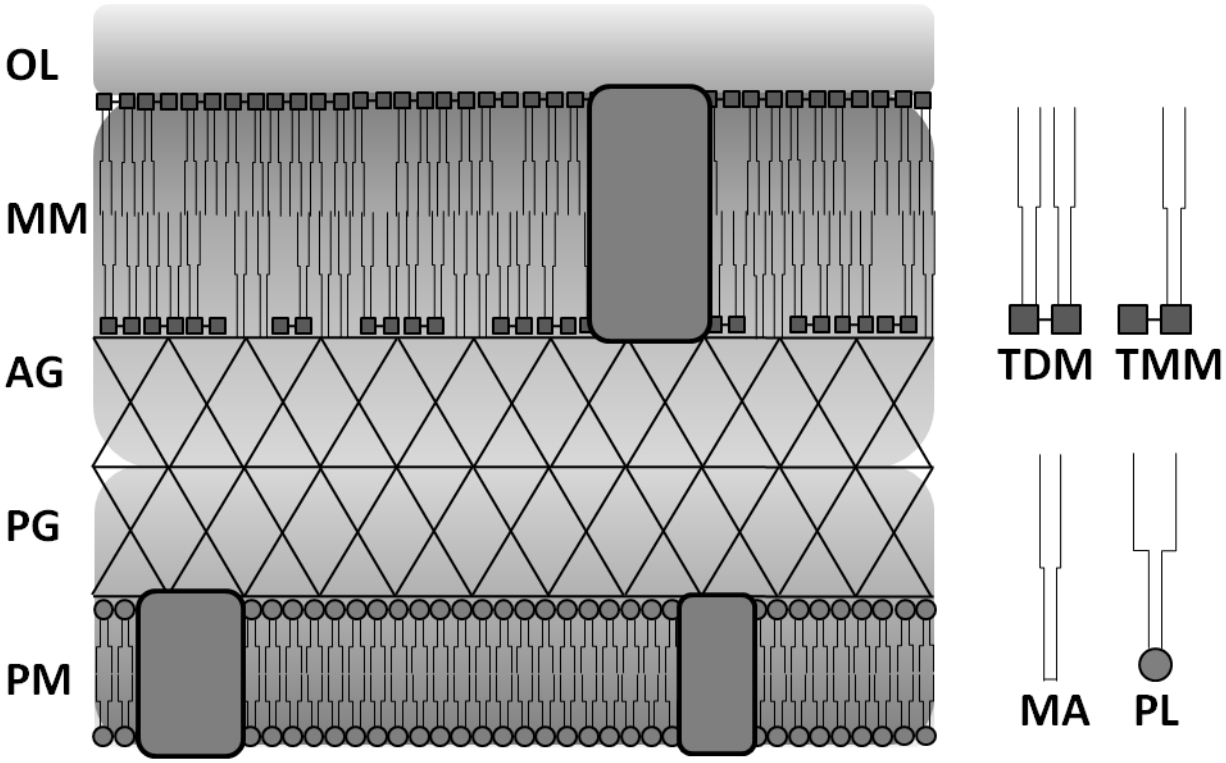

Figure 1: Cell envelope structure of *C. glutamicum*. PM: plasma membrane; **PG**: peptidoglycan layer; **AG**: arabinogalactan layer; **MM**: mycolic acid membrane; **OL**: outer layer; **TDM**: trehalose dimycolate; **TMM**: trehalose monomycolate; **MA:** mycolic acids; **PL**: phospholipids; **Boxes**: membrane proteins. Structure and composition are adapted from Puech *et al.* (2001).

In *C. glutamicum*, the mycolic acid layer has also been investigated for its contribution to amino acid excretion. L-glutamate excretion can be triggered under different conditions like biotin limitation, the addition of surfactants, antibiotics, or by temperature upshifts (Shiio *et al.*, 1962; Nara *et al.*, 1964; Takinami *et al.*, 1964; Delaunay *et al.*, 1999; Radmacher *et al.*, 2005b). The mechanosensitive channel MscCG has been shown to be involved in L-glutamate transport across the plasma membrane (Nakamura *et al.*, 2007). Restricted by the hydrophobicity of the mycolic acid layer, porin proteins located in the mycolic acid layer probably allow the efflux of amino acids to the surrounding. Four different porins were identified in *C. glutamicum* and mycolylation of two of them has been shown recently (Huc *et al.*, 2013). Notably, mycolic acid synthesis is not essential in *C. glutamicum*. Strains unable to synthesise trehalose constantly excreted L-glutamate to the medium, an effect caused by the lack of trehalose mycolates in these mutants (Gebhardt *et al.*, 2007).

The investigation of trehalose metabolism in *C. glutamicum* is thus of interest for the optimisation of *C. glutamicum* production strains as well as for the identification of new drug targets for the treatment of tuberculosis.

1.3 Trehalose synthesis in *C. glutamicum*

Trehalose plays an important role in many organisms. It protects proteins and membranes during anhydrobiosis, serves as transport sugar in the haemolymph of arthropods, acts as compatible solute under conditions of hyperosmotic stress, and it is an important precursor for the mycolic acid membrane in Corynebacterineae (Strom & Kaasen, 1993; Crowe *et al.*, 1998; Arguelles, 2000; Luzardo *et al.*, 2000; Tropis *et al.*, 2005).

In *C. glutamicum*, changes of the external osmolality trigger a sequence of adaptation mechanisms to adjust the osmotic strength of the cytosol to the external conditions to maintain the turgor pressure of the cell. An immediate response to hyperosmotic conditions is the uptake of K^+ to prevent the loss of water from the cell (Wolf *et al.*, 2003). For long-term adaptation, K^+ is then replaced by the accumulation of compatible solutes. These can either be taken up from the medium like glycine betaine, or they can be synthesised endogenously, like L-glutamate, L-proline, and trehalose. Trehalose synthesis becomes the most important adaptation mechanism under conditions of nitrogen starvation in the absence of compatible solutes in the medium (Wolf *et al.*, 2003).

In *C. glutamicum*, *M. tuberculosis*, and *M. smegmatis* three pathways are present for the synthesis of trehalose (Figure 2) (De Smet *et al.*, 2000; Wolf *et al.*, 2003). In contrast to many other bacteria, the most important pathway for trehalose synthesis under hyperosmotic conditions in *C. glutamicum* is the TreYZ-pathway. Two enzymes, maltooligosyltrehalose synthase (TreY) and maltooligosyltrehalose trehalohydrolase (TreZ), convert maltodextrines, which are intermediates of the glycogen metabolism in *C. glutamicum*, to trehalose. Expression of *treY* and *treZ* is constitutive to enable a fast response to sudden osmotic upshifts and is only slightly induced under hyperosmotic conditions (Wolf *et al.*, 2003). The OtsAB-pathway converts the activated precursors UDP-glucose and glucose-6-phosphate to trehalose by the sequential action of trehalose-6-phosphate synthase (OtsA) and trehalose-6-phosphate phosphatase (OtsB). Although *otsA* expression is slightly enhanced after osmotic upshifts, its activity is dispensable for trehalose synthesis under these conditions and thus the physiological function of this pathway in *C. glutamicum* remains unclear (Wolf *et al.*, 2003). In the third pathway, trehalose synthase (TreS) catalyses the conversion of maltose to trehalose, but in *C. glutamicum* this pathway is only relevant for trehalose synthesis during growth with maltose as substrate (Tzvetkov *et al.*, 2003). Although this reaction is reversible, flux from trehalose to maltose seems to prevail in the cell. TreS could

thus be important for trehalose degradation after conditions of hyperosmotic stress (Wolf *et al.*, 2003; Kim *et al.*, 2010a; Miah *et al.*, 2013).

TreS catalyses the interconversion of maltose and trehalose by a double displacement mechanism. A nucleophilic attack of the glucosidic bond by the catalytic L-aspartate residue leads to the intramolecular release of glucose, which reorients without leaving the catalytic site of the enzyme, and attacks the enzyme-bound intermediate (Zhang *et al.*, 2011). Besides the transglucosylating activity of TreS, the release of small amounts (<10%) of glucose as a byproduct was also observed *in vitro* (Koh *et al.*, 1998; Pan *et al.*, 2004; Kim *et al.*, 2010a). Two additional pathways for trehalose synthesis are known in other bacteria. Trehalose glycosyltransferring synthase (TreT) catalyses the formation of trehalose from ADP-glucose and glucose (Qu *et al.*, 2004) and trehalose phoshphorylase (TreP) uses glucose-1-phosphate and glucose as substrates for trehalose synthesis (Maruta *et al.*, 2002). However, both pathways are not present in corynebacteria.

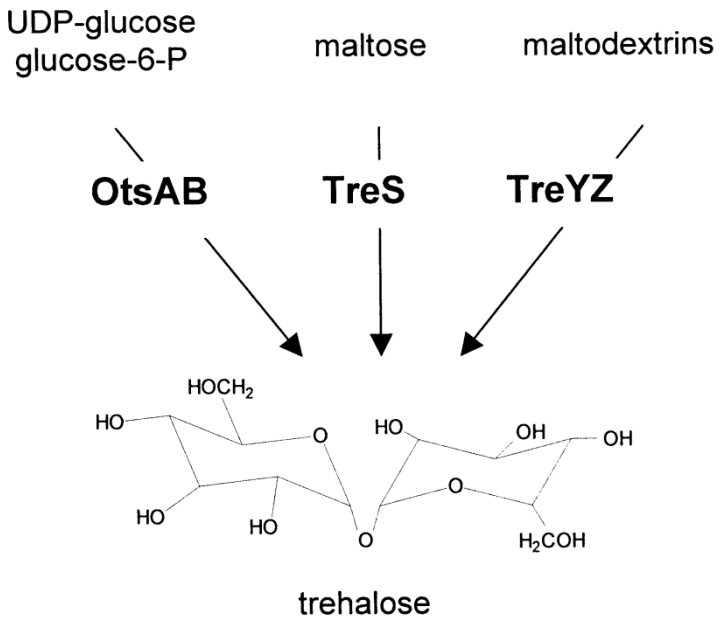

Figure 2: Trehalose synthesis in *C. glutamicum*. OtsA: trehalose-6-phosphate synthase; **OtsB**: trehalose-6-phosphate phosphatase; **TreS**: trehalose synthase; **TreY**: maltooligosyltrehalose synthase; **TreZ**: maltooligosyltrehalose trehalohydrolase. Adapted from Wolf *et al.* (2003) with modifications.

M. tuberculosis and *M. smegmatis* possess the same pathways for trehalose synthesis as *C. glutamicum.* While viable *C. glutamicum* mutants lacking all three pathways for trehalose synthesis have been successfully created (Wolf *et al.*, 2003; Tropis *et al.*, 2005), this was not

possible in mycobacteria and trehalose synthesis is thus thought to be essential in these bacteria (Woodruff *et al.*, 2004; Murphy *et al.*, 2005). Trehalose synthesis and its metabolism are thus interesting drug targets for the treatment of mycobacterial infections.

1.4 Trehalose catabolism in *C. glutamicum*

C. glutamicum can use different substrates like sugars, sugar alcohols, organic acids, or peptides as carbon and energy sources. In mixed-substrate cultivations, the co-utilisation of most carbon sources is observed for this bacterium (Arndt & Eikmanns, 2008). Besides its role as osmoprotectant and precursor for the synthesis of mycolic acids, trehalose also serves as substrate for growth for *C. glutamicum* (Henrich, 2011).

The transport system responsible for trehalose uptake was recently identified (Henrich, 2011). The gene cluster *cg0830* – *cg0835* (*tus*-genes) encodes an ABC trehalose uptake system with high affinity (K_M = 0.16 µM) but low transport capacity (v_{max} = 2.5 nmol × mg^{-1} cdw × min^{-1}). Genes in this cluster encode two putative membrane proteins, *cg0831* (*tusF*) and *cg0832* (*tusG*), a putative periplasmic solute binding protein, *cg0834* (*tusE*), and an ATPase protein, *cg0835* (*tusK*) (Henrich, 2011). Further, two genes encoding proteins with unknown function are also encoded in the *tus*-cluster. The gene *cg0830* encodes a predicted membrane protein with two transmembrane domains, *cg0833* putatively encodes a soluble cytosolic protein (Schulte, 2011). Both are not required but beneficial for trehalose uptake (Rehorst, 2013). The genes *cg0830* and *cg0833* form a transcriptional operon with *tusF* and *tusG,* while *tusE* and *tusK* are transcribed monocistronically (Henrich, 2011; Schulte, 2011). *C. glutamicum* utilises trehalose only as a co-substrate, but spontaneous mutants were isolated that can use trehalose as sole carbon source (Henrich, 2011). Because the *tus*-genes are expressed independently of the carbon source and because of the low transport capacity of the trehalose uptake system, this has been assumed to be rather important for the recycling of trehalose, which is released in the periplasm during TDM synthesis, than for the utilisation of trehalose as carbon source. This assumption is also based on the recent identification of the trehalose uptake system LpqY-SugA-SugB-SugY in *M. tuberculosis* and *M. smegmatis*, which is characterised by its constitutive expression, its high specificity for trehalose, its low transport velocity, and its importance for virulence (Kalscheuer *et al.*, 2010). The finding of a trehalose uptake system in *M. tuberculosis* was surprising since this bacterium is thought to thrive on fatty acids due to the absence of sugar substrates in

human phagocytes and especially the absence of trehalose synthesis in mammals (Marrero *et al.*, 2010).

After trehalose uptake and the TreS catalysed conversion to maltose, trehalose is degraded via the same pathways as maltose (Figure 3), which can enter the cell via the ABC transporter $MusFGK_2E$ (Henrich *et al.*, 2013). It is then metabolised by the enzyme 4-α-glucanotransferase (MalQ), which forms maltodextrines and glucose, which is then phosphorylated by a glucokinase (Glk) to glucose-6-phosphate. A maltodextrine phosphorylase (MalP) phosphorolytically cleaves maltodextrines to form glucose-1-phosphate, which is then isomerised to glucose-6-phosphate by phosphoglucomutase (Pgm). The latter is then degraded via reactions of central carbon metabolism.

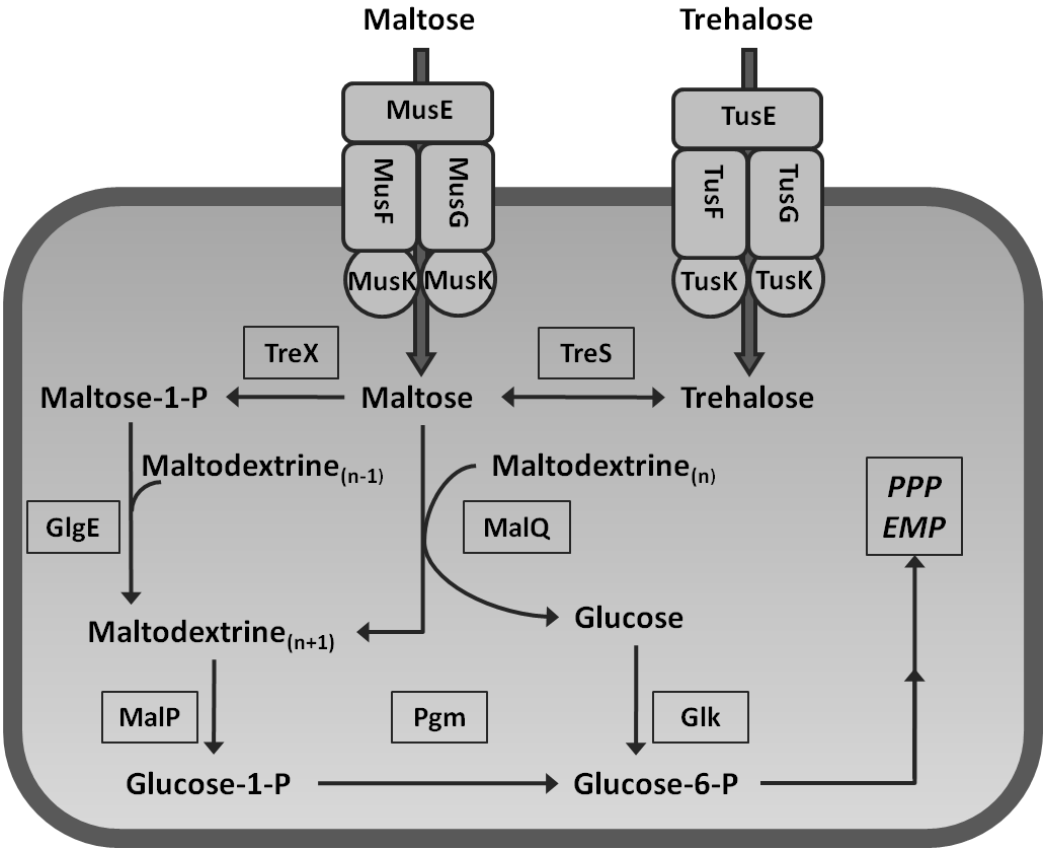

Figure 3: Uptake and degradation of trehalose and maltose in *C. glutamicum*. PPP: pentose phosphate pathway; **EMP**: Embden-Meyerhof pathway. For further abbreviations see text.

The presence of a second pathway for maltose and trehalose degradation in *C. glutamicum* has been shown (Henrich, 2011) in succession to its identification in *M. tuberculosis* and *M. smegmatis* as the sole pathway for trehalose degradation in these bacteria (Kalscheuer *et al.*, 2010). Accordingly, maltose is phosphorylated to maltose-1-phosphate by a maltokinase

(TreX) and incorporated into α-glucans, intermediates of glycogen metabolism in *C. glutamicum* (Seibold & Eikmanns, 2007), by a maltosyltransferase (GlgE) (Figure 3). However, it is not yet understood under which conditions this pathway is active and what impact it has on the metabolism of maltose and trehalose.

In contradiction to its function as carbon source, trehalose accumulation as byproduct is frequently observed during bioreactor cultivation of *C. glutamicum* (Vallino & Stephanopoulos, 1993; Gourdon & Lindley, 1999; Wittmann & Heinzle, 2001). Considering the presence of an uptake system for trehalose and enzymes for its degradation, this observation was unexpected. This also indicates the presence of a trehalose export system in *C. glutamicum* but neither the mechanism of trehalose excretion to the medium nor a regulatory mechanism, which could be expected to hinder the uptake of trehalose, has been investigated in *C. glutamicum* yet.

1.5 Trehalose as precursor for TMM synthesis

Further support for the presence of a trehalose export system comes from the investigation of TMM and TDM synthesis in *C. glutamicum*. The main features of this pathway are supposed to be similar in different members of the Corynebacterineae, albeit additional steps for the synthesis of more complex mycolic acid derivatives are required in some members of this group. In contrast to mycobacteria, corynebacterial mutants defective in mycolic acid synthesis or transport are viable and thus, the latter are important model organisms for the examination of mycolic acid synthesis and transport.

The precursors for mycolic acid synthesis are two fatty acids. *C. glutamicum* possesses two type-I fatty acid synthases, FAS-IA and FAS-IB (Radmacher *et al.*, 2005a). Products of these enzymes are mostly C_{16} – C_{18} fatty acids during growth on glucose as substrate (Radmacher *et al.*, 2005a). In *M. smegmatis* and *M. tuberculosis*, a FAS-II enzyme complex is present that further elongates FAS-I products (Bloch, 1977). As shown in Figure 4, mycolic acid synthesis then proceeds with the activation of two fatty acids via adenylation and carboxylation, respectively (Trivedi *et al.*, 2004; Portevin *et al.*, 2005; Gande *et al.*, 2007). A polyketide synthase encoded by *cg3178* in *C. glutamicum* catalyses the decarboxylative condensation of the two activated precursors to an α-alkyl, β-keto-acyl intermediate (Gande *et al.*, 2004; Portevin *et al.*, 2004). During condensation, the substrates and products are covalently linked to the polyketide synthase domains via thioester bonds (Gande *et al.*, 2004) and the

condensation product is probably transferred to a mannosylphosphopolyprenol carrier ('X' in Figure 4) that has been identified as a TMM precursor in *M. smegmatis* (Besra *et al.*, 1994). The final α-alkyl, β-hydroxy mycolic acid motif is then formed by the reduction of the precursor (Lea-Smith *et al.*, 2007).

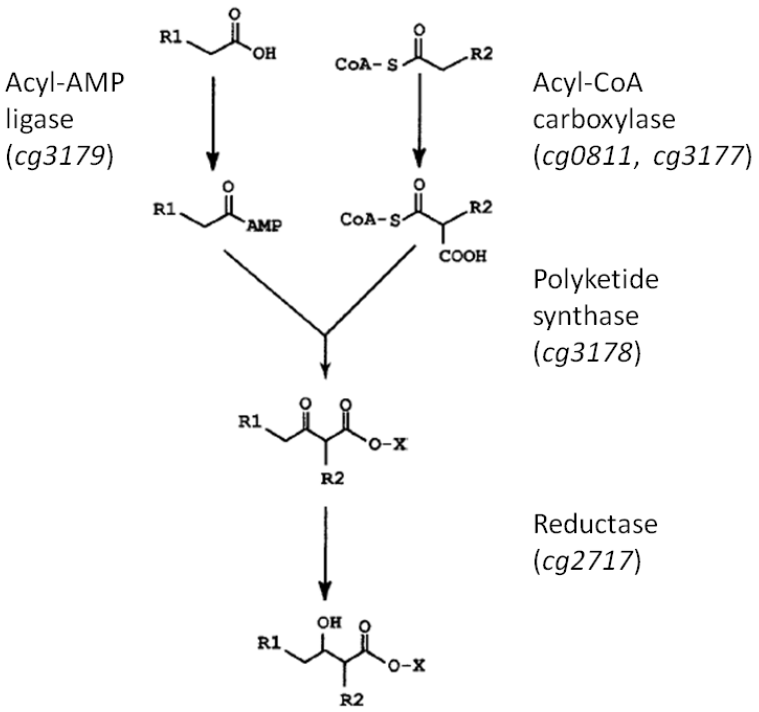

Figure 4: Final steps of mycolic acid synthesis. Gene **n**umbers for *C. glutamicum* genes encoding the presented enzymes are given in brackets. X denotes the mannosylphosphopolyprenol carrier identified as a putative mycolic acid carrying precursor for TMM in *M. smegmatis.* Modified after Portevin *et al.* (2005).

The lasts steps of TMM synthesis in Corynebacterineae are still discussed controversially in the literature. Especially the localisation of the TMM forming transfer of mycolic acids onto trehalose remains uncertain. Nevertheless, TMM has been shown to be the mycolic acid donor for the formation of TDM and the mycolylation of arabinogalactane. Thereby, one molecule of trehalose is released to the periplasm per reaction cycle, which is catalysed by six mycolyltransferases with partial redundancy in *C. glutamicum* (Brand *et al.*, 2003; De Sousa-D'Auria *et al.*, 2003). ABC trehalose uptake systems recently identified in mycobacteria (Kalscheuer *et al.*, 2010) and in *C. glutamicum* (Henrich, 2011) are probably important for the re-uptake of trehalose released to the periplasm during TDM synthesis.

Based on studies in *M. tuberculosis* and *C. matruchotii*, a pathway has been proposed, in which the mycolic acid moiety is transferred from a mannosylphosphopolyprenol carrier to trehalose-6-phosphate, yielding TMM-phosphate, by a hypothetical mycolyltransferase. TMM-phosphate could then be dephosphorylated by a hypothetical phosphatase in the cytosol (Shimakata & Minatogawa, 2000; Takayama *et al.*, 2005). This model is supported by the observation that [^{14}C]-labelled trehalose was only incorporated into trehalose glycolipids after its uptake in *M. tuberculosis* (Kalscheuer *et al.*, 2010).

Furthermore, it was recently published by several groups that inhibition of MmpL3 led to the accumulation of TMM in *M. tuberculosis* and *M. smegmatis* (Grzegorzewicz *et al.*, 2012; La Rosa *et al.*, 2012; Tahlan *et al.*, 2012; Varela *et al.*, 2012). MmpL proteins (mycobacterial membrane protein large) belong to the RND (restriction, nodulation, cell division) family, secondary active efflux transporters with broad substrate spectrum, which are found in all domains of life. These proteins have 12 transmembrane domains (TMD) and two large periplasmic domains between TMD 1 and 2 and TMD 7 and 8, which are responsible for substrate specificity (Yu *et al.*, 2005). In *M. tuberculosis*, a total of 13 *mmpL*-genes are present. Identified substrates for MmpL transporters in *M. tuberculosis* comprise lipids found in the cell envelope like phthiocerol dimycocerosate for MmpL7 (Camacho *et al.*, 2001) and diacyltrehalose sulfate, a precursor for sulfolipid-I synthesis, for MmpL8 (Converse *et al.*, 2003; Domenech *et al.*, 2004). Four *mmpL*-genes are also present in *C. glutamicum* and simultaneous inactivation of two of these genes led to the absence of mycolic acids in the cell envelope. In contrast to the situation in mycobacteria, no accumulation of TMM was observed in this mutant (Varela *et al.*, 2012). Thus, also transport was not shown biochemically, MmpL3 and homologous proteins in *C. glutamicum* were suggested to export TMM from the cytosol to the periplasm (Grzegorzewicz *et al.*, 2012; La Rosa *et al.*, 2012; Tahlan *et al.*, 2012; Varela *et al.*, 2012). Nevertheless, the role of MmpL transporters in the glycolipid metabolism of *C. glutamicum* remains uncertain.

In contrast, a second hypothesis assumes that trehalose and a mycolic acid precursor are exported independently and react to TMM in the periplasm. Trehalose is assumed to be the precursor for TMM synthesis rather than trehalose-6-phosphate since trehalose synthesis via either of three pathways in *C. glutamicum* is sufficient to enable TMM synthesis (Tzvetkov *et al.*, 2003; Wolf *et al.*, 2003). Most importantly, in *C. glutamicum* Δ*otsA* Δ*treS* Δ*treY* Δ*tus*, a mutant which is unable to synthesise and to take up trehalose, trehalose mycolate synthesis

could be restored by the addition of trehalose to the medium (Henrich, 2011). Further proof for this theory was given by the identification of an ABC transporter in *C. matruchotii*, which probably exports short-chain mycolic acids to the periplasm (Wang *et al.*, 2006). Besides the export of an activated mycolic acid precursor, a prerequisite for TMM synthesis in the periplasm is the export of trehalose from the cytosol to the periplasm. Although trehalose is known to accumulate in the culture supernatant of *C. glutamicum*, the mechanism of trehalose excretion has not been investigated yet and the export system is not known.

1.6 Aims of this project

The model of periplasmic TMM synthesis in *C. glutamicum* from trehalose and a mycolic acid precursor requires the export of both a mycolic acid precursors and trehalose to the periplasm. This model is supported by the ability of *C. glutamicum* Δ*otsA* Δ*treS* Δ*treY* Δ*tus* to use external trehalose for TMM synthesis but was challenged by the recent identification of MmpL proteins in *C. glutamicum* and related species and their assignment to the export of TMM to the periplasm.

To validate the assumption of periplasmic TMM formation, trehalose excretion in *C. glutamicum* should be investigated qualitatively and quantitatively in this work. *C. glutamicum* test strains should be constructed to investigate trehalose export. Analytical techniques for the sensitive and specific quantification of intra- and extracellular trehalose concentrations should be developed to allow the mechanistic analysis of trehalose excretion. Besides testing unspecific mechanism probably contributing to trehalose accumulation in the culture supernatant, a set of genes putatively encoding sugar export systems in *C. glutamicum* should be tested for their contribution to trehalose excretion. In parallel, the identification of the assumed trehalose export system should be achieved by the screening of a *C. glutamicum* mutant library. To enable the identification of mutants with altered intracellular trehalose concentrations, a trehalose sensor based on the trehalose binding protein of *C. glutamicum* should be constructed.

Further, trehalose transport should be investigated in *C. glutamicum* to resolve the apparent contradiction of trehalose accumulation in the supernatant of *C. glutamicum* cultures in spite of the presence of an uptake system in this bacterium. In this context, the biotechnological significance of engineering trehalose uptake in *C. glutamicum* should be addressed.

2 Material and Methods

2.1 Bacterial strains, plasmids, and oligonucleotides

All bacterial strains used in this work are shown in Table 1.

Table 1: Strains used in this work.

C. glutamicum	Genotype or application	Reference
ATCC 13032	Wild type	(Abe *et al.*, 1967)
Δ*cg0284*	Deletion of *cg0284*	This study
Δ*cg3174*	Deletion of *cg3174*	This study
Δ*cg3174* Δ*cg0284*	Deletion of *cg3174* and *cg0284*	This study
IM*cg2893*	Insertion of pDrive in *cg2893*	This study
DM1729	Lysine overproduction strain, pyc^{P458S}, hom^{V59A}, $lysC^{T311I}$	(Georgi *et al.*, 2005)
DM1729 IM*cg0834*	DM1729 with insertion of pDrive in *cg0834*	This study
Δ*malQ*	Deletion of *malQ*	(Henrich, 2011)
Δ*malQ* Δ*treX*	Deletion of *malQ* and *treX*	This study
Δ*malQ* Δ*treX* Δ*tus*	Deletion of *malQ, treX,* and the *cg0831 – cg0835* gene cluster	This study
Δ*malQ* Δ*treX* Δ*tus* IM*cg0206*	Deletion of *malQ*, *treX*, the *cg0831 – cg0835* gene cluster, and insertion of pDrive in *cg0206*	This study
Δ*malQ* Δ*treX* Δ*tus* IM*cg0340*	Deletion of *malQ*, *treX*, the *cg0831 – cg0835* gene cluster, and insertion of pDrive in *cg0340*	This study
Δ*malQ* Δ*treX* Δ*tus* IM*cg0501*	Deletion of *malQ*, *treX*, the *cg0831 – cg0835* gene cluster, and insertion of pDrive in *cg0501*	This study
Δ*malQ* Δ*treX* Δ*tus* IM*cg0772*	Deletion of *malQ*, *treX*, the *cg0831 – cg0835* gene cluster, and insertion of pDrive in *cg0772*	This study
Δ*malQ* Δ*treX* Δ*tus* IM*cg1212*	Deletion of *malQ*, *treX*, the *cg0831 – cg0835* gene cluster, and insertion of pDrive in *cg1212*	This study
Δ*malQ* Δ*treX* Δ*tus* IM*cg1289*	Deletion of *malQ*, *treX*, the *cg0831 – cg0835* gene cluster, and insertion of pDrive in *cg1289*	This study
Δ*malQ* Δ*treX* Δ*tus* IM*cg1399*	Deletion of *malQ*, *treX*, the *cg0831 – cg0835* gene cluster, and insertion of pDrive in *cg1399*	This study
Δ*malQ* Δ*treX* Δ*tus* IM*cg1526*	Deletion of *malQ*, *treX*, the *cg0831 – cg0835* gene cluster, and insertion of pDrive in *cg1526*	This study
Δ*malQ* Δ*treX* Δ*tus* IM*cg2618*	Deletion of *malQ*, *treX*, the *cg0831 – cg0835* gene cluster, and insertion of pDrive in *cg2618*	This study
Δ*malQ* Δ*treX* Δ*tus* IM*cg2739*	Deletion of *malQ*, *treX*, the *cg0831 – cg0835* gene cluster, and insertion of pDrive in *cg2739*	This study
Δ*malQ* Δ*treX* Δ*tus* IM*cg2893*	Deletion of *malQ*, *treX*, the *cg0831 – cg0835* gene cluster, and insertion of pDrive in *cg2893*	This study
Δ*malQ* Δ*treX* Δ*tus* IM*cg2895*	Deletion of *malQ*, *treX*, the *cg0831 – cg0835* gene cluster, and insertion of pDrive in *cg2895*	This study
Δ*malQ* Δ*treX* Δ*tus* IM*cg2971*	Deletion of *malQ*, *treX*, the *cg0831 – cg0835* gene cluster, and insertion of pDrive in *cg2971*	This study
Δ*malQ* Δ*treX* Δ*tus* IM*cg3038*	Deletion of *malQ*, *treX*, the *cg0831 – cg0835* gene cluster, and insertion of pDrive in *cg3038*	This study

C. glutamicum	Genotype or application	Reference
Δ*malQ* Δ*treX* Δ*tus* Δ*cg3178*	Deletion of *malQ*, *treX*, the *cg0831* – *cg0835* gene cluster, and *cg3178*	This study
Δ*malQ* Δ*treX* Δ*tus* IM*cg3226*	Deletion of *malQ*, *treX*, the *cg0831* – *cg0835* gene cluster, and insertion of pDrive in *cg3226*	This study
Δ*malQ* Δ*treX* Δ*tus* IM*cg3240*	Deletion of *malQ*, *treX*, the *cg0831* – *cg0835* gene cluster, and insertion of pDrive in *cg3240*	This study
Δ*malQ* Δ*treX* Δ*tus* IM*cg3245*	Deletion of *malQ*, *treX*, the *cg0831* – *cg0835* gene cluster, and insertion of pDrive in *cg3245*	This study
Δ*malQ* Δ*treX* Δ*tus* IM*cg3301*	Deletion of *malQ*, *treX*, the *cg0831* – *cg0835* gene cluster, and insertion of pDrive in *cg3301*	This study
Δ*malQ* Δ*treX* Δ*tus* IM*cg3334*	Deletion of *malQ*, *treX*, the *cg0831* – *cg0835* gene cluster, and insertion of pDrive in *cg3334*	This study
Δ*malQ* Δ*treX* Δ*tus* IM*cg3353*	Deletion of *malQ*, *treX*, the *cg0831* – *cg0835* gene cluster, and insertion of pDrive in *cg3353*	This study
Δ*malQ* Δ*treX* Δ*tus* IM*cg3387*	Deletion of *malQ*, *treX*, the *cg0831* – *cg0835* gene cluster, and insertion of pDrive in *cg3387*	This study
Δ*malQ* Δ*treX* Δ*tus* IM*cg3395*	Deletion of *malQ*, *treX*, the *cg0831* – *cg0835* gene cluster, and insertion of pDrive in *cg3395*	This study
Δ*malQ* Δ*mscCG* Δ*mscL*	Deletion of *malQ*, *mscCG,* and *mscL*	(Henrich, 2011)
Δ*malQ* Δ*treX* Δ*mscCG* Δ*mscL*	Deletion of *malQ*, *treX, mscCG,* and *mscL*	This study
Δ*malQ* Δ*treX* Δ*treS*	Deletion of *malQ*, *treX*, and *treS*	This study
Δ*mus*	Deletion of the *cg2703* – *cg2708* gene cluster	(Henrich, 2011)
Δ*treS*	Deletion of *treS*	(Wolf *et al.*, 2003)
Δ*treS* Δ*tus*	Deletion of *treS* and the *cg0831* – *cg0835* gene cluster	This study
Δ*otsA* Δ*treS* Δ*treY*	Deletion of *otsA*, *treS*, and *treY*	(Wolf *et al.*, 2003)
Δ*otsA* Δ*treS* Δ*treY* Δ*tus*	Deletion of *otsA*, *treS*, *treY*, and the *cg0831* –*cg0835* gene cluster	(Henrich, 2011)
E. coli	**Genotype or application**	**Reference**
DH5α-mcr	*endA1 supE44 thi-1 λ-recA1 gyrA96 relA1 deoR* Δ(*lacZYA-argF*) *U196 Φ80lacZΔM15 mcrA* Δ(*mmr hsdRMS mcrBC*)	(Grant *et al.*, 1990)
BL21 (DE3)	F^- *dcm ompT hsdS*(r_B^- m_B^-) *gal λ*(DE3)	(Studier & Moffatt, 1986)
JM109	*endA1 recA1 gyrA96 thi-1 hsdR17* (r_K^- m_K^+) *relA1 supE44* Δ*(lac-proAB)* [F' *traD36 proAB laqI*^{q} *lacZΔM15*]	(Yanisch-Perron *et al.*, 1985)

All plasmids used in this work are shown in Table 2.

Table 2: Plasmids used in this work.

Plasmid	Relevant characteristic or application	Reference
pBB1	Constitutive overexpression of genes in *E. coli* and *C. glutamicum*. P_{tac}, Cm^R	(Krause *et al.*, 2010)
pET29b(+)	IPTG-inducible overexpression of genes in *E. coli* BL21 (DE3). P_{T7}, Kan^R, C-terminal 6×Histag, *lacI*.	Novagen, Darmstadt
pTre1	Trehalase gene from *R. marinus* ligated to pET23a(+)	(Jorge *et al.*, 2007)
pET29b_tre_rmr	Overexpression of a trehalase gene from *R. marinus* in *E. coli* BL21 (DE3)	This study
pET29b_tusE	Overexpression of *tusE* in *E. coli* BL21 (DE3)	This study

Plasmid	Relevant characteristic or application	Reference
pET29b_tusEΔN25	Overexpression of *tusE*ΔN25 in *E. coli* BL21 (DE3)	This study
pET29b_tusEΔN32	Overexpression of *tusE*ΔN32 in *E. coli* BL21 (DE3)	This study
pET29b_TreSen1-34	Overexpression of trehalose nanosensors TreSen1 - 34 in *E. coli* BL21 (DE3)	This study
pDrive	Cloning vector. Kan^R, Amp^R, *lacZα.*	Qiagen, Hilden
pJET	Cloning vector. Amp^R.	Thermo Scientific ,USA
pK19mobsacB	Plasmid for gene deletion in *C. glutamicum*. Kan^R, $oriV_{E. coli}$, *oriT*, *mob*, *sacB*	(Schäfer *et al.*, 1994)
pK19mobsacB_Δ*cg0284*	Plasmid for deletion of *cg0284* in *C. glutamcium*	This study
pK19mobsacB_Δ*cg3174*	Plasmid for deletion of *cg3174* in *C. glutamcium*	This study
pK19mobsacB_Δ*cg3178*	Plasmid for deletion of *cg3178* in *C. glutamcium*	This study
pK19mobsacB_Δ*treX*	Plasmid for deletion of *treX* in *C. glutamcium*	This study
pK19mobsacB_Δ*treStreX*	Plasmid for deletion of *treS* and *treX* in *C. glutamcium*	This study
pK19mobsacB_Δ*tus*	Plasmid for deletion of the *cg0831 – cg0835* gene cluster	(Henrich, 2011)
pRSETb_AT1.03, pRSETb_AT1.03^{YEMK}, pRSETb_AT3.10^{MGK}, pRSETb_AT1.03$^{R122K/R126K}$	Overexpression of AT1.03, AT1.03^{YEMK}, AT3.10^{MGK}, and AT103$^{R122K/R126K}$ in *E. coli*	(Imamura *et al.*, 2009)
pBB1_AT1.03, pBB1_AT1.03^{YEMK}, pBB1_AT3.10^{MGK}, pBB1_AT1.03$^{R122K/R126K}$	Overexpression of AT1.03, AT1.03^{YEMK}, AT3.10^{MGK}, and AT103$^{R122K/R126K}$ in *C. glutamicum*	This study
pRSETb_FLIPmal-2µ,	Overexpression of FLIPmal-2µ in *E. coli*	(Fehr *et al.*, 2002)
pXMJ19	IPTG-inducible overexpression of genes in *E. coli* and *C. glutamicum*. P_{tac}, $lacI^q$, Cm^R.	(Jakoby *et al.*, 1999)
pXMJ19_tus	Overexpression of the *cg0831 – cg0835* gene cluster in *C. glutamicum*.	(Henrich, 2011)
pXMJ19_otsBA$_{E. coli}$	Overexpression of the *otsBA*-operon from *E. coli* JM109 in *C. glutamicum*.	(Padilla *et al.*, 2004a)
pXMJ19_*cg2893*	Overexpression of *cg2893* in *C. glutamicum*.	This study
pXMJ19_*cg2895*	Overexpression of *cg2895* in *C. glutamicum*.	This study

All oligonucleotides used in this work are shown in Table 3.

Table 3: Oligonucleotides used in this work. Restriction sites are underlined and the corresponding restriction endonucleases are given in brackets.

Oligonucleotide	Sequence	Application
delcg0284 fw a	CCCGGGTCGCAAGTGGATTGTG (*Xma*I)	Deletion of *cg0284*
delcg0284 rv a	CCAACTTCCATACTCCATTCCATATTCTGCGGCCTCAAC	Deletion of *cg0284*
delcg0284 fw b	GGAATGGAGTATGGAAGTTGGCCTTCATGCCGATCTTCC	Deletion of *cg0284*
delcg0284 rv b	GGATCCCTGCTTCTCCTCCCATTC (*Bam*HI)	Deletion of *cg0284*
delcg0284 check fw	CCGCAGGTAAGTTAGTG	Test-primer for deletion of *cg0284*
delcg0284 check rv	GACATAGGTGCCAAGTC	Test-primer for deletion of *cg0284*
delcg3174 fw a	GAATTCCCAGGTGGCTCTGATGT (*Eco*RI)	Deletion of *cg3174*
delcg3174 rv a	CCAACTTCCATACTCCATTCCCGGCGATGACGA	Deletion of *cg3174*

Oligonucleotide	Sequence	Application
	CTAAC	
delcg3174 fw b	GGAATGGAGTATGGAAGTTGGCGATACCGTGG CATCTC	Deletion of *cg3174*
delcg3174 rv b	GGATCCACCAGACGGTCGATAGG (*Bam*HI)	Deletion of *cg3174*
delcg3174 check fw	AAGGCCCTGAAAGTGTC	Test-primer for deletion of *cg3174*
delcg3174 check rv	CTTCCACTGCGGTCATA	Test-primer for deletion of *cg3174*
delcg3178 fw a	CCCGGGTGGTTGAGGCGGATAG *(Xma*I)	Deletion of *cg3178*
delcg3178 rv a	CCAACTTCCATACTCCATTCCAACGGCCAATCG GTAG	Deletion of *cg3178*
delcg3178 fw b	GGAATGGAGTATGGAAGTTGGGACTTCGCCAA GAAGACC	Deletion of *cg3178*
delcg3178 rv b	CCCGGGCCGTCAGCTCTCCGTTAC *(Xma*I)	Deletion of *cg3178*
delcg3178 check fw	CTCCTCAGCCTCGTT	Test-primer for deletion of *cg3178*
delcg3178 check rv	TTCCGTCAGCTCTCC	Test-primer for deletion of *cg3178*
deltreSX fw a	GGATCCTGGCCTGGAGAATTCGGATA (*Bam*HI)	Deletion of *treS* and *treX*
deltreSX rv a	CCAACTTCCATACTCCATTCCTCTTCCGATTCGT GCTCAAC	Deletion of *treS* and *treX*
deltreSX fw b	GGAATGGAGTATGGAAGTTGGCGTTGTACGAG GTTGCCTAT	Deletion of *treS* and *treX*
deltreSX rv b	CTGCAGTAAGGACACGCCTCTGCATT (*Pst*I)	Deletion of *treS* and *treX*
deltreSX check fw	TTGCTCGCCGCTACTTC	Test-primer for deletion of *treS* and *treX*
deltreSX check rv	TCTGCGGTGGAGGAAGA	Test-primer for deletion of *treS* and *treX*
deltreX fw a	GAATTCATCCTGAACGCCTGTACCTT (*Eco*RI)	Deletion of *treX*
deltreX rv a	CCAACTTCCATACTCCATTCCAAGTGTTCTCGCC ACATTCG	Deletion of *treX*
deltreX fw b	GGAATGGAGTATGGAAGTTGGCGTTGTACGAG GTTGCCTAT	Deletion of *treX*
deltreX rv b	CTGCAGTAAGGACACGCCTCTGCATT (*Pst*I)	Deletion of *treX*
deltreX check fw	AGCTGGAACTCCTTCAC	Test-primer for deletion of *treX*
deltreX check rv	TCTGCGGTGGAGGAAGA	Test-primer for deletion of *treX*
IMcg0206 fw	TCAACGTGCCCTTAGGAATC	Integration mutagenesis *cg0206*
IMcg0206 rv	AATACCAAGGCGCCAGCAGC	Integration mutagenesis *cg0206*
IMcg0206 check	GCAATGATCGGTCCTTTAGC	Test-primer for integration mutagenesis
IMcg0340 fw	TGGCATCCACATGCATCG	Integration mutagenesis *cg0340*
IMcg0340 rv	TGCGTAGCTGATGGAGAAGG	Integration mutagenesis *cg0340*
IMcg0340 check	ATCCTGCGAGACTTCAC	Test-primer for integration mutagenesis
IMcg0501 fw	CTTTGGAGCACGCCGATGAG	Integration mutagenesis *cg0501*
IMcg0501 rv	ACACTGGTCGGCGACCAATG	Integration mutagenesis *cg0501*
IMcg0501 check	ACAGGACTGCAGACAGAAAC	Test-primer for integration mutagenesis
IMcg0772 fw	CTTCATCGCTGGTCTG	Integration mutagenesis *cg0772*
IMcg0772 rv	CCACCGACGTAGTTTC	Integration mutagenesis *cg0772*
IMcg0772 check	CGGCGGACATATCAAAC	Test-primer for integration mutagenesis
IMcg1212 fw	CCTCCACGGTGTTGGATACG	Integration mutagenesis *cg1212*
IMcg1212 rv	CCCGTAATCAGATCGCGTTC	Integration mutagenesis *cg1212*
IMcg1212 check	AGCTTGGTCGAACTCTTCTG	Test-primer for integration mutagenesis
IMcg1289 fw	CCAGTTATCGGTGGTGTTC	Integration mutagenesis *cg1289*
IMcg1289 rv	AGGCGATCCACCAATCGTC	Integration mutagenesis *cg1289*
IMcg1289 check	TGCCAACGGCGAAAGTC	Test-primer for integration mutagenesis
IMcg1399 fw	CTTCCATGGCGTTCATTCCG	Integration mutagenesis *cg1399*

Oligonucleotide	Sequence	Application
IMcg1399 rv	GGTGCAGCTCTTGGAGTGTG	Integration mutagenesis *cg1399*
IMcg1399 check	GGCGACCTTTAAGGCTTTAC	Test-primer for integration mutagenesis
IMcg1526 fw	TATCGCTCCAGCGACAC	Integration mutagenesis *cg1526*
IMcg1526 rv	ACGGAGCCAACCAGAAG	Integration mutagenesis *cg1526*
IMcg1526 check	CAGTAGTACCGGCATAAG	Test-primer for integration mutagenesis
IMcg2618 fw	TGCATCACAGTGGTGATCAG	Integration mutagenesis *cg2618*
IMcg2618 rv	GATGATGCCCTGCTGTTCTG	Integration mutagenesis *cg2618*
IMcg2618 check	CCGCGATGTGTTCTTCTCTG	Test-primer for integration mutagenesis
IMcg2739 fw	ATACCGCCGATCACGAGTCC	Integration mutagenesis *cg2739*
IMcg2739 rv	GTGTGGCTGGTTTCGTACTC	Integration mutagenesis *cg2739*
IMcg2739 check	GAAGGAACTTCCCGGCTGTG	Test-primer for integration mutagenesis
IMcg2893 fw	GCGTTTGCTCCAACTG	Integration mutagenesis *cg2893*
IMcg2893 rv	AACCACACCGCCTAAG	Integration mutagenesis *cg2893*
IMcg2893 check	CCGACCATTCGTTACAG	Test-primer for integration mutagenesis
IMcg2895 fw	AGTACTATGCGCAGCTCTCC	Integration mutagenesis *cg2895*
IMcg2895 rv	ACATCACCGGCAGATAGTCC	Integration mutagenesis *cg2895*
IMcg2895 check	ACACTTGTCACCGTGTTC	Test-primer for integration mutagenesis
IMcg2971 fw	TGCTGATGACGGTTACG	Integration mutagenesis *cg2971*
IMcg2971 rv	TGGTGGTCAAGGAGAAG	Integration mutagenesis *cg2971*
IMcg2971 check	GCTTCATGCTGTGAAAGG	Test-primer for integration mutagenesis
IMcg3038 fw	CGTGCGTGGTGATTG	Integration mutagenesis *cg3038*
IMcg3038 rv	GATGCGGTGTGGATG	Integration mutagenesis *cg3038*
IMcg3038 check	GAAAGGCCTGCTCGTTG	Test-primer for integration mutagenesis
IMcg3226 fw	ATCGGAATTGGCGGCGAATG	Integration mutagenesis *cg3226*
IMcg3226 rv	TGTAGGTGCCGAAGATGTAG	Integration mutagenesis *cg3226*
IMcg3226 check	AGGTGACACGCCTTACATTC	Test-primer for integration mutagenesis
IMcg3240 fw	TCCGGCGTCGATACTTTC	Integration mutagenesis *cg3240*
IMcg3240 rv	AGGATTCCGCCAATGAGC	Integration mutagenesis *cg3240*
IMcg3240 check	TGGCGCATGATGAACTC	Test-primer for integration mutagenesis
IMcg3245 fw	CTGCACCTGCATTCGAAATC	Integration mutagenesis *cg3245*
IMcg3245 rv	TGCTGCTATTGCCCAGTTTG	Integration mutagenesis *cg3245*
IMcg3245 check	AAGTAGCTGCTGGTCGAGTC	Test-primer for integration mutagenesis
IMcg3301 fw	GCCGCATGGTCGTTATCCTG	Integration mutagenesis *cg3301*
IMcg3301 rv	GCAACCGCATAGCCTGGAAG	Integration mutagenesis *cg3301*
IMcg3301 check	TGCTTATCGACGCCCACTTC	Test-primer for integration mutagenesis
IMcg3334 fw	CCGCACTATCGCAGCATTG	Integration mutagenesis *cg3334*
IMcg3334 rv	TTCGGGTTGCCACTGTCAC	Integration mutagenesis *cg3334*
IMcg3334 check	AACAGCCCGATTCAAG	Test-primer for integration mutagenesis
IMcg3353 fw	AAAGCAGCGGTGATTGG	Integration mutagenesis *cg3353*
IMcg3353 rv	GAGCAGGGTGACAAATGTG	Integration mutagenesis *cg3353*
IMcg3353 check	ACCAGAATCGGGAGGAC	Test-primer for integration mutagenesis
IMcg3387 fw	TCTACGGACCAGGATTTG	Integration mutagenesis *cg3387*
IMcg3387 rv	ACGAACCAGCCATTTG	Integration mutagenesis *cg3387*
IMcg3387 check	GGGCTAAATGCTCCAAAC	Test-primer for integration mutagenesis
IMcg3395 fw	CACGCGGTCACTCCACATAC	Integration mutagenesis *cg3395*
IMcg3395 rv	GAGGTTTCTTCGGAGCTTTC	Integration mutagenesis *cg3395*
IMcg3395 check	GCGGGCTTTACGGTTATGCG	Test-primer for integration mutagenesis
M13 fw	TGTAAAACGACGGCCAGT	Test-primer for integration mutagenesis
M13 rv	CAGGAAACAGCTATGAC	Test-primer for integration mutagenesis

Oligonucleotide	Sequence	Application
tusE_fw_NdeI	CATATGTCCTCGATTTCCCGCAAGA (*Nde*I)	Cloning of *tusE* in pET29b
tusEΔN25_fw_NdeI	CATATGTGTAGTTCAGACTCAAGCTC (*Nde*I)	Cloning of *tusE*ΔN25 in pET29b
tusEΔN32_fw_NdeI	CATATGGACTCCACAGATTCCACC (*Nde*I)	Cloning of *tusE* ΔN32 in pET29b
tusE_rv_HindIII	AAGCTTGCTGGAAGCGTTTTCG (*Hin*dIII)	Cloning of *tusE, tusE*ΔN25, and *tusE*ΔN32 in pET29b
tusE_fw_KpnI	GGTACCGGAGGCGCCATGTCCTCGATTTCCCG (*Kpn*I)	PCR *tusE* for sensor construction (TreSen1)
tusEΔN32_fw_KpnI	GGTACCGGAGGCGCCGACTCCACAGATTCC (*Kpn*I)	PCR *tusE* for sensor construction (TreSen2, 8)
tusEΔN47_fw_KpnI	GGTACCGGAGGCGCCATGCCCATCACCTTTGCG (*Kpn*I)	PCR *tusE* for sensor construction (TreSen3)
tusE_fw2_KpnI	GGTACCATGTCCTCGATTTCCCG (*Kpn*I)	PCR *tusE* for sensor construction (TreSen4)
tusEΔN32_fw2_KpnI	GGTACCGACTCCACAGATTCCAC (*Kpn*I)	PCR *tusE* for sensor construction (TreSen5)
tusEΔN47_fw2_KpnI	GGTACCCCCATCACCTTTGCG (*Kpn*I)	PCR *tusE* for sensor construction (TreSen6)
tusEΔN25_fw_KpnI	GGTACCTGTAGTTCAGACTCAAGC (*Kpn*I)	PCR *tusE* for sensor construction (TreSen7, 11, 12, 13)
tusE_Tr8_rv	TGGTGCTTCTGGGATG	PCR *tusE*N1-174 for sensor construction (TreSen8)
tusE_Tr8_b_fw	GCAAACTGGGCTGACC	PCR *tusE*N1-174 for sensor construction (TreSen8)
tusE_Tr8_B_rv_ HindIII	AAGCTTCTAGCTGGAAGCGTTTTC (*Hin*dIII)	PCR *tusE*N174-424 for sensor construction (TreSen8)
tusEΔN20_fw_KpnI	GGTACCATCGCACTGGCCG (*Kpn*I)	PCR *tusE* for sensor construction (TreSen9)
tusEΔN29_fw_KpnI	GGTACCTCAAGCTCCGACTCCAC (*Kpn*I)	PCR *tusE* for sensor construction (TreSen10)
tusEΔN27_fw_KpnI	GGTACCGACTCAAGCTCCGACTC (*Kpn*I)	PCR *tusE* for sensor construction (TreSen16)
tusEΔN28_fw_KpnI	GGTACCTCAAGCTCCGACTCCAC (*Kpn*I)	PCR *tusE* for sensor construction (TreSen17)
tusEΔN30_fw_KpnI	GGTACCTCCGACTCCACAGATTC (*Kpn*I)	PCR *tusE* for sensor construction (TreSen18)
tusEΔN31_fw_KpnI	GGTACCGACTCCACAGATTCCACC (*Kpn*I)	PCR *tusE* for sensor construction (TreSen19)
tusEΔN26_fw_KpnI	GGTACCTCAGACTCAAGCTCCGAC (*Kpn*I)	PCR *tusE* for sensor construction (TreSen20)
tusEΔN33_fw_KpnI	GGTACCTCCACAGATTCCACCGCTAG (*Kpn*I)	PCR *tusE* for sensor construction (TreSen32)
tusEΔN34_fw_KpnI	GGTACCACAGATTCCACCGCTAGCG (*Kpn*I)	PCR *tusE* for sensor construction (TreSen33)
tusEΔN35_fw_KpnI	GGTACCGATTCCACCGCTAGCGAAG (*Kpn*I)	PCR *tusE* for sensor construction (TreSen34)
tusE_rv_KpnI	GGTACCGGCGCCGCTGGAAGCGTTTTC (*Kpn*I)	PCR *tusE* for sensor construction (TreSen1 - 3)
tusE_rv2_KpnI	GGTACCGCTGGAAGCGTTTTC (*Kpn*I)	PCR *tusE* for sensor construction (TreSen4 - 10, 14 - 34)
tusEΔC1_rv_KpnI	GGTACCGGAAGCGTTTTCGATCGC (*Kpn*I)	PCR *tusE* for sensor construction (TreSen11)
tusEΔC3_rv_KpnI	GGTACCGTTTTCGATCGCTGCC (*Kpn*I)	PCR *tusE* for sensor construction (TreSen12)
tusEΔC5_rv_KpnI	GGTACCGATCGCTGCCTTCAT (*Kpn*I)	PCR *tusE* for sensor construction (TreSen13)
yfp_Tr8_fw	CGAAATCATCCCAGAAGCACCAATGGTGAGCAAGGGCGAG	PCR *eyfp* for sensor construction (TreSen8)
yfp_Tr8_rv	CCACGAGGTCAGCCCAGTTTGCCTTGTACAGCTCGTCCATGC	PCR *eyfp* for sensor construction (TreSen8)
eyfp_fw_KpnI	GGTACCATGGTGAGCAAGGGCG (*Kpn*I)	PCR *mVenus* for sensor construction (TreSen15 - 34)
eyfp_rv_HindIII	CAAGCTTTTACTTGTACAG (	PCR *mVenus* for sensor construction (TreSen15 - 34)
ecfp_fw_BamHI	GGATCCATGGTGAGCAAGGGC (*Bam*	PCR *ecfp*ΔC10 for sensor construction (TreSen15 - 34)
ecfpΔC10_rv_KpnI	GGTACCCCCGGCGGCGGTCAC (*Kpn*I)	PCR *ecfp*ΔC10 for sensor construction (TreSen15 - 34)
mVenusΔN6_fw_	GGTACCGAGCTGTTCACCGGG (*Kpn*I)	PCR *mVenus*ΔN6 for sensor construction

Oligonucleotide	Sequence	Application
KpnI		(TreSen15 - 34)
mVenus_rv_HindIII	AAGCTTCTTGTACAGCTCGTC (*Hin*dIII)	PCR *mVenus*ΔN6 for sensor construction (TreSen15 - 34)
Q5_K55A_fw	TGCGATGGGCGCAAACGACACCGACAAAG	Site-directed mutagenesis (*tusE*^{K55A})
Q5_K55E_fw	TGCGATGGGCGAAAACGACACC	Site-directed mutagenesis (*tusE*^{K55E})
Q5_K55_rv	AAGGTGATGGGGCCGCGG	Site-directed mutagenesis (*tusE*^{K55A} and *tusE*^{K55E})
Q5_D110A_fw	ATGGCGCTCGCCGTCATCTGG	Site-directed mutagenesis (*tusE*^{D110A})
Q5_D110N_fw	CATGGCGCTCAACGTCATCTG	Site-directed mutagenesis (*tusE*^{D110N})
Q5_D110_rv	GACGTCGTAGTCAGAGTTGC	Site-directed mutagenesis (*tusE*^{D110A} and *tusE*^{D110N})
Q5_W113A_fw	CGACGTCATCGCGACCGCAGACTTCGC	Site-directed mutagenesis (*tusE*^{W113A})
Q5_W113A_rv	AGCGCCATGACGTCGTAG	Site-directed mutagenesis (*tusE*^{W113A})
Q5_E259A_fw	GCAGCGACCGCAGAAGAAACC	Site-directed mutagenesis (*tusE*^{E259A})
Q5_E259A_rv	AAGGGATGCCTTGGAGATG	Site-directed mutagenesis (*tusE*^{E259A})
Q5_W277A_fw	CGCCATTAACGCGCCATACATGTACACCAACTC	Site-directed mutagenesis (*tusE*^{W277A})
Q5_W277A_rv	TAGGCGGTTTGGCCTTCG	Site-directed mutagenesis (*tusE*^{W277A})
Q5_W277F_fw	GCCATTAACTTTCCATACATGTACACCAAC	Site-directed mutagenesis (*tusE*^{W277F})
Q5_W277F_rv	GTAGGCGGTTTGGCCTTC	Site-directed mutagenesis (*tusE*^{W277F})
Q5_Y313A_fw	CCTTGGTGGCGCCAACAACGGCATCAACG	Site-directed mutagenesis (*tusE*^{Y313A})
Q5_Y313A_rv	GGTGGATACGCCGACGCC	Site-directed mutagenesis (*tusE*^{Y313A})
Q5_Y313F_fw	CTTGGTGGCTTCAACAACGGCATC	Site-directed mutagenesis (*tusE*^{Y313F})
Q5_Y313F_rv	GGTGGATACGCCGACGCC	Site-directed mutagenesis (*tusE*^{Y313F})
Q5_R381A_fw	CGCAGCACCAGCCCCAGTGTCTC	Site-directed mutagenesis (*tusE*^{R381A})
Q5_R381_rv	TTTTCCAGGGATTCCTTC	Site-directed mutagenesis (*tusE*^{R381A})
cg2893_fw_HindIII	AAGCTTATGACTTCAGAAACCTTACAG (*Hin*dIII)	PCR *cg2893* for overexpression
cg2893_rv_SalI	GTCGACCTAGTGCGCATTATTGGCTCCC (*Sal*I)	PCR *cg2893* for overexpression
cg2895_fw_HindIII	AAGCTTATGACTGTTCAGGAATTCGAC (*Hin*dIII)	PCR *cg2895* for overexpression
cg2895_rv_SalI	GTCGACCTACTTCACCTTGTGCGGTG (*Sal*I)	PCR *cg2895* for overexpression

2.2 Media and cultivation of *E. coli* and *C. glutamicum*

2.2.1 Media

For cultivation of *E. coli*, LB medium (10 g/l tryptone, 5 g/l yeast extract, 10 g/l NaCl) or TB medium (12 g/l tryptone, 24 g/l yeast extract, 4 ml/l glycerol, 100 mM K_2HPO_4/KH_2PO_4 buffer pH7.4) was used. *C. glutamicum* precultures were grown in 2TY medium (16 g/l tryptone, 10 g/l yeast extract, 5 g/l NaCl) or BHI medium (37 g/l brain heart infusion). For shake flask cultivation, CgC minimal medium was used (5 g/l $(NH_4)_2SO_4$, 5 g/l urea, 21 g/l MOPS, 1 g/l K_2HPO_4, 1 g/l KH_2PO_4, 0.25 g/l $MgSO_4 \times 7\ H_2O$, 10 mg/l $CaCl_2$, 10 mg/l $FeSO_4 \times 7\ H_2O$, 10 mg/l $MnSO_4 \times H_2O$, 1 mg/l $ZnSO_4 \times H_2O$, 0.2 mg/l $CuSO_4$, 0.02 mg/l $NiCl_2 \times 6\ H_2O$, 200 µg/l biotin). The pH was adjusted to 6.8 (NaOH) for cultivations with sugars as carbon sources, to 6.3 for cultivations with organic acids as carbon sources and to 6.5 for cultivations with sugars and

organic acids as carbon sources. For bioreactor cultivations, CgXII minimal medium was used (same composition as CgC medium but 20 g/l $(NH_4)_2SO_4$, 33 mg/l protocatechuic acid, no addition of MOPS, pH 7.0).

For agar plates, 16 g/l agar was added to the liquid medium. If appropriate, *E. coli* strains were grown in the presence of 30 µg/ml chloramphenicol, 100 µg/ml kanamycin or 100 µg/ml carbenicillin. For *C. glutamicum* strains 6 µg/ml chloramphenicol or 25 µg/ml kanamycin were added if appropriate.

2.2.2 Cultivation of *C. glutamicum* in shake flasks

Growth experiments with *C. glutamicum* strains were performed in 50 ml CgC minimal medium in baffled 500 ml shake flasks at 30°C and 110 rpm on a rotary shaker. Precultures were grown in 2TY broth or BHI medium over night and cells were washed twice with 0.9% NaCl solution before inoculating the main culture. Carbon sources and antibiotics were added as appropriate.

2.2.3 Bioreactor cultivation of *C. glutamicum*

Bioreactor cultivations of *C. glutamicum* strains were carried out in a 2 l glass fermenter (Biostat B, Sartorius, Göttingen) equipped with standard electrodes for the online-measurement of pH, temperature, and the partial pressure of dissolved oxygen. The fractions of O_2 and CO_2 in the fermenter off-gas were determined photo-acoustically (BCP-O_2, Bluesens, Herten) or via infrared absorption (BCP-CO_2, Bluesens, Herten), respectively. For batch cultivations 1 l CgXII minimal medium was used. The carbon source was chosen as adequate for the experiment. Temperature and pH-value were set at 30°C and 7.0, respectively, and the latter was controlled by the addition of 8% (v/v) H_2SO_4 and 5 M KOH. The fermenter was aerated with 1.3 l/min ambient air filtered sterile (0.2 µM). The dissolved oxygen saturation was maintained above 30% by adjusting the stirrer speed between 200 rpm and 1200 rpm. Antifoam 204 (Sigma-Aldrich, USA) was added manually when necessary.

2.3 Molecular biology methods

2.3.1 DNA purification, digestion, and ligation

For the preparation of chromosomal DNA from *C. glutamicum*, cells from 5 ml of an overnight culture were harvested by centrifugation and resuspended in 1 ml TE buffer (10 mM Tris-HCl pH 8.0, 1 mM EDTA) plus lysozyme (15 mg/ml). After incubation for 3 h at37°C, 3 ml lysis buffer (10 mM Tris-HCl pH 8.2, 400 mM NaCl, 2 mM EDTA), 220 µl 10% sodium dodecyl sulfate (SDS) solution, and 150 µl proteinase K (20 mg/ml) were added. After incubation over night at 37°C, 2 ml saturated NaCl-solution were added and precipitated proteins were removed by centrifugation. The supernatant was mixed with an equal volume of cold ethanol. Precipitated DNA was coiled up on a glass pipette, washed with 70% ethanol, dried, and resuspended in 200 µl TE buffer.

Plasmid DNA from *E. coli* and *C. glutamicum* strains was prepared using the High Pure Plasmid Isolation Kit (Roche, Switzerland). To improve disruption of *C. glutamicum* cells, these were incubated in resuspension buffer plus 10 µg/ml lysozyme for 1.5 h in addition to the standard procedure recommended by the manufacturer. For DNA digestion and ligation, FastDigest restriction endonucleases and T4 DNA Ligase (Thermo Scientific, USA), respectively, were used.

2.3.2 Polymerase chain reaction

For amplification of target genes by PCR (Mullis *et al.*, 1986), EconoTaq® PLUS GREEN 2×Master Mix (Lucigen, USA), Phusion® High-Fidelity DNA Polymerase (New England Biolabs, USA), or PRECISOR High-Fidelity DNA Polymerase (BioCat, Heidelberg) were used with plasmid DNA or chromosomal DNA as template for the amplification. Oligonucleotides were purchased from Eurofins MWG Operon (Ebersberg). PCR products were cloned using the CloneJet PCR Cloning Kit (Thermo Scientific, USA) or the QIAGEN PCR Cloning Kit (QIAGEN, Hilden). Sequencing of DNA was carried out by GATC Biotech (Konstanz).

2.3.3 Site-directed DNA mutagenesis

Site-directed mutagenesis of plasmid DNA was achieved using the Q5® Site-Directed Mutagenesis Kit (New England Biolabs, USA). PCR primers were designed with the NEBaseChanger™ software (www.nebasechanger.neb.com).

2.3.4 Agarose gel electrophoresis

DNA fragments resulting from PCR reactions or the digestion of plasmid DNA were separated by agarose gel electrophoresis. Samples were loaded on 1% agarose gels and run in 1 × TAE buffer (Sambrook & Russel, 2001). After separation, DNA was stained in 1 µg/ml ethidium bromide solution and visualised using the UVP BioDoc-It™ Imaging system (Analytik Jena, Jena). The NucleoSpin® Extract II Kit (Macherey-Nagel, Düren) was used to isolate DNA from agarose gels.

2.3.5 Competent *E. coli* and *C. glutamicum* cells and transformation

Chemically competent *E. coli* cells were prepared and transformed by standard procedures (Inoue *et al.*, 1990). 250 ml SOB medium (20 g/l tryptone, 5 g/l yeast extract, 0.6 g/l NaCl, 0.2 g/l KCl, 2.48 g/l $MgSO_4 \times 7\ H_2O$) were inoculated from an LB culture and grown to OD_{600} = 0.3 (37°C, 200 rpm). The cells were cooled on ice for 10 min, pelletized (850 × g, 15 min, 4°C), and resuspended in 80 ml TB buffer (3.025 g/l PIPES, 1.67 g/l $CaCl_2$,18.63 g/l KCl, pH 6.7 (KOH), autoclave, add 6.92 g/l $MnCl_2$). After incubation on ice for 10 min, centrifugation was repeated and cells were resuspended in 20 ml TB buffer. 1.4 ml dimethyl sulfoxide was added, the suspension was aliquoted, frozen in liquid nitrogen and stored at -80°C. For transformation, 1 µl – 5 µl plasmid solution were added and incubated on ice for 15 min. A heat shock was then performed for 45 s at 42°C and 1 ml LB medium was added. The suspension was incubated at 37°C for 1 h and plated on selective agar plates.

Electro-competent *C. glutamicum* cells were prepared by the method of van der Rest *et al.* (1999). Therefore, 10 ml LB plus 2% glucose were inoculated and incubated for 8 h (30°C, 125 rpm). Then, 200 ml LB-I medium (LB plus 4 g/l isonicotinic acid, 25 g/l glycine, 1 ml/l Tween 80) were inoculated to OD_{600} = 0.25 and cultivated for 12 h at 20°C and 125 rpm. Then, the OD_{600} was measured, cells were harvested by centrifugation (2164 × g, 10 min, 4°C) and washed with 50 ml cold 10% glycerol solution. After centrifugation, the pellet was resuspended in 1 ml per OD_{600} 10% glycerol solution, frozen in liquid nitrogen and stored at -80°C.

Competent *C. glutamicum* cells were transformed wit 1 µl – 5 µl plasmid solution using a MicroPulser (Bio-Rad, München) set at 2.5 kV. Afterwards, 1 ml BHI medium was added, a heat shock was performed (46°C, 10 min), cells were incubated at 30°C and 125 rpm for 1 h and plated on selective agar plates.

2.3.6 Integration mutagenesis and gene deletion in *C. glutamicum*

Inactivation of chromosomal genes in *C. glutamicum* was either achieved by integration mutagenesis or gene deletion.

For gene inactivation by integration mutagenesis, the pDrive plasmid was integrated into the target gene by homologous recombination. Therefore, a 500 bp stretch of DNA homologous to the central part of the target gene was amplified by PCR and ligated to the pDrive plasmid. *C. glutamicum* was then transformed with the resulting plasmid and spread on LB agar plates containing 25 µg/ml kanamycin. The disruption of the target gene in kanamycin resistant cells was tested by PCR using a target gene specific primer and the plasmid specific M13_fw or M13_rv primer.

For gene deletion, the method of Schäfer *et al.* (1994) was applied. Therefore, pK19mobsacB-derived plasmids were used to replace chromosomal regions with truncated DNA sequences by two successive events of homologous recombination.

DNA sequences of 500 bp homologous to the up- and downstream regions of the target gene were amplified by PCR. These two PCR products were fused together in a second PCR step via oligonucleotide linkers (5'-GGAATGGAGTATGGAAGTTGG-3'). The PCR product was ligated to pK19mobsacB, a plasmid enabling positive (kanamycin-resistance gene) and negative (levansucrase gene, expression is lethal in the presence of sucrose) selection. After transformation of *C. glutamicum* with the resulting plasmid, kanamycin resistant cells were selected on LB agar plates. These were grown in 5 ml LB medium for 12 h under non-selective conditions. Cells were then spread on LB agar plates plus 10% sucrose for the selection of plasmid-free cells. Finally, PCR using primers flanking the target sequence was applied to verify successful target gene deletion.

2.3.7 RNA hybridisation experiments

Total RNA was isolated with the Nucleospin® RNA II Kit (Macherey-Nagel, Düren). RNA hybridisation experiments were performed as described previously (Möker *et al.*, 2004) in a Minifold Slot-Blot system (Schleicher & Schuell, Dassel). DIG-11-dUTP-labelled RNA antisense probes used for mRNA detection were constructed in a previous work (Schulte, 2011).

2.4 Biochemical methods

2.4.1 Heterologous expression in *E. coli* BL21 (DE3)

For overexpression of heterologous genes, *E. coli* BL21 (DE3) was transformed with the respective expression plasmid. A single colony was picked from a LB agar plate and transferred into 5 ml LB medium. After incubation at 37°C for several hours 50 ml – 200 ml TB medium was inoculated to an OD_{600} of 0.1. When the OD_{600} reached 0.8 – 1.0, 1 mM IPTG was added to induce gene expression. Cells were harvested by centrifugation after 16 h of incubation at 25°C – 37°C and stored at -20°C.

2.4.2 Chromatographic purification of proteins

For cell disruption, a French Pressure Cell Press (Thermo Scientific, USA) was used. Cell debris was removed by centrifugation (2164 × g, 30 min, 4°C).

Protein purification was carried out on an Äkta Purifier FPLC-system (GE Healthcare, Freiburg). For purification via ion metal affinity chromatography (IMAC), a HisTrap™ FF crude 1 ml column (GE Healthcare, Freiburg) was used. For protein binding to the column, washing, and elution, a three-step gradient of buffer A (20 mM K_2HPO_4/KH_2PO_4 buffer pH 7.5, 500 mM NaCl, 10 mM imidazole) and buffer B (20 mM K_2HPO_4/KH_2PO_4 buffer pH 7.5, 500 mM NaCl, 500 mM imidazole) of individually determined ratio between 0% – 100% (v/v) solvent B was used at a flow rate of 1 ml/min.

For further purification via size exclusion chromatography (SEC), samples were concentrated in Vivaspin 2 ml centrifugal concentrators (Sigma-Aldrich, USA) and loaded onto a Superdex 200 10/300 GL column (GE Healthcare, Freiburg). The buffer was chosen individually for each protein. The flow rate was adjusted to 0.5 ml/min.

2.4.3 Investigation of trehalose binding via intrinsic protein fluorescence

Intrinsic protein fluorescence of purified TusE-His_6 or TusEΔN25-His_6 (100 µg/ml in 20 mM K_2HPO_4/KH_2PO_4 buffer pH 7.5, 150 mM NaCl) was excited at 289 nm in a luminescence spectrometer (Thermo Scientific, USA) at 30°C. 10 µM or 150 µM trehalose stock solution or buffer as negative control were added repeatedly and the fluorescence intensity (F) at 336 nm (800 V detector current) was recorded. The relative fluorescence change (ΔF) was calculated according to equation 1 and plotted against the trehalose concentration (c_{Tre}). F_0

is the fluorescence intensity without ligand, F_{max} is the maximum fluorescence intensity measured in the presence of ligand.

$$\Delta F = \frac{F(c_{Tre}) - F_0}{F_{\max} - F_0} \quad \text{(eq. 1)}$$

2.4.4 Fluorescence measurements with metabolite nanosensors

For fluorescence measurements in *E. coli* or *C. glutamicum* cell lysates, cells were disrupted in a Precellys 24 homogenizer (Peqlab, Erlangen) with 250 µl glass beads (0.1 – 0.25 mm diameter) in 100 mM MOPS (pH 7.5). Cell debris was removed by centrifugation (17500 × g, 20 min, 4°C). The supernatant was diluted appropriately with the same buffer and transferred to black 96 well plates (Corning, USA). Fluorescence measurements were performed in an Infinite® 200 PRO microplate reader (Tecan, Crailsheim) with the temperature set to 30°C and the gain level adjusted between 60 and 100. For Förster Resonance Energy Transfer (FRET)-experiments with the ECFP-EYFP FRET-pair, the excitation wavelength was set to 435 nm and fluorescence intensities were recorded at 480 nm and 525 nm. The fluorescence ratio (R) was calculated by dividing the latter value by the former. R was plotted against the trehalose concentration (c_{Tre}). Data were fitted to the Hill equation (eq. 2) to determine the dissociation constant (K_d). R_0 is the initial FRET-ratio in the absence of ligand, ΔR_{max} is the maximum change of the fluorescence intensity and n the Hill coefficient.

$$R(c_{Tre}) = R_0 + \frac{\Delta R_{\max} \times c_{Tre}^n}{K_d^n + c_{Tre}^n} \quad \text{(eq. 2)}$$

2.4.5 *In situ* calibration of metabolite nanosensors

For *in situ* calibration of metabolite nanosensors, cells were permeabilised with 0.05% CTAB. Therefore, CTAB, a series of different ligand concentrations, and water (ad 50 µl) were mixed in a 96 well plate. *C. glutamicum* cells expressing genetically encoded nanosensors were washed and resuspended in 50 mM MOPS pH 7.5. Both solutions were preheated to 30°C before equal volumes of both were mixed. Fluorescence ratios were determined immediately as described above (2.4.4).

2.4.6 Determination of maltose and trehalose transport rates

Cells were grown in 2TY broth and harvested in the exponential growth phase. Cells were washed twice with 0.9% NaCl solution and resuspended in CgC minimal medium to OD_{600} = 3. 1 ml cell solution was mixed with 980 µl CgC minimal medium and incubated at 30°C for 3 min. The experiment was started by the addition of 20 µl radiolabelled [U-^{14}C]-maltose (580 mCi × mmol^{-1}, American Radiolabeled Chemicals, USA) premixed with unlabelled maltose to adjust the final maltose concentration between 50 µM and 5 mM) or 20 µl radiolabelled [U-^{14}C]-trehalose (600 mCi × mmol^{-1}, Trenzyme, Konstanz) premixed with unlabelled trehalose to adjust the final concentration to 50 µM. Samples of 200 µl were vacuum filtered through glass fibre prefilters (Millipore, USA) and cells were washed twice with 100 mM LiCl. The intracellular radioactivity was determined via liquid scintillation (Rotiszint® eco plus scintillation cocktail, Carl Roth, Karlsruhe) in a LS 6500 scintillation counter (Beckmann, Krefeld).

2.4.7 Investigation of solute release after hypoosmotic shocks

To investigate solute excretion triggered by hypoosmotic shocks, the cells were loaded with [^{14}C]-labelled substrate. To enable glycine betaine uptake, the expression of *betP*, which encodes a glycine betaine uptake system, was induced by pre-cultivating *C. glutamicum* in BHI medium plus 0.5 M NaCl overnight. The cells were washed twice in cold downshock buffer (100 mM Mes/Tris pH 8, 5 mM Na_2HPO_4, 5 mM KH_2PO_4) to release compatible solutes synthesised or taken up during pre-cultivation, and resuspended in uptake buffer (100 mM MES/Tris pH 8, 0.9 M NaCl, 30 mM glucose, 30 mM urea, 30 mM KCl). Osmolalities of solutions were determined by freezing point depression (Osmomat 030, Gonotec, Berlin). Hypoosmotic shocks were conducted by dilution of substrate loaded cells in downshock buffer. 200 µl samples were filtered, washed with 3 ml isoosmotic buffer and measured by liquid scintillation (see 2.4.6).

2.5 Analytical methods

2.5.1 Determination of protein concentrations

Protein concentrations were determined with the Bio-Rad Protein Assay (Bio-Rad, München) using BSA as a standard.

2.5.2 SDS-PAGE and Western-Blot analysis

For separation of proteins by sodium-dodecyl-sulphate-polyacrylamide-gel-electrophoresis (SDS-PAGE) (Laemmli, 1970) protein solutions were mixed with 4 × sample buffer (400 mM Tris-HCl pH 6.7, 20% glycerol, 0.004% bromophenol blue, 4% (v/v) ß-mercaptoethanol, 4% SDS) and incubated for 10 min at 95°C. 12% separation gels (12 ml 30% acrylamide/bisacrylamide (Carl Roth, Karlsruhe), 7.5 ml separation gel buffer (1.5 M Tris-HCl, 8 mM Na_2EDTA, 0.4% SDS, pH 8.8), 10 ml H_2O, 15 µl TEMED, 300 µl 10% APS) combined with 6% stacking gels (2 ml 30% acrylamide/bisacrylamide, 2.5 ml stacking gel buffer (0.5 M Tris-HCl, 8 mM Na_2EDTA, 0.4% SDS, pH 6.8), 5.2 ml H_2O, 15 µl TEMED, 75 µl 10% APS) were used for separation. Separation was performed in separation buffer (3 g/l Tris, 14.4 g/l glycine, 5 g/l SDS) at 25 mA. Gels were stained with an aqueous solution of 0.2% Serva Blue G, 45% (v/v) methanol, and 10% (v/v) acetic acid and destained with 20% (v/v) ethanol plus 10% (v/v) acetic acid.

For Western-Blot analysis proteins were separated by SDS-PAGE and transferred to a Roti®-PVDF membrane (Carl Roth, Karlsruhe) by semi-dry blotting (Kyhse-Andersen, 1984) using a Hoefer SemiPhor™ TE77 transfer unit (GE Healthcare, Freiburg) with 10 mM CAPS pH 11 plus 10% (v/v) methanol as transfer buffer. Subsequently, the membrane was blocked in wash buffer (50 mM Tris-HCl pH 7.4, 0.9% NaCl) plus 5% milk powder for 1 h before murine 6×-His epitope tag antibody (Thermo Scientific, USA) was added (1:2000 (v/v)). After 1 h of incubation, the membrane was washed thrice with wash buffer and anti-mouse IgG alkaline phosphatase antibody (Sigma-Aldrich, USA) was added to the wash buffer (1:10000 (v/v)) and incubated for 1 h. After three further wash steps, 10 ml detection buffer (10 mM Tris-HCl pH 8.8) plus each 66 µl 5% NBT in 70% (v/v) dimethyl formamide and 2.5% BCIP in dimethyl formamide was added for detection.

2.5.3 Carbohydrate analysis via TLC

Thin-layer-chromatography (TLC) was applied for the qualitative analysis of carbohydrates in culture supernatants and of intracellular carbohydrates. ADAMANT silica gel 60 TLC plates (20 × 20 cm, Carl Roth, Karlsruhe) were used as stationary phase. If necessary, samples were desalted (Chromafix® PS-Mix, Macherey-Nagel, Düren) and concentrated by evaporation. For the analysis of intracellular carbohydrates, cells were separated from the medium and disrupted with isopropanol as described in 2.5.5. TLC plates were run up to twelve times in

pyridine/1-butanol/H_2O (30/70/10 (v/v/v)). Carbohydrates were visualised by spraying with 4% (v/v) H_2SO_4 in methanol followed by heating to 110°C. ^{14}C-labelled carbohydrates were visualised in a BAS-1800 imager (Fujifilm, Japan) after exposure of BAS-MP imager plates (Fujifilm, Japan) to the TLC plate for 2 – 5 days.

2.5.4 Quantitative analysis of carbohydrates and organic acids by HPLC

High-pressure liquid chromatography (HPLC) was used to determine the concentrations of carbohydrates and organic acids in culture supernatants. An Elite LaChrom system (Hitachi, Japan) equipped with UV- and refractive index detector was used. The stationary phase consisted of a ChromCart 30×4 mm Nucleogel® Sugar 810 H pre-column and a 300×7.8 mm Nucleogel® Sugar 810 H main-column (Macherey-Nagel, Düren) heated to 40°C. As mobile phase, 10 mM H_2SO_4 was used with a flow rate of 0.5 ml/min.

2.5.5 Quantitative analysis of trehalose using an enzymatic assay

To determine trehalose concentrations, a trehalase from *Rhodothermus marinus* described previously (Jorge *et al.*, 2007) was used. 20 µl of culture supernatants were mixed with 1 µl trehalase solution (for purification of the enzyme see 3.2.3), 29 µl H_2O, and 50 µl 100 mM bis-tris-propane buffer pH 7.6. After incubation for 3 h at 80 °C, the glucose released by the hydrolysis of trehalose was determined. Therefore, 20 µl of the trehalase pretreated sample was mixed with 50 µl 200 mM Tris-HCl pH 7.7 plus 2 mM $MgCl_2$, 10 µl 6 mM NADP, 10 µl 18 mM ATP, and 10 µl 1:20 diluted hexokinase/glucose-6-phosphate dehydrogenase solution (3 mg/ml, Roche, Mannheim). The absorption at 340 nm was recorded before and 20 min after the addition of the enzyme solution. Trehalose standards were treated equally to enable the calculation of trehalose concentrations.

To determine intracellular trehalose concentrations, 0.5 ml cell suspension was vacuum filtered using glass fibre prefilters (Millipore, USA) and washed twice with 1.5 ml 0.9% NaCl solution. To release intracellular trehalose, the filters were incubated in 70% (v/v) isopropanol for 30 min. The solvent was removed completely in a vacuum concentrator (Eppendorf, Hamburg) and the residue was redissolved in 150 µl H_2O before trehalose concentrations were determined as described above.

For the calculation of intracellular concentrations, a specific intracellular volume of 1.6 µl ×

mg^{-1} cdw (Botzenhardt, 2004) and a cell dry weight (cdw) concentration of 0.36 mg cdw × ml^{-1} × OD^{-1} were used.

2.5.6 Quantitative analysis of amino acids via HPLC

Amino acids in culture supernatants were measured on an Elite LaChrom HPLC system (Hitachi, Japan). Before injection, samples were derivatised with o-phthalaldehyde (OPA) (Thermo Scientific, USA). The stationary phase consisted of a RP18 Multospher 40×4 mm pre-column (CS-Chromatographie Service, Langerwehe) and a Nucleodur® RP-18 125×4 mm main column (Macherey-Nagel, Düren) heated to 35°C. Solvent A consisted of 40 mM sodium acetate, 0.06% sodium azide, 5% (v/v) methanol/acetonitrile (1/1, v/v). Solvent B consisted of methanol/acetonitrile (1/1, v/v). The solvent gradient was as follows: 0 – 8 min, 95 – 60% A, 8 – 11 min, 60 – 0% A, 11 – 12 min, 0% A, – 8 min, 95 – 60% A, 12 – 15 min, 0 – 95% A. The flow rate was adjusted to 0.8 ml/min. For fluorescence detection, an excitation wavelength of 230 nm and an emission wavelength of 455 nm were used.

2.5.7 Glycolipid extraction and analysis by TLC

For glycolipid extraction, cells from 50 ml of a *C. glutamicum* culture were washed twice with 0.9% NaCl-solution and successively extracted with 10 ml $CHCl_3$/CH_3OH (1:2, 1:1, and 2:1 (v/v)). The extracts were pooled and the solvent was removed in a rotary evaporator (RE-111 Rotavapor, Büchi, Switzerland). The crude glycolipid preparation was weighted and dissolved in $CHCl_3$/CH_3OH/H_2O (65:25:4 (v/v/v)) to a final concentration of 20 µg/µl. The sample constituents were separated on Durasil 25 TLC plates (Macherey-Nagel, Düren) in $CHCl_3$/CH_3OH/H_2O (65:25:4 (v/v/v)). For staining, the plate was sprayed with 0.2% anthrone in H_2SO_4 followed by heating to 110°C.

3 Results

3.1 The trehalose import system as a target for optimisation of *C. glutamicum* strains

C. glutamicum is industrially applied mainly for the production of amino acids (Becker & Wittmann, 2012) but genetic engineering has been used successfully to construct strains overproducing other high value or bulk products in a laboratory scale. Genetically modified strains have also been constructed that overproduce trehalose (Padilla *et al.*, 2004a; Carpinelli *et al.*, 2006). This non-reducing disaccharide can be used for different purposes like the cryoprotection of cells (Eroglu *et al.*, 2002; Barbas & Mascarenhas, 2009), stabilisation of enzymes during freeze-drying (Carpenter *et al.*, 1987), stabilisation of vaccines for long-term storage (Kim *et al.*, 2010b), or as a food additive (Patist & Zoerb, 2005).

The gene cluster *cg0830* – *cg0835* (*tus*-genes) has recently been shown to encode an ABC trehalose uptake system with high affinity (K_M = 0.16 µM) and low transport capacity (2.5 nmol × mg cdw^{-1} × min^{-1}) in *C. glutamicum* (Henrich, 2011). Preventing the reuptake and metabolisation of fermentation products has been used to construct strains with increased product formation in the past (Ikeda *et al.*, 1994; Ikeda & Katsumata, 1995). The trehalose uptake system of *C. glutamicum* is thus a potential target for strain optimisation and the effect of *tus*-gene deletion was examined in trehalose overproducing strains in this work. In spite of the presence of a trehalose uptake system, *C. glutamicum* is known to accumulate trehalose as a byproduct in the culture supernatant during bioreactor cultivation (Vallino & Stephanopoulos, 1993; Gourdon & Lindley, 1999; Wittmann & Heinzle, 2001). Since fermentation byproducts can hamper the purification of the product and can also reduce the product yield (Lee *et al.*, 2001; Bideaux *et al.*, 2006), the *tus*-gene expression during the cultivation of L-lysine producing *C. glutamicum* strains was examined in this work and it was attempted to reduce the accumulation of trehalose as a byproduct.

3.1.1 Trehalose recycling improves L-lysine production

To resolve the apparent contradiction of trehalose accumulation in spite of the presence of a trehalose uptake system in *C. glutamicum* and to evaluate the influence of trehalose

accumulation on amino acid production, trehalose transport was investigated in the L-lysine producing strains *C. glutamicum* DM1729 (pXMJ19) carrying an empty plasmid and *C. glutamicum* DM1729 (pXMJ19_*tus*) carrying a plasmid for the overexpression of the *tus*-genes. Both strains were cultivated in CgXII minimal medium in a bioreactor. When the initial amount of 4% glucose was consumed, another 4% was added. The OD_{600} and the concentrations of glucose, L-lysine, and trehalose in the supernatant were determined.

C. glutamicum DM1729 (pXMJ19) grew to a final OD_{600} of 107 ± 1.5 with a growth rate of 0.23 ± 0.07 h^{-1} (Figure 5). 37.2 ± 6.2 mM L-lysine were produced with a molar yield of 75.8 ± 18.0 mmol × mol^{-1} glucose. Trehalose mainly accumulated in the second half of the fermentation and reached a final concentration of 4.7 ± 2.1 mM.

Expression of the *tus*-genes during cultivation was examined in an mRNA hybridisation experiment. At different time points total cellular RNA was isolated and transcripts of *tusK*, *tusFG*, and *tusE* were visualised with DIG-11-labelled RNA probes (Figure 7). The transcription of all genes examined here was weak compared to the 16S RNA used as a control. *tusK* transcripts were not detectable at any time point while *tusFG* transcripts were clearly detectable only at the beginning of the cultivation. *tusE* transcripts were detected after 0 h and 6 h of cultivation but decreased below the detection limit afterwards. Therefore, the down-regulation of *tus*-gene expression seems to prevent trehalose reuptake during the fermentation, leading to the accumulation of trehalose in the culture broth.

Consequently, the influence of *tus*-gene overexpression on L-lysine production and trehalose accumulation was examined in *C. glutamicum* DM1729 (pXMJ19_*tus*) (Figure 6). The growth conditions were identical as for *C. glutamicum* DM1729 (pXMJ19). Overexpression of the *tus*-genes was induced by the addition of 1 mM IPTG to the medium. The growth rate was 0.22 ± 0.04 h^{-1} and the final OD_{600} was 103 ± 8. The final L-lysine and trehalose concentrations were 46.8 ± 2.8 mM and 0.57 ± 0.2 mM, respectively, and the molar L-lysine yield was 93.0 ± 1.1 mmol × mol^{-1} glucose.

In mRNA hybridisation experiments, transcripts of *tusK*, *tusFG*, and *tusE* were detectable at all time points for *C. glutamicum* DM1729 (pXMJ19_*tus*) (Figure 7). While the signal for *tusK* transcription was weak for the first three time points (0 h, 9 h, and 13 h) and increased afterwards, signals for *tusFG* and *tusE* transcripts were stronger at the beginning of the cultivation and slightly decreased after 9 h.

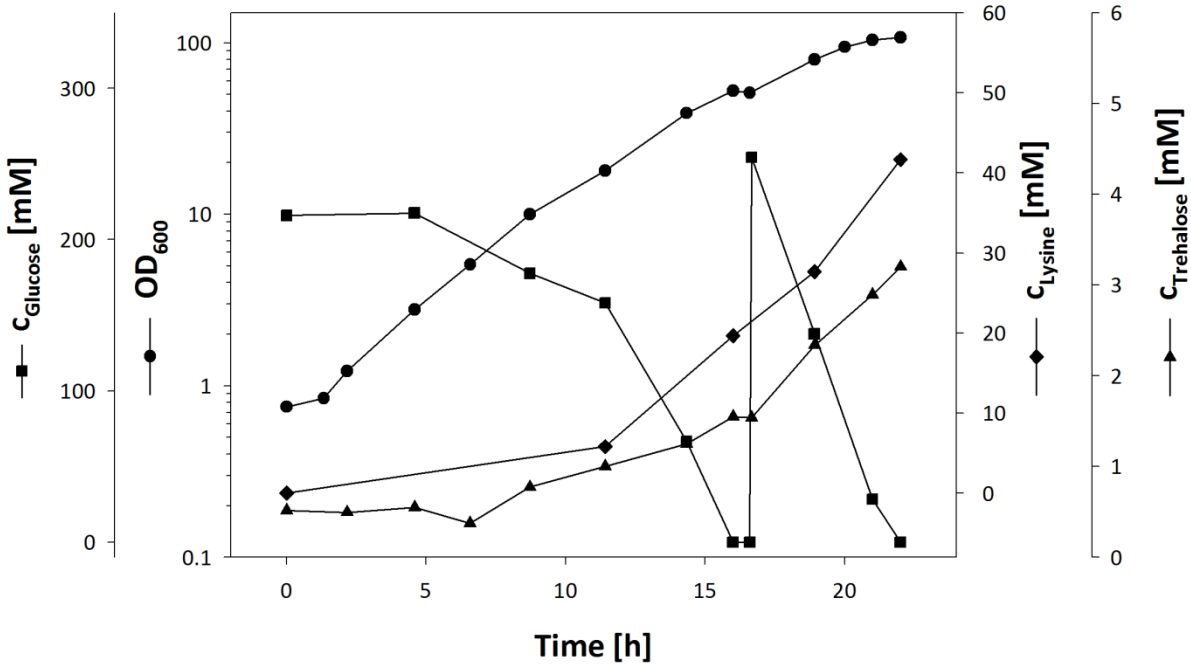

Figure 5: L-lysine production with *C. glutamicum* DM1729 (pXMJ19). 4% glucose was added as carbon source at the beginning of the cultivation and again after its depletion after 16.5 h. The experiment was performed in triplicate and the results of one representative fermentation are shown here.

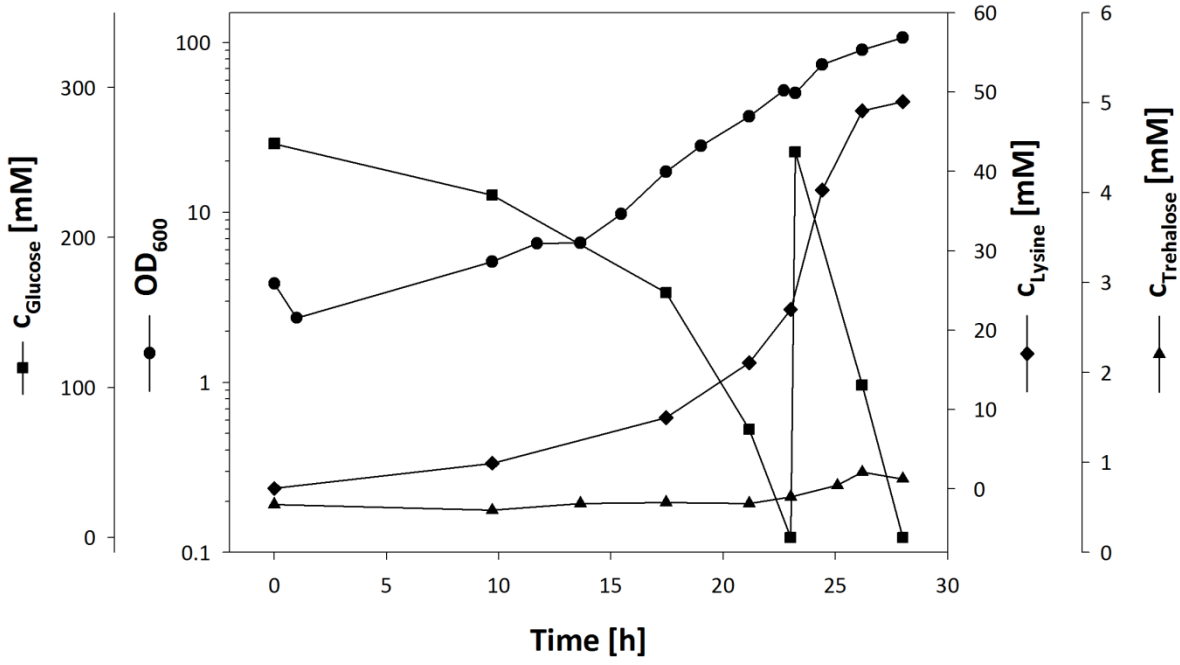

Figure 6: L-lysine production with *C. glutamicum* DM1729 (pXMJ19_tus). The plasmid encodes the tus-genes under the control of an IPTG-inducible promoter. The experiment was performed in triplicate and the results of one representative fermentation are shown here.

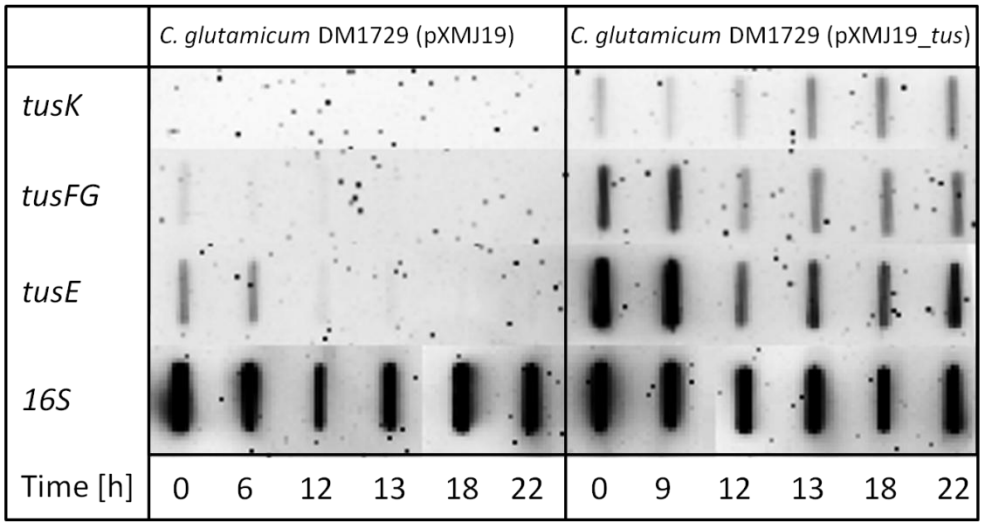

Figure 7: Analysis of *tus*-gene expression by RNA-hybridisation. Total RNA was isolated during bioreactor cultivation of *C. glutamicum* DM1729 (pXMJ19) and *C. glutamicum* DM1729 (pXMJ19_*tus*) at several time points (compare Figure 5 and 6) and transcripts of *tusK*, *tusFG*, and *tusE* were visualised with DIG-11-labelled RNA probes. 16S RNA was used as a control.

In conclusion, trehalose accumulated in the supernatant during the cultivation of *C. glutamicum* DM1729 (pXMJ19) because the expression of the *tus*-genes rapidly decreased under the conditions applied here. Overexpression of the *tus*-genes increased the amounts of the corresponding transcripts and led to a significant reduction of trehalose concentrations in the culture supernatant of *C. glutamicum* DM1729 (pXMJ19_*tus*). Furthermore, the average L-lysine yield for this strain was 23% higher than for the control strain.

3.1.2 Deletion of the *tus*-genes increases trehalose production

Genetically engineered *C. glutamicum* strains deficient in trehalose degradation can be applied for trehalose overproduction (Padilla *et al.*, 2004a; Padilla *et al.*, 2004b). The impact of trehalose recycling via the recently discovered trehalose uptake system (Henrich, 2011) on trehalose production has not been tested yet and was examined in this work.

For the construction of trehalose overproducing *C. glutamicum* strains, the *otsBA* operon from *E. coli* JM109 was amplified by PCR and ligated to pXMJ19 as described earlier (Padilla *et al.*, 2004a), resulting in the plasmid pXMJ19_$otsBA_{E.\ coli}$. *C. glutamicum* Δ*treS*, in which the trehalose synthase gene encoding the first enzyme in the trehalose degradation pathway is deleted, and *C. glutamicum* Δ*treS* Δ*tus*, in which also the gene cluster encoding the trehalose uptake system is deleted, were transformed with pXMJ19_$otsBA_{E.coli}$. *C. glutamicum* Δ*treS*

(pXMJ19_*otsBA*$_{E.coli}$) and *C. glutamicum* Δ*treS* Δ*tus* (pXMJ19_*otsBA*$_{E.coli}$) were cultivated with 2% sucrose and the OD_{600} and the intra- and extracellular trehalose concentrations were determined during growth (Figure 8).

C. glutamicum Δ*treS* (pXMJ19_*otsBA*$_{E.coli}$) grew with a rate of 0.43 ± 0.01 h^{-1} to a final OD_{600} of 32.9 ± 1.4 while the growth rate and the final OD_{600} for *C. glutamicum* Δ*treS* Δ*tus* (pXMJ19_*otsBA*$_{E.coli}$) were 0.40 ± 0.01 h^{-1} and 29.1 ± 1.9, respectively. The time course of the intracellular trehalose concentration was similar for both strains. Constant levels of 17 mM (*C. glutamicum* Δ*treS* (pXMJ19_*otsBA*$_{E.coli}$)) and 25 mM (*C. glutamicum* Δ*treS* Δ*tus* (pXMJ19_*otsBA*$_{E.coli}$)), respectively, were detected within the first 5 h of cultivation, which increased to 35 ± 3 mM and 34 ± 3 mM after 8 h. These values dropped to 17 ± 1 mM after 24 h for *C. glutamicum* Δ*treS* (pXMJ19_*otsBA*$_{E.coli}$), and was even lower for *C. glutamicum* Δ*treS* Δ*tus* (pXMJ19_*otsBA*$_{E.coli}$) (9 ± 2 mM). For both strains, the extracellular trehalose concentration increased steadily within the first 8 h to 1.94 ± 0.2 mM and 2.99 ± 0.14 mM.

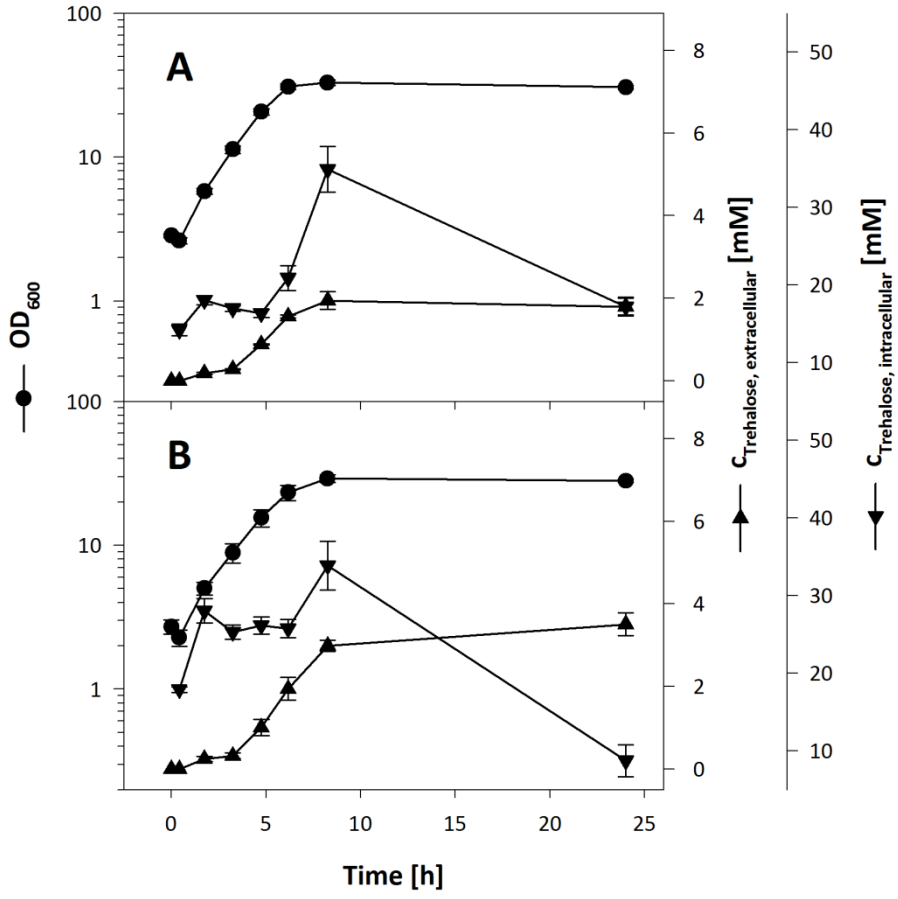

Figure 8: Trehalose overproduction in *C. glutamicum* Δ*treS* (pXMJ19_*otsBA*$_{E. coli}$) (A) and *C. glutamicum* Δ*treS* Δ*tus* (pXMJ19_*otsBA*$_{E. coli}$) (B). 2% sucrose was used as carbon source. For induction, 100 µM IPTG was added to the medium.

It remained constant afterwards for *C. glutamicum* Δ*treS* (pXMJ19_$otsBA_{E.coli}$) but further increased to 3.50 ± 0.28 mM for *C. glutamicum* Δ*treS* Δ*tus* (pXMJ19_$otsBA_{E.coli}$) after 24 h. Calculating the total amounts of trehalose produced intra- and extracellularly by each strain, *C. glutamicum* Δ*treS* Δ*tus* (pXMJ19_$otsBA_{E.coli}$) produced 40% more trehalose (3.65 ± 0.32 mM, $Y_{P/S}$ = 62.5 mmol × mol^{-1} sucrose) than the control strain (2.61 ± 0.30 mM, $Y_{P/S}$ = 44.7 mmol × mol^{-1} sucrose). This shows that the deletion of the *tus*-genes is beneficial for the production of trehalose in *C. glutamicum* strains.

3.2 Investigation of trehalose export in *C. glutamicum*

The cell wall of *C. glutamicum* contains a trehalose glycolipid bilayer similar to the outer membrane of Gram-negative bacteria (Puech *et al.*, 2001). The incorporation of external trehalose into these glycolipids has been found to be independent of trehalose uptake in *C. glutamicum* and is therefore assumed to take place in the periplasmic space (Henrich, 2011). In consequence, trehalose synthesised in the cytosol via either of three pathways (Wolf *et al.*, 2003) has to be exported to the periplasm. Furthermore, genetically engineered *C. glutamicum* strains accumulate high amounts of trehalose in the culture supernatant. For example, *C. glutamicum* Δ*mluI*/pLPI*galUotsBA*01 has been reported to accumulate 29 mM trehalose in the supernatant using 555 mM glucose as a substrate (Padilla *et al.*, 2004b). An unknown trehalose export system is thus assumed to be present in *C. glutamicum*. However, trehalose export in *C. glutamicum* has not been shown biochemically so far.

Trehalose excretion was thus investigated both qualitatively and quantitatively in this work. Therefore, a suitable *C. glutamicum* test strain had to be constructed and analytical methods had to be established for the sensitive, specific, and quantitative detection of intra- and extracellular trehalose. The contribution of several transport proteins to trehalose export was then examined.

3.2.1 Construction of a test strain for the investigation of trehalose excretion

In *C. glutamicum*, trehalose can be produced via three different pathways (Wolf *et al.*, 2003). While the OtsAB-pathway and the TreYZ-pathway each synthesise trehalose in two steps from activated precursors, trehalose synthesis is also possible by the TreS-catalysed isomerisation of maltose, which can be taken up into the cell by an ABC transporter (Henrich, 2011). TreS is also the first enzyme for trehalose degradation in *C. glutamicum,* which then proceeds via the TreX- or MalQ-pathways (Henrich, 2011). To study trehalose excretion, maltose was chosen as substrate for trehalose production via the TreS-pathway. Therefore, a strain was needed that does not degrade maltose. The genes *treX* and *malQ* were thus deleted in *C. glutamicum*. In addition, the genes encoding the trehalose uptake system were deleted to prevent the reuptake of exported trehalose, resulting in the strain *C. glutamicum* Δ*malQ* Δ*treX* Δ*tus*. As a control strain, *C. glutamicum* Δ*malQ* Δ*treX* Δ*treS* was constructed by the deletion of *treS* in *C. glutamicum* Δ*malQ* Δ*treX. C. glutamicum* and both

mutant strains were examined in growth experiments in CgC minimal medium using glucose plus maltose or glucose plus trehalose as carbon sources (Figure 9).

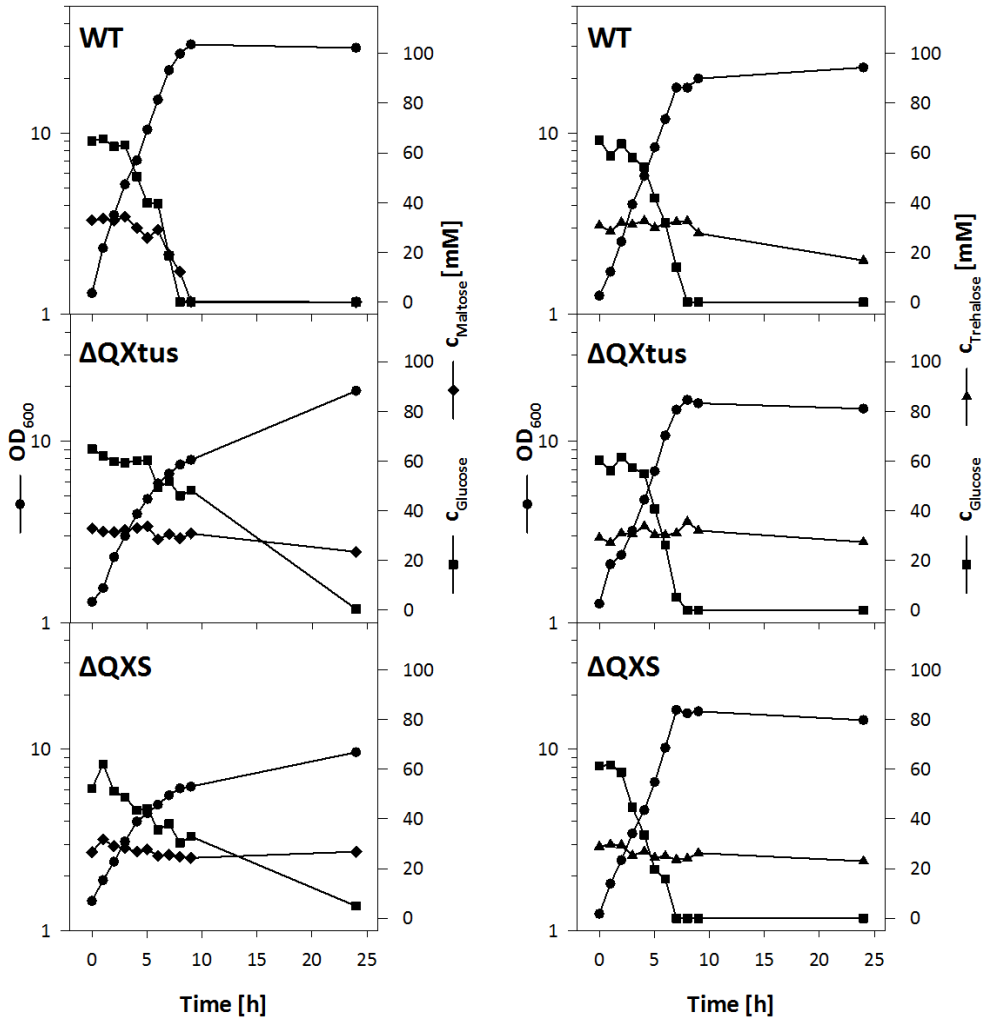

Figure 9: Growth of *C. glutamicum* (WT), *C. glutamicum* Δ*malQ* Δ*treX* Δ*tus* (ΔQXtus), and *C. glutamicum* Δ*malQ* Δ*treX* Δ*treS* (ΔQXS) on 1% glucose plus 1% maltose (left panel) or 1% glucose plus 1% trehalose (right panel).

While *C. glutamicum* could use all three substrates for growth, *C. glutamicum* Δ*malQ* Δ*treX* Δ*tus* as well as *C. glutamicum* Δ*malQ* Δ*treX* Δ*treS* only used glucose within 24 h. Further, the growth rates for both mutant strains were reduced to 0.20 h^{-1} in the presence of maltose and glucose compared to 0.39 h^{-1} for *C. glutamicum*. The specific glucose consumption rate was also reduced from 26.0 µmol × mg^{-1} cdw × h^{-1} for *C. glutamicum* to 12.3 µmol × mg^{-1} cdw × h^{-1} and 16.4 µmol × mg^{-1} cdw × h^{-1} for *C. glutamicum* Δ*malQ* Δ*treX* Δ*tus* and *C. glutamicum* Δ*malQ* Δ*treX* Δ*treS*, respectively (Figure 9). In contrast to *C. glutamicum*, the culture supernatants of both mutants showed a brownish colour after 24 h (Figure 10). Using

glucose plus trehalose as substrates, the growth rates of the two mutant strains were only slightly reduced to 0.35 h^{-1} compared to 0.38 h^{-1} for *C. glutamicum*. All strains completely consumed the added glucose within 8 h while trehalose consumption was only observed for *C. glutamicum*.

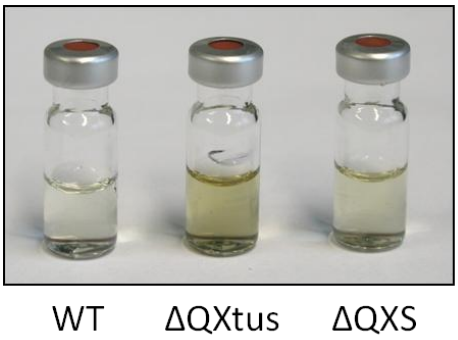

Figure 10: Culture supernatants of *C. glutamicum* (WT), *C. glutamicum* Δ*malQ* Δ*treX* Δ*tus* (ΔQXtus) and *C. glutamicum* Δ*malQ* Δ*treX* Δ*treS* (ΔQXS). Cells were cultivated in minimal medium containing glucose plus maltose for 24 h.

In conclusion, *C. glutamicum* Δ*malQ* Δ*treX* Δ*tus* and *C. glutamicum* Δ*malQ* Δ*treX* Δ*treS* were successfully constructed. As expected, both strains were no longer able to use maltose or trehalose as co-substrates for growth. In the presence of maltose, growth of both strains and the consumption of glucose were impaired.

3.2.2 Radiochemical analysis of trehalose excretion by *C. glutamicum* Δ*malQ* Δ*treX* Δ*tus*

C. glutamicum Δ*malQ* Δ*treX* Δ*tus*, *C. glutamicum* Δ*malQ* Δ*treX* Δ*treS*, and *C. glutamicum* Δ*mus* were then used to study trehalose excretion. [^{14}C]-labelled maltose was used as substrate to study the uptake of maltose, the intracellular conversion of maltose to trehalose, and the excretion of trehalose. *C. glutamicum* Δ*malQ* Δ*treX* Δ*treS* was used as a control strain since this strain is not able to isomerise maltose to trehalose. *C. glutamicum* Δ*mus*, which lacks the genes encoding the maltose uptake system, was used as a control to exclude the extracellular conversion of maltose to trehalose. All strains were cultivated in 2TY, harvested during the exponential growth phase, washed twice and resuspended in 10 mM KH_2PO_4/K_2HPO_4 buffer pH 6.8. 300 µM labelled maltose was added and the cells were incubated for 5 h at 30°C. Samples were taken after several time points to determine the total radioactivity and the intracellular amount of substrate. Supernatants as well as cell extracts were analysed via TLC.

C. glutamicum Δ*malQ* Δ*treX* Δ*tus* and *C. glutamicum* Δ*malQ* Δ*treX* Δ*treS* completely imported the substrate within 50 min with similar uptake rates (11.2 ± 2.7 nmol × mg^{-1} cdw × min^{-1} and 11.9 ± 3.5 nmol × mg^{-1} cdw × min^{-1}, respectively) while *C. glutamicum* Δ*mus* did not import any maltose even after prolonged incubation (Figure 11).

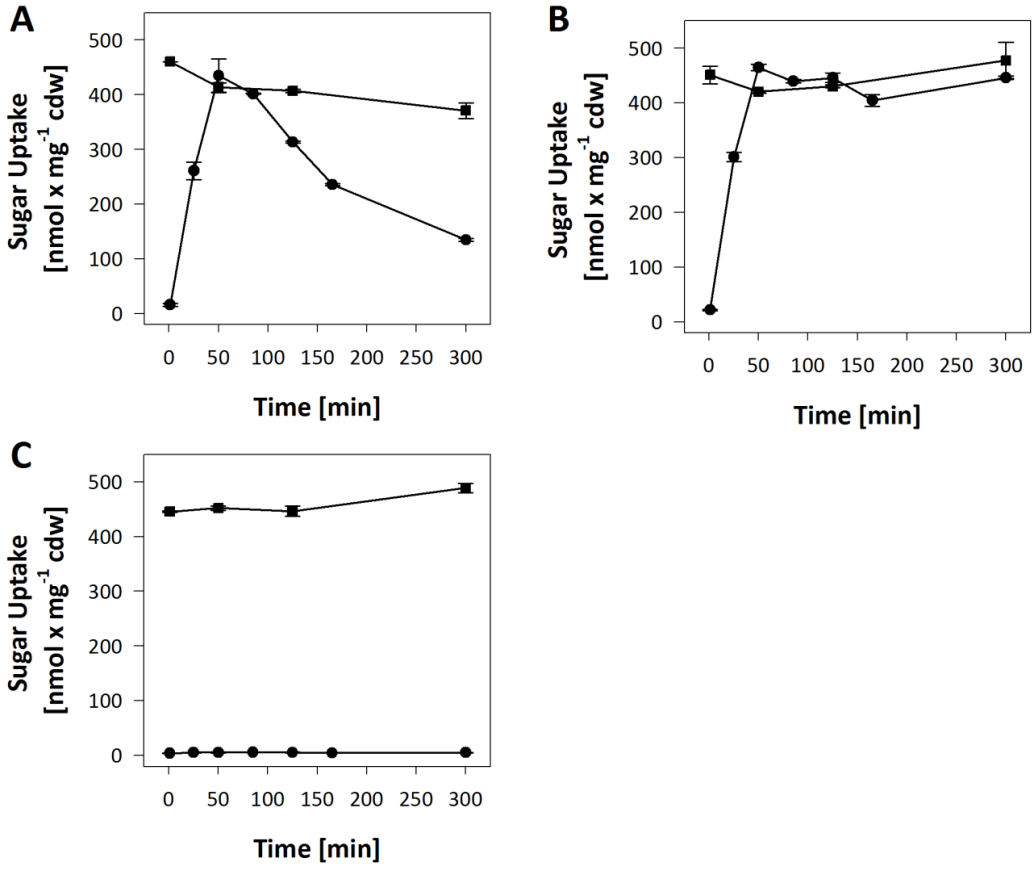

Figure 11: Trehalose export experiment with [^{14}C]-maltose as substrate. 300 µM [^{14}C]-labelled maltose was added at 0 min and the time courses of the intracellular amount of radiolabel (●) and of the total amount of radiolabel (■) were recorded for *C. glutamicum* Δ*malQ* Δ*treX* Δ*tus* (A), *C. glutamicum* Δ*malQ* Δ*treX* Δ*treS* (B), and *C. glutamicum* Δ*mus* (C).

After the substrate was depleted, the intracellular amount of sugar remained constant for *C. glutamicum* Δ*malQ* Δ*treX* Δ*treS* but decreased from 435 ± 31 nmol × mg cdw^{-1} to 135 ± 3 nmol × mg^{-1} cdw after 300 min for *C. glutamicum* Δ*malQ* Δ*treX* Δ*tus*. Assuming that trehalose is the only labelled metabolite excreted in the experiment, this corresponds to a trehalose excretion rate of 1.23 ± 0.09 nmol × mg^{-1} cdw × min^{-1}. Unexpectedly, the total radioactivity decreased by 19% for *C. glutamicum* Δ*malQ* Δ*treX* Δ*tus* within 300 min but remained stable for the other strains.

In *C. glutamicum* Δ*malQ* Δ*treX* Δ*tus* the intracellular ratio of maltose to trehalose was not

known. To examine whether TreS efficiently catalysed the formation of trehalose from maltose in the cytosol, cells were separated from the medium by filtration, washed, and disrupted in 70% isopropanol. The samples were concentrated and analysed via TLC (Figure 12). Intracellular trehalose and maltose were detected after 50 min, 80 min, and 110 min for *C. glutamicum* Δ*malQ* Δ*treX* Δ*tus*. *C. glutamicum* Δ*malQ* Δ*treX* Δ*treS* accumulated maltose in the cells but did not produce trehalose. No other compound than maltose or trehalose was detected in the cell extracts.

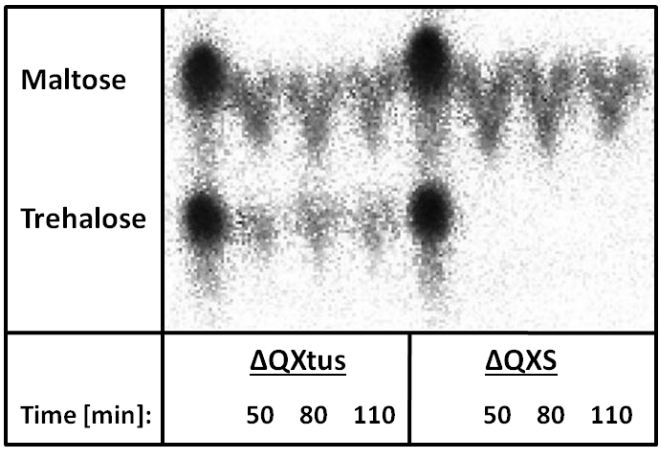

Figure 12: Separation of [^{14}C]-labelled intracellular sugars via TLC. *C. glutamicum* Δ*malQ* Δ*treX* Δ*tus* (ΔQXtus) and *C. glutamicum* Δ*malQ* Δ*treX* Δ*treS* (ΔQXS) were cultivated in the presence of 300 µM [^{14}C]-maltose and samples were taken at various time points.

The experiments shown above prove that maltose is taken up and converted to trehalose by TreS in the cytosol. To investigate whether trehalose can also be excreted from the cytosol, culture supernatants from the experiment shown in Figure 11 were analysed via TLC (Figure 13). At the beginning of the experiment, maltose was present in the samples of all three strains. For *C. glutamicum* Δ*malQ* Δ*treX* Δ*tus,* the substrate was depleted after 50 min and after 300 min, a substance with identical retention as trehalose was detected in the supernatant. *C. glutamicum* Δ*malQ* Δ*treX* Δ*treS* also imported the substrate completely but no trehalose was excreted. *C. glutamicum* Δ*mus* neither imported [^{14}C]-maltose nor formed trehalose from extracellular substrate. Two weak spots, of which one migrated slightly faster and one slightly slower than maltose, were detected in all supernatants. Since these spots were already present in all samples after 1 min of incubation and even in the maltose standard solution, they were contaminations with unknown identity from the [^{14}C]-substrate solution.

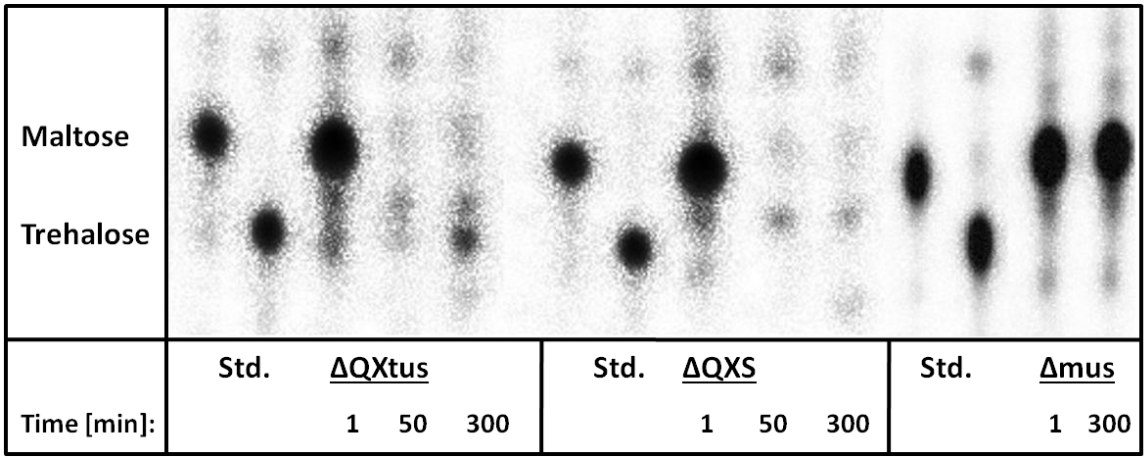

Figure 13: TLC analysis of culture supernatants with [^{14}C]-maltose as substrate. ΔQXtus: *C. glutamicum* Δ*malQ* Δ*treX* Δ*tus;* **ΔQXS***: C. glutamicum ΔmalQ ΔtreX ΔtreS;* **Δmus:** *C. glutamicum* Δ*mus*; **Std**.: Maltose and trehalose standards. Samples were taken from the experiment shown in Figure 11. Prior to TLC analysis, samples were desalted and concentrated as described in the methods section.

In conclusion, these experiments show that trehalose is exported by *C. glutamicum* Δ*malQ* Δ*treX* Δ*tus* after the uptake of maltose and the TreS-dependent conversion to trehalose. Maltose and trehalose were clearly detectable in cell extracts of this strain. Control strains lacking TreS or the maltose uptake system were not able to produce trehalose.

However, it was not possible to determine the exact trehalose export rate in this experiment. The total radioactivity decreased, indicating active metabolism and the formation of CO_2 from labelled maltose. Further, the generation of trehalose from unlabelled precursors in the cell could not be excluded in the experiment, which would alter the ratio of labelled to unlabelled substrate. Hence, a quantitative analysis of trehalose concentrations in the supernatant was necessary to determine the exact rate of trehalose excretion.

3.2.3 Enzymatic assay for quantitative trehalose detection

To further characterise trehalose export, a quantification of trehalose concentrations in the cytosol and in culture supernatants of *C. glutamicum* strains was needed. HPLC analysis was not suitable for this purpose since maltose was used as substrate for trehalose production and the separation of maltose and trehalose was not possible with the available equipment. An enzymatic assay was developed here as an alternative. Trehalases are enzymes that catalyze trehalose hydrolysis yielding two molecules of glucose per molecule of trehalose.

Glucose can then be phosphorylated and oxidised to 6-phosphogluconolactone by hexokinase and glucose-6-phosphate dehydrogenase. The concomitant reduction of NADP to NADPH can be detected photometrically at 340 nm. The reaction scheme is depictured in Figure 14.

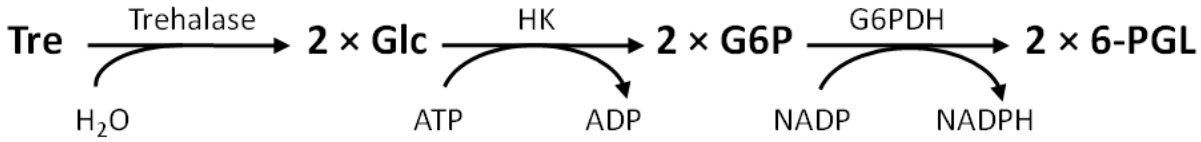

Figure 14: Enzymatic assay for the determination of trehalose concentrations. Tre: Trehalose; **Glc**: glucose; **G6P**: glucose-6-phosphate; **6-PGL**: 6-phosphogluconolactone; **HK**: hexokinase; **G6PDH**: glucose-6-phosphate dehydrogenase.

A plasmid encoding a trehalase cloned from the thermophilic bacterium *Rhodothermus marinus* (Jorge *et al.*, 2007) was provided by the authors. The gene was overexpressed in *E. coli* BL21 (DE3) and the protein carrying a C-terminal His_6-tag was purified via IMAC and SEC. SDS-PAGE and Western-blot analysis showed that the protein was purified to near homogeneity (Figure 15). SEC elution fractions were collected, 20% glycerol (final concentration) was added and aliquots were stored at -80°C.

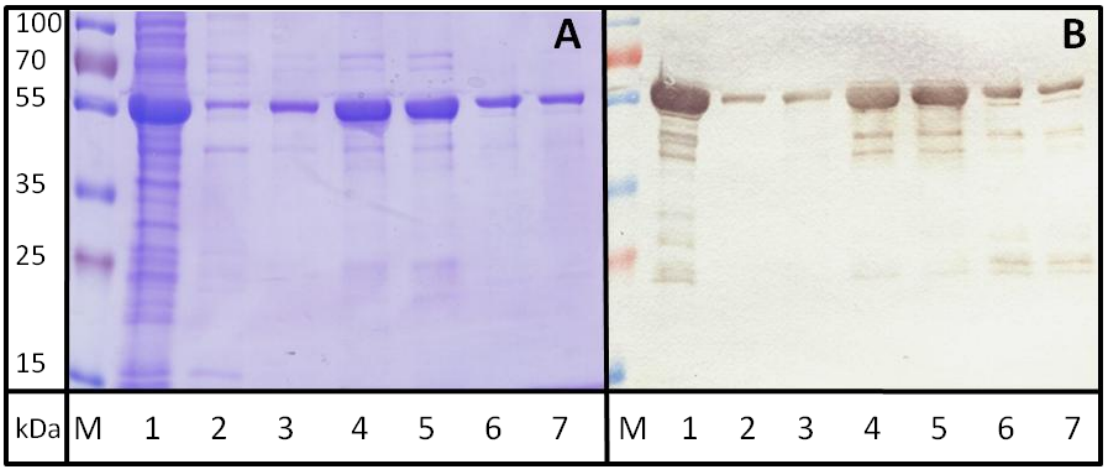

Figure 15: Purification of trehalase after overproduction in *E. coli*. A: SDS-PAGE analysis; **B:** Western-blot analysis (anti-His_6); **M:** Protein marker; **1:** cell lysate; **2 – 5:** IMAC elution fractions; **6 – 7:** SEC elution fractions. Elution fractions 3, 4, and 5 were pooled, concentrated by filtration (30 kDa cut-off) and further purified via SEC using 20 mM Tris-HCl buffer pH 7.6. Fractions 6 and 7 were used for enzymatic determination of trehalose concentrations.

An enzymatic assay using purified trehalase for trehalose detection was established (see 2.5.5). Results of the enzymatic measurement of trehalose standards are shown in Figure 16. A linear correlation of the absorption difference at 340 nm for samples containing 0.1 mM to 5 mM trehalose was obtained. Importantly, maltose was not a substrate for the enzyme.

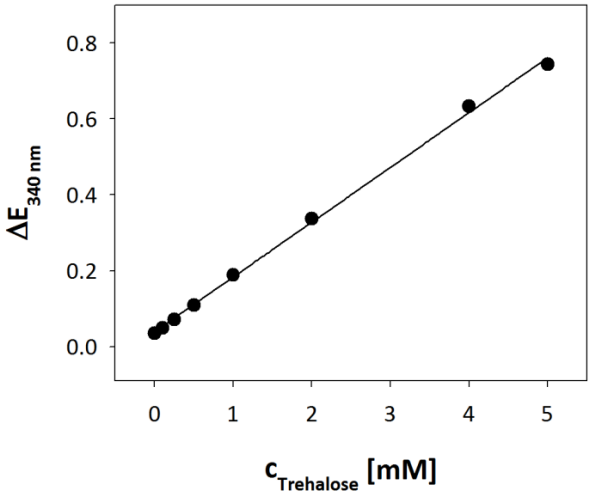

Figure 16: Enzymatic assay for trehalose quantification. Trehalose standards were incubated in the presence of purified trehalase at 80°C for 3 h and the liberated glucose was detected enzymatically. $\Delta E_{340\,nm}$ is the change of absorbance at 340 nm caused by NADP reduction.

3.2.4 Quantitative analysis of trehalose excretion

To determine the rate of trehalose release in *C. glutamicum* Δ*malQ* Δ*treX* Δ*tus*, the strain was pre-cultivated in minimal medium plus 2% glucose. When all glucose was consumed, maltose was added to start the production of trehalose. The concentration of trehalose in the supernatant was determined enzymatically. *C. glutamicum* Δ*malQ* Δ*treX* Δ*treS* was used as negative control since this strain does not convert maltose to trehalose.

C. glutamicum Δ*malQ* Δ*treX* Δ*tus* consumed all glucose within 10 h and grew to an OD_{600} of 28.7 ± 0.6 (Figure 17 A). After the addition of maltose, the OD_{600} further increased to 48.3 ± 0.3 after 23 h. 5.22 ± 0.27 mM trehalose were detected after 51.5 h corresponding to a yield of 0.19 ± 0.01 mol × mol^{-1} maltose. Trehalose accumulated with a constant rate of 0.19 ± 0.01 nmol × mg^{-1} cdw × min^{-1} for 21.5 h after the addition of maltose. *C. glutamicum* Δ*malQ* Δ*treX* Δ*treS* grew to a similar OD_{600} with glucose as substrate but no further increase of the OD_{600} was observed after the addition of maltose. This strain did not produce significant amounts of trehalose from maltose (Figure 17 B).

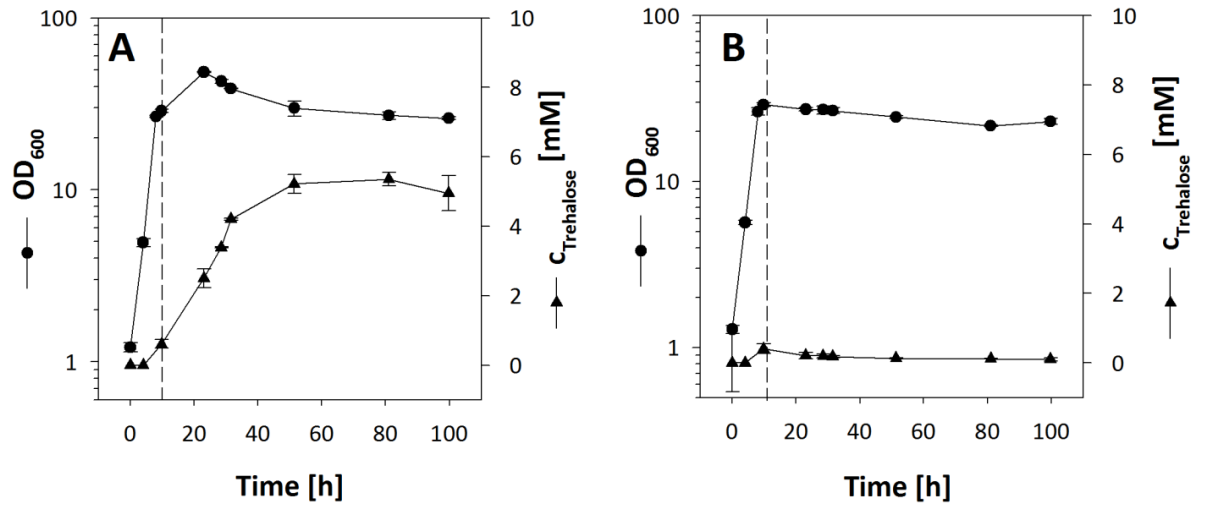

Figure 17: Trehalose export by *C. glutamicum* Δ*malQ* Δ*treX* Δ*tus* (A) and *C. glutamicum* Δ*malQ* Δ*treX* Δ*treS* (B). Cells were cultivated in minimal medium with 100 mM glucose. The dashed lines indicate the addition of 29 mM maltose after 10 h.

3.2.5 Contribution of mechanosensitive channels to the excretion of trehalose

Mechanosensitive channels are passive transport systems that are responsible for the release of osmotically active solutes under hypoosmotic conditions (Martinac *et al.*, 1987). In *E. coli*, these transporters have been linked to the export of metabolites like glutamate, trehalose, lactose, and ATP from cells subjected to hypoosmotic conditions (Berrier *et al.*, 1992; Schleyer *et al.*, 1993). Two mechanosensitive channels have been described in *C. glutamicum,* MscL and MscCG (Ruffert *et al.*, 1999). To test a possible contribution of these channels to the accumulation of trehalose in the culture broth during cultivation of *C. glutamicum*, the strain *C. glutamicum* Δ*malQ* Δ*treX* Δ*mscL* Δ*yggB* was constructed, which lacks the two genes coding for mechanosensitive channels and which is also deficient in maltose degradation. After growth of this strain in minimal medium plus 2% glucose and addition of 1% maltose as substrate for trehalose production, trehalose accumulation in the supernatant with a rate of 0.13 nmol × mg cdw^{-1} × min^{-1} was detected. Since this rate was similar for *C. glutamicum* Δ*malQ* Δ*treX* Δ*tus* (0.19 nmol × mg^{-1} cdw × min^{-1}), it can be concluded that trehalose release to the medium occurred independent of the function of MscCG and MscL under the conditions applied here.

To test for the contribution of so far unidentified mechanosensitive channels to trehalose excretion in *C. glutamicum* Δ*malQ* Δ*treX* Δ*tus*, the release of trehalose after hypoosmotic shocks was tested. Under these conditions, compatible solutes like glycine betaine are

released from the cell by the opening of mechanosensitive channels (Ruffert *et al.*, 1997). Cells were loaded with 300 µM [^{14}C]-maltose in the presence of 250 µM glycine betaine to induce intracellular trehalose accumulation. As a control, the uptake of 250 µM [^{14}C]-labelled glycine betaine in the presence of 300 µM maltose was measured in a parallel experiment. When cells were exposed to a hypoosmotic shock from 1790 mOsmol × kg^{-1} to 280 mOsmol × kg^{-1}, the combined intracellular amount of maltose and trehalose (which cannot be distinguished here, compare Figure 12) was only slightly reduced from 169 nmol × mg^{-1} cdw to 146 nmol × mg^{-1} cdw (Figure 18).

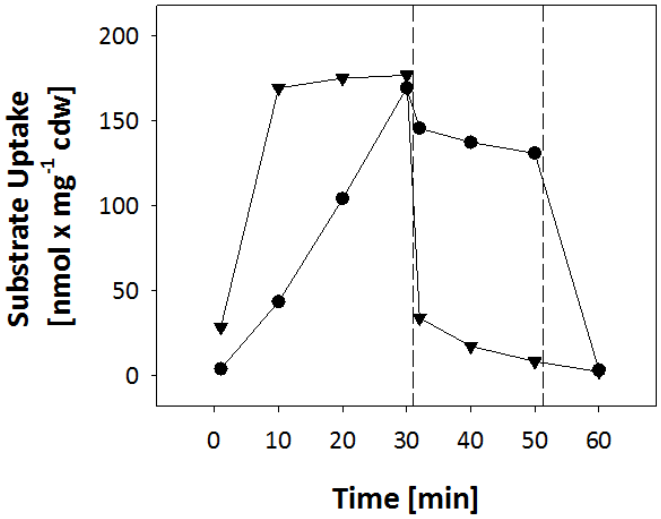

Figure 18: Metabolite excretion after hypoosmotic shocks. Cells were incubated in the presence of 250 µM glycine betaine and 300 µM maltose in both experiments. Either [^{14}C]-maltose (●) or [^{14}C]-glycine betaine (▼) was used. Opening of mechanosensitive channels was triggered by performing an osmotic downshock from 1790 mOsmol × kg^{-1} to 280 mOsmol × kg^{-1} after 31 min (first dashed line). After 51 min 0.1% CTAB was added (second dashed line).

The drop of the amount of intracellular substrate to 3 nmol × mg^{-1} cdw after the addition of 0.1% CTAB confirmed that the labelled substrate was not metabolised to immobile products during the experiment. The excretion of [^{14}C]-labelled glycine betaine in the control experiment confirmed the opening of osmoregulated channels under the experimental conditions (Figure 18).

The experiments described here show that mechanosensitive channels do not release trehalose after hypoosmotic shocks in *C. glutamicum* and that MscCG and MscL are not responsible for trehalose excretion during shake flask cultivation.

3.2.6 Contribution of putative sugar export systems to the excretion of trehalose

C. glutamicum has been shown to release trehalose to the medium in the experiments described above. Since mechanosensitive channels were excluded as an unspecific trehalose export mechanism, carrier-mediated export seemed likely. The physiological function of metabolite export in bacteria is not understood in most cases and sugar export has only been investigated in a few cases. A family of three proteins named SetA, B and C (sugar efflux transporter) catalysing the export of arabinose and β-galactosides like lactose and IPTG has been described in *E. coli* (Liu *et al.*, 1999a; Koita & Rao, 2012). Also, *ydeA* is known to encode an export protein for arabinose and IPTG in *E. coli* (Carolé *et al.*, 1999). A single trehalose exporter is known in insects, where this sugar serves as carbon capacitor and can be exported from fat cells to the haemolymph (Sakurai *et al.*, 2008). The sequences of these proteins were used as queries in BLASTP searches (Altschul *et al.*, 1997) to identify candidate genes encoding sugar transporters in *C. glutamicum* by Natalie Brühl (unpublished data) (Table 4).

Table 4: Identification of genes putatively encoding sugar export proteins in *C. glutamicum*. BLASTP searches were conducted with gene sequences of previously described sugar efflux transporters as query (Natalie Brühl, unpublished data).

Gene (annotation, family)	*C. glutamicum* homologues (score, E-value)
mdtD (putative arabinose efflux transporter, MFS)	*cg0206* (194 bit, 1^{-50}), *cg1399* (161 bit, 6^{-41}), *cg1289* (160 bit, 2^{-40}), *cg2893* (132 bit, 5^{-32}), *cg2739* (127 bit, 1^{-30})
kgtP (alpha-ketoglutarate transporter, MFS)	*cg3226* (176 bit, 2^{-45}), *cg3395* (176 bit, 3^{-45}), *cg0501* (145 bit, 5^{-36}), *cg0340* (130 bit, 2^{-31})
ydhP (predicted transporter, MFS)	*cg0772* (214 bit, 7^{-57}), *cg3334* (72 bit, 4^{-14})
setA (sugar efflux transporter, MFS)	*cg3245* (32 bit, 0.052)
setB (sugar efflux transporter, MFS)	*cg1212* (35 bit, 0.009), *cg2739* (31 bit, 0.08)
setC (sugar efflux transporter, MFS)	*cg1212* (35 bit, 0.005)
mhpT (predicted 3-hydroxyphenyl-propionic acid transporter, MFS)	*cg3353* (121 bit, 5^{-29}), *cg2618* (116 bit, 2^{-27}), *cg3301* (99 bit, 5^{-22})
yebQ (predicted transporter, MFS)	*cg1399* (175 bit, 4^{-45}), *cg1289* (166 bit, 2^{-42}), *cg2893* (138 bit, 1^{-33}), *cg2971* (123 bit, 2^{-29}), *cg0206* (104 bit, 7^{-24}), *cg1526* (103 bit, 1^{-23})
ydhC (putative arabinose efflux transporter, MFS)	*cg3038* (114 bit, 6^{-27})
ynfM (putative arabinose efflux transporter, MFS)	*cg3240* (268 bit, 3^{-73})
ydeA (arabinose efflux transporter, MFS)	*cg3334* (102 bit, 2^{-23}), *cg0772* (100 bit, 2^{-22}), *cg3245* (42 bit, 6^{-5})
TRET1 (*Anopheles gamibiae*, facilitated trehalose transporter, MFS)	*cg0223* (139 bit, 2^{-34})

The best hits for each query were selected and a total of 23 genes were inactivated in the trehalose excreting test strain, *C. glutamicum* Δ*malQ* Δ*treX* Δ*tus*, in this work. The inactivation of genes encoding trehalose export systems was expected to deteriorate its rate of export. The resulting strains were thus grown on 2% glucose as substrate and 1% maltose was added as substrate for trehalose production after glucose depletion. Trehalose concentrations were determined in the supernatants to calculate trehalose accumulation rates (Figure 19). Compared to the parental strain, *C. glutamicum* Δ*malQ* Δ*treX* Δ*tus*, none of the strains tested released trehalose with a significantly reduced rate. The sole exception was *C. glutamicum* Δ*malQ* Δ*treX* Δ*tus* IM*cg2893*, which no longer excreted trehalose. This mutant was analysed in more detail (section 3.2.7).

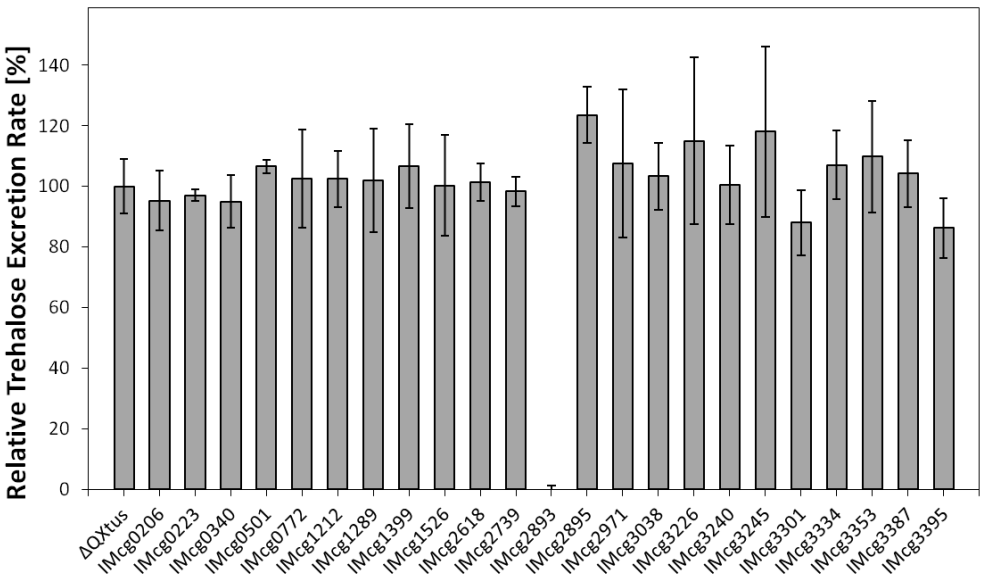

Figure 19: Trehalose excretion rates after inactivation of putative sugar exporters. Candidate genes were inactivated in *C. glutamicum* Δ*malQ* Δ*treX* Δ*tus* (ΔQXtus). The trehalose excretion rates of the mutant strains were determined after the addition of maltose as substrate (see 0) and are depictured as relative values with the excretion rate of the parental strain set to 100%.

3.2.7 Investigation of trehalose excretion in *C. glutamicum* Δ*malQ* Δ*treX* Δ*tus* IM*cg2893*

The gene *cg2893* encodes a permease of the major facilitator superfamily (MFS). The gene locus is shown in Figure 20. The genes *cg2893*, *cg2894*, and *cg2895* are transcribed in the same direction, while *poxB* and *cg2896*, which lie up- and downstream, respectively, are transcribed in the reverse direction. The genes *cg2893* and *cg2894* overlap by 10 nucleotides and *cg2894* and *cg2895* are only separated by 17 nucleotides. Hence, *cg2893*, *cg2894*, and

cg2895 possibly form an operon of co-transcribed genes. Like *cg2893*, *cg2895* encodes a MFS permease while *cg2894* encodes a TetR-type transcriptional regulator.

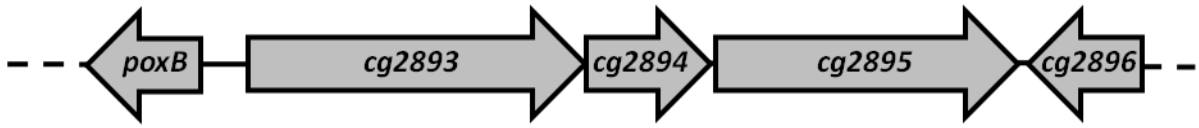

Figure 20: Gene cluster *cg2893* – *cg2895*. *poxB* encodes pyruvate dehydrogenase, *cg2893* and *cg2895* encode MFS-type permeases, *cg2894* encodes a TetR-type regulator protein and *cg2896* encodes an endoglucanase.

C. glutamicum Δ*malQ* Δ*treX* Δ*tus* IM*cg2893* no longer accumulated trehalose in the culture supernatant using maltose as substrate (see Figure 19). Growth of this mutant in minimal medium plus glucose was nearly absent and the cells aggregated during cultivation (Figure 21). Analysis of the culture supernatants via TLC (Figure 22) after the addition of maltose to *C. glutamicum* Δ*malQ* Δ*treX* Δ*tus* IM*cg2893* revealed that maltose consumption was also impaired in comparison to *C. glutamicum* Δ*malQ* Δ*treX* Δ*tus*, which completely consumed the substrate within 8 h after its addition. The lack of trehalose excretion by this mutant was thus most likely an indirect effect of poor growth and maltose uptake.

Since inactivation of *cg2893* caused a severe growth phenotype which hampered the investigation of the function of the encoded protein, the gene was cloned and overexpressed in *C. glutamicum* Δ*malQ* Δ*treX* Δ*tus* (pXMJ19_*cg2893*). If this gene encoded an exporter for trehalose, this strain should export trehalose with an increased rate. Trehalose accumulation rates were determined as described above. *C. glutamicum* Δ*malQ* Δ*treX* Δ*tus* (pXMJ19) carrying an empty plasmid was used as control (Figure 23). No significant differences concerning the trehalose accumulation rate were observed between both strains.

Figure 21: *C. glutamicum* Δ*malQ* Δ*treX* Δ*tus* IM*cg2893* forms cell aggregates in minimal medium plus glucose.

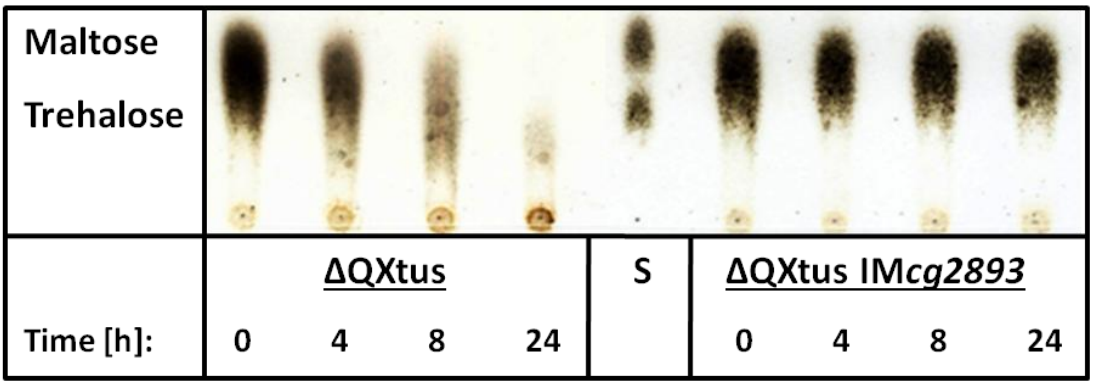

Figure 22: TLC analysis of culture supernatants of *C. glutamicum* Δ*malQ* Δ*treX* Δ*tus* (ΔQXtus) and *C. glutamicum* Δ*malQ* Δ*treX* Δ*tus* IM*cg2893* (ΔQXtus IM*cg2893*) after maltose addition. S: standard solution. Carbohydrates were visualised with 4% H_2SO_4 in methanol and heating to 110°C.

Due to the severe growth phenotype of *C. glutamicum* Δ*malQ* Δ*treX* Δ*tus* IM*cg2893* plasmid encoded expression of *cg2893* in this strain was not tested. To rule out negative effects of *cg2893* inactivation on the expression of *cg2895*, which lies downstream of *cg2893* in the hypothetical operon and also encodes a MFS type permease, the influence of disruption and overexpression of the latter on trehalose excretion was tested. Growth of *C. glutamicum* Δ*malQ* Δ*treX* Δ*tus* IM*cg2895* with glucose was similar to the parental strain (μ = 0.34 h^{-1} and 0.38 h^{-1}, respectively) and significant differences in the trehalose excretion rates were measured neither after inactivation nor overexpression of *cg2895* (Figure 19 and 23).

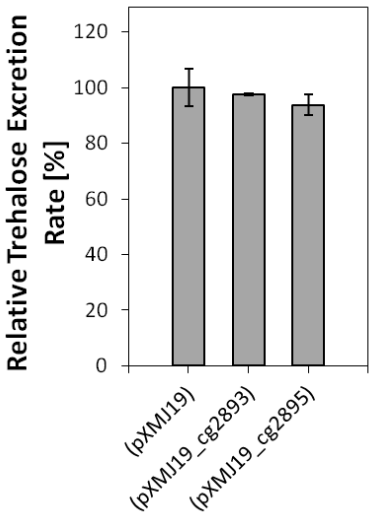

Figure 23: Effect of *cg2893* and *cg2895* overexpression on the trehalose accumulation rate in the medium. For induction of gene expression, 100 µM IPTG was added to the medium. (**pXMJ19**): *C. glutamicum* Δ*malQ* Δ*treX* Δ*tus* (pXMJ19); (**pXMJ19_*cg2893***): *C. glutamicum* Δ*malQ* Δ*treX* Δ*tus* (pXMJ19_*cg2893*); (**pXMJ19_*cg2895***): *C. glutamicum* Δ*malQ* Δ*treX* Δ*tus* (pXMJ19_*cg2895*).

These experiments indicate that the lack of trehalose excretion by *C. glutamicum* Δ*malQ* Δ*treX* Δ*tus* IM*cg2893* was most likely a secondary effect of poor growth and substrate consumption. Since overexpression of this gene did not increase the trehalose accumulation rate, this gene is unlikely to encode a trehalose exporter. The severe growth defect of this strain was reminiscent of strains impaired in mycolic acid metabolism. The role of Cg2893 in glycolipid synthesis was thus further investigated and is described in section 3.4.4.

3.2.8 Transcriptional regulation of the putative trehalose export system

Analysis of differential expression of genes under diverse conditions has been successfully applied for the identification of genes coding for export proteins in the past (Trötschel *et al.*, 2005; Kind *et al.*, 2011). Thereby, mRNA extracted from cells grown under inducing and non-inducing conditions is transcribed to cDNA and the latter is spotted on a DNA chip containing DNA probes for (nearly) all genes of an organism. Genes that are up- or downregulated under one of the applied conditions can be identified comparing transcript amounts of the two samples. If the transcription of gene(s) encoding the trehalose export system was regulated in the test strain *C. glutamicum* Δ*malQ* Δ*treX* Δ*tus*, these could also be identified applying DNA microarray analysis. To test whether *de novo* protein synthesis is required to trigger trehalose export in this strain, translation was inhibited using chloramphenicol. Therefore, cells were pre-cultivated in minimal medium with 1% glucose as carbon source. After depletion of the substrate, 100 µg/ml chloramphenicol and 1% maltose were added to the culture. In parallel, the experiment was performed without chloramphenicol. The OD_{600}, the intra-, and the extracellular concentrations of trehalose were recorded (Figure 24).

Within 24 h after the addition of maltose, the OD_{600} increased in both experiments from about 20 to 26 (no chloramphenicol) and 32 (plus chloramphenicol), respectively. The intracellular trehalose concentration was in the low millimolar range before maltose addition in both cases. Without chloramphenicol, it linearly increased to 85 ± 4 mM after 8.5 h and reached 124 ± 3 mM after 24 h. In the presence of chloramphenicol, the increase of the internal trehalose concentration occurred with a higher rate and reached 154 ± 3 mM after 24 h. Under the latter condition, the accumulation of trehalose in the supernatant was also faster (0.16 ± 0.01 nmol × mg^{-1} cdw × min^{-1} compared to 0.09 ± 0.00 nmol × mg^{-1} cdw × min^{-1} with and without chloramphenicol, respectively). Although the internal trehalose concentration was higher when chloramphenicol was added, the excretion rate

was not reduced but even increased. This excluded the necessity of *de novo* protein synthesis to induce trehalose excretion in the experiment described here. In conclusion, the trehalose uptake system cannot be identified via transcriptional analyses under the applied conditions.

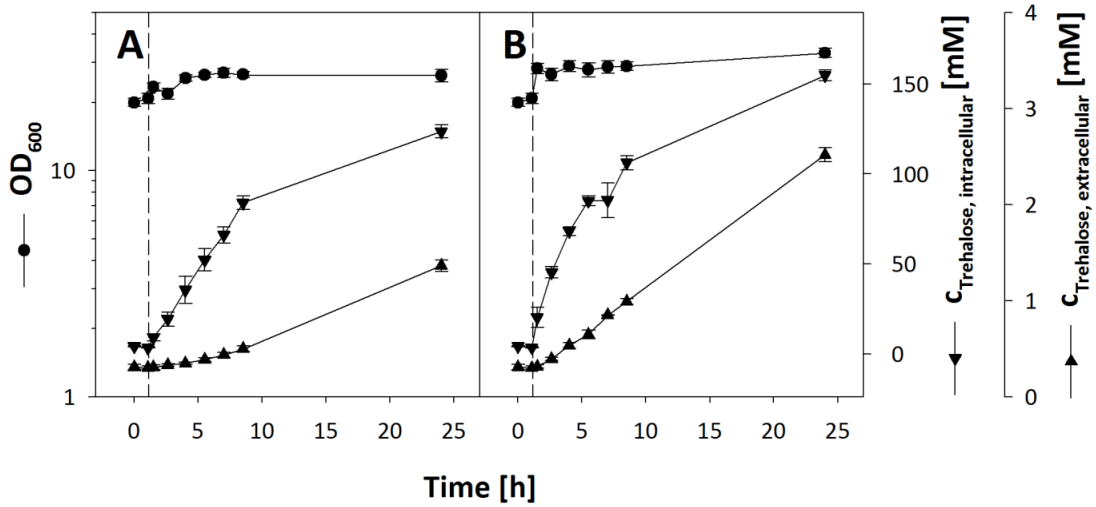

Figure 24: Dependence of trehalose release to the medium on *de novo* protein synthesis. *C. glutamicum* Δ*malQ* Δ*treX* Δ*tus* was pre-cultivated with glucose (not depicted) before 15 mM maltose was added (dashed line) (**A**). 100 µg/ml chloramphenicol was added to block protein synthesis prior to maltose addition (**B**).

3.3 Construction and application of a genetically encoded trehalose nanosensor

C. glutamicum was shown to export trehalose in this study but the exporter could not be identified so far. A set of candidate genes was inactivated but none of the encoded proteins contributed to trehalose export. Since this rational approach was not successful, screening of a *C. glutamicum* mutant library was considered as an alternative. To construct a library based on gene inactivation, transposon mutagenesis could be applied, for example. Alternatively, genomic DNA of *C. glutamicum* could be fragmented, cloned in a suitable vector, and overexpressed in an appropriate host to construct a genomic library. However, the screening of such a library has to be considered as well. A likely phenotype after inactivation or overexpression of an exporter is an altered intracellular concentration of the export substrate and this could be detected with a genetically encoded FRET-nanosensor. Genetically encoded FRET-nanosensors consist of a ligand binding domain fused to two fluorescent proteins forming a FRET-pair. Binding of the ligand causes a conformational change of the binding domain and is translated into an altered FRET-efficiency between the coupled fluorescent proteins. This enables the determination of intracellular solute concentrations in a non-disruptive manner using fluorescence detection (Fehr *et al.*, 2002). Bacterial periplasmic binding proteins (PBPs) are frequently used as binding domains for nanosensor construction (Jeffery, 2010). PBPs serve as receptors for the active uptake of mono- and oligosaccharides, amino acids, oligopeptides, cations, vitamins, etc. (Quiocho & Ledvina, 1996). This large family of proteins shows a common shape. Two globular domains are connected by a central hinge and a substrate binding pocket is formed on the interface of these domains (Quiocho & Ledvina, 1996). PBPs undergo a pronounced conformational change from an open to a closed state upon ligand binding and are thus well suited for the application in biosensors (Dwyer & Hellinga, 2004).

FRET-nanosensors have been constructed to detect ions like Ca^{2+} (Nakai *et al.*, 2001) and phosphate (Gu *et al.*, 2006), small metabolites like ATP (Imamura *et al.*, 2009), mono- and disaccharides like glucose (Fehr *et al.*, 2003), maltose (Fehr *et al.*, 2002), and sucrose (Chen *et al.*, 2012), and amino acids like L-glutamate (Okumoto *et al.*, 2005) and L-leucine (Mohsin *et al.*, 2013), for example. FRET-nanosensors have been used to show the uptake of maltose by yeast cells (Fehr *et al.*, 2002), the transport of glucose across the membrane of the endoplasmatic reticulum of HepG2 cells (Fehr *et al.*, 2005), to measure steady-state glucose levels in plants (Deuschle *et al.*, 2006), or to depict the accumulation of arabinose and

maltose in *E. coli* (Kaper *et al.*, 2008). Furthermore, a sucrose sensor was used to identify a family of sucrose export proteins by screening a set of membrane proteins of unknown function from *Arabidopsis thaliana* expressed in human embryonic kidney cells (Chen *et al.*, 2012). It was thus reasoned that a trehalose nanosensor could be used as a tool for the detection of intracellular trehalose and to screen a *C. glutamicum* mutant library to identify proteins involved in trehalose export. A trehalose nanosensor has not yet been described in the literature and should be constructed in this work. The periplasmic trehalose binding protein of *C. glutamicum* was therefore characterised and finally used for the construction of a trehalose sensor. Since FRET-nanosensors have not been tested for the application in *C. glutamicum* yet, a set of ATP-nanosensors was expressed in this organism and used to establish techniques for the application of FRET-sensors in this host.

3.3.1 Establishing metabolite nanosensors in *C. glutamicum*

FRET-nanosensors for ATP have been described in the literature and have been used to study the energy metabolism of human epithelial cells (Imamura *et al.*, 2009). The set of sensors applied here comprises two sensors with millimolar dissociation constants for ATP (AT1.03 and AT1.03^{YEMK}), one sensor with a micromolar ATP dissociation constant (AT3.10^{MGK}) and a control sensor that does not respond to even 10 mM ATP (AT1.03$^{R122K/R126K}$). For expression, the genes encoding these sensor constructs were ligated to the *E. coli – C. glutamicum* shuttle vector pBB1. Successful expression in *C. glutamicum* was verified by fluorescence imaging showing the expression and correct folding of both fluorescence protein domains of the sensor (Figure 25).

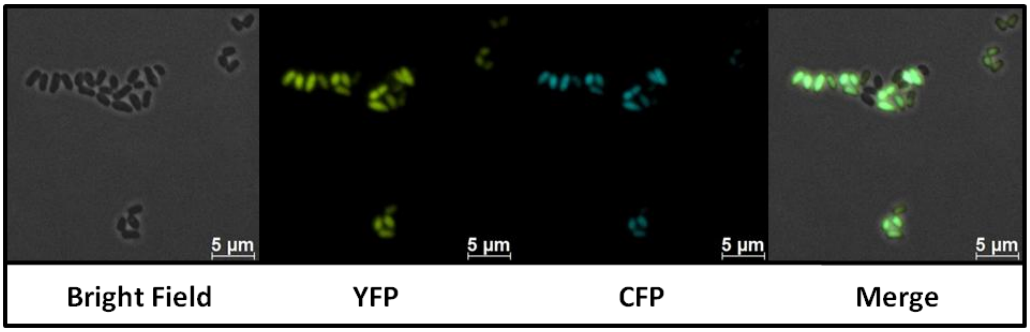

Figure 25: Expression of ATP-nanosensors in *C. glutamicum* cells. As an example for all four ATP-sensors used in this study the expression of AT1.03^{YEMK} is shown here in *C. glutamicum* (pBB1_AT1.03^{YEMK}). Images were taken using an Axio Imager M1 fluorescence microscope equipped with an Axiocam HRm camera and an EC Plan Neofluar 100 × /1.3 Oil Ph3 objective (Carl Zeiss).

Table 5: Dissociation constants of ATP-nanosensors in cell lysates and permeabilised cells. K_d-values for sensors in *E. coli* cell lysates were taken from the literature (Imamura et al., 2009). The maximum signal changes upon ATP-addition are given in brackets. n. d. not determined.

Sensor	*E. coli* (cell lysates)	*C. glutamicum* (cell lysates)	*C. glutamicum* (permeabilised cells)
AT1.03	3.3 mM	1.25 mM (0.44)	1.25 mM (0.23)
AT1.03^{YEMK}	1.2 mM	0.71 mM (1.93)	1.5 mM (0.75)
AT3.10^{MGK}	14 µM	24 µM (0.31)	91 µM (0.71)
AT1.03$^{R122K/R126K}$	> 10 mM	-	n. d.

Next, cell lysates of *C. glutamicum* (pBB1_AT1.03), *C. glutamicum* (pBB1_AT1.03^{YEMK}), *C. glutamicum* (pBB1_AT3.10^{MGK}), and *C. glutamicum* (pBB1_AT1.03$^{R122K/R126K}$) were prepared to perform *in vitro* calibrations of the ATP-sensors. Results of these experiments are shown in Figure 26 and Table 5. All K_d values were in the same range as expected from the literature. AT3.10^{MGK} showed a very high affinity for ATP with a K_d-value of 24 µM. For AT1.03 and AT1.03^{YEMK} the values were 1.25 mM and 0.71 mM. The control sensor AT1.03$^{R122K/R126K}$ did not respond to the addition of ATP.

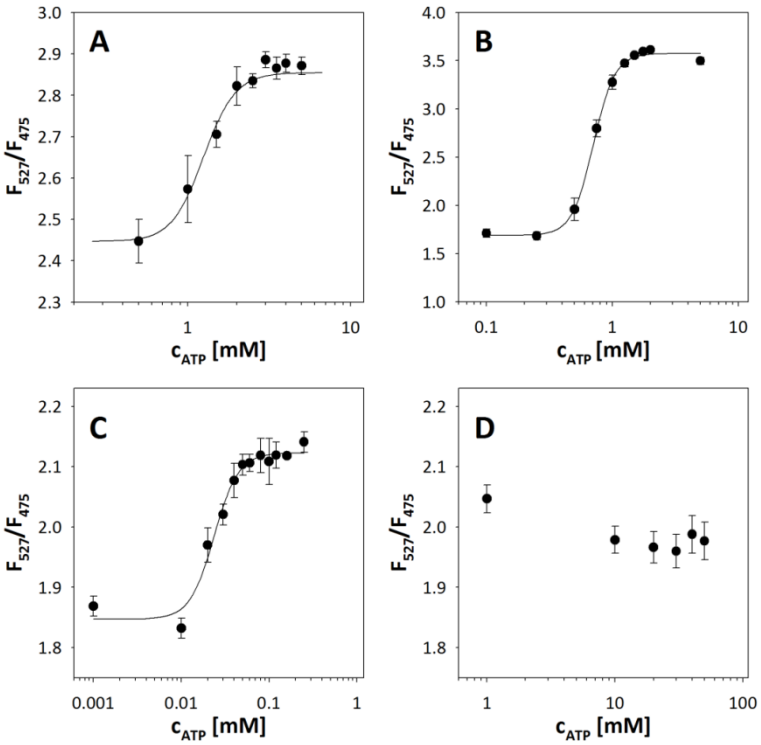

Figure 26: *In vitro* calibration of ATP-nanosensors in *C. glutamicum* cell lysates. A: *C. glutamicum* (pBB1_AT1.03); **B:** *C. glutamicum* (pBB1_AT1.03^{YEMK}); **C:** *C. glutamicum* (pBB1_AT3.10^{MGK}); **D:** *C. glutamicum* (pBB1_AT1.03$^{R122K/R126K}$). The FRET-efficiency (F_{527}/F_{475}) was calculated by division of the yellow by the cyan fluorescence intensity.

The influence of cytosolic contents on the sensor response was studied in *C. glutamicum* cells permeabilised with 0.05% CTAB. While the K_d-value for AT1.03 remained unchanged, those of AT1.03^{YEMK} and AT3.10^{MGK} increased to 1.5 mM and 91 µM, respectively. Further, the maximum signal changes (ΔR_{max}) of the sensors were different in permeabilised cells compared to cell lysates. While ΔR_{max} was higher in cell lysates for AT1.03 (0.44 and 0.23) and AT1.03^{YEMK} (1.93 and 0.75), the opposite was true for AT3.10^{MGK} (0.31 and 0.71) (Table5). To test the function of the ATP sensors *in vivo*, different inhibitors of ATP synthesising reactions were added to a *C. glutamicum* (pBB1_AT1.03^{YEMK}) culture (Figure 27).

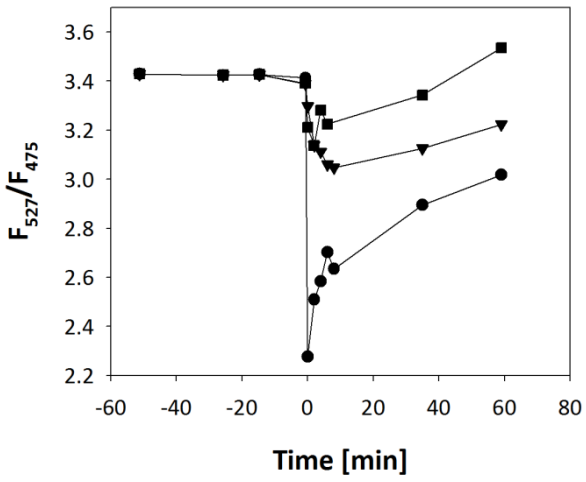

Figure 27: In vivo response of AT1.03YEMK to the perturbation of ATP synthesis. *C. glutamicum* was cultivated in CgC minimal medium plus 1% glucose. At t = 0 min 0.1% CTAB (●), 20 mM azide (▼), or 1 mM cyanide (■) was added. The FRET-efficiency F_{527}/F_{475} was calculated by division of the yellow by the cyan fluorescence intensity.

CTAB leads to cell permeabilisation and therefore ATP synthesis by the respiratory chain is blocked completely, leaving only substrate-level phosphorylation for ATP generation. Addition of 0.1% CTAB caused a drop of the FRET-efficiency of AT1.03^{YEMK} from 3.41 to 2.25, reflecting the immediate dilution of the intracellular ATP concentration due to cell permeabilisation. A partial restoration of the FRET-efficiency to 3.02 within 60 min was observed. Cyanide and azide are inhibitors of the cytochrome-aa3-oxidase. Cyanide was added at a concentration of 1 mM to partially block the activity of this enzyme (Sugiyama *et al.*, 1973). The FRET-efficiency slightly decreased from 3.39 to 3.21 after the addition and slowly increased to 3.53 after 60 min. 20 mM azide was added to completely inhibit cytochrome-aa3-oxidase. Within 10 min, a decrease of the sensor signal from 3.39 to 3.05 was observed. Only a partial recovery of the signal (3.22 after 60 min) was possible,

correlating with the assumption of a total inhibition of the cytochrome-aa3-oxidase branch of the respiratory chain under these conditions.

In conclusion, a set of ATP-nanosensors was successfully applied for ATP measurements in *C. glutamicum*. Techniques for the calibration of FRET-nanosensors in cell lysates and permeabilised cells were established and the experiments showed that the sensor response is altered in the intracellular environment compared to experiments in cell lysates. This is likely to hamper the quantitative detection of ATP by this method. Nevertheless, these sensors were applied successfully to show relative changes of the intracellular ATP concentrations in *C. glutamicum* upon perturbation of ATP synthesis.

3.3.2 The gene *cg0834* encodes the binding protein of the trehalose ABC uptake system

The applicability of genetically encoded FRET-nanosensors in *C. glutamicum* could be shown with the help of a set of ATP-sensors. To construct a trehalose nanosensor, the trehalose binding protein of *C. glutamicum* was characterised next.

The *tus*-gene cluster comprises a gene encoding a putative periplasmic sugar binding protein, *cg0834* (*tusE*) (Henrich, 2011). The function of the encoded protein was examined in this work. To collect information about the protein, a bioinformatic analysis of the predicted primary sequence encoded by *cg0834* was conducted. The gene encodes a protein of 424 amino acids with a calculated molecular weight of 45 kDa. The primary structure has 30% identity and 48% similarity to the trehalose/maltose binding protein from *Thermococcus litoralis* and 27% identity and 42% similarity to the maltose binding protein MalE from *E. coli*. The domain annotation given in the KEGG database (Kanehisa & Goto, 2000) classifies the protein as a member of either the ABC transporter substrate binding protein cluster 1 (E-value 4.9^{-27}), members of which are specific for oligosaccharides, glycerol-3-phsphate, and iron (Tam & Saier, 1993), or cluster 8 (E-value 4.4^{-26}), members of which are specific for iron complexes (Tam & Saier, 1993). The protein probably also contains a PepSY domain (E-value = 0.51, amino acids 10 to 47), which is found in a large number of secreted bacterial proteins (Yeats *et al.*, 2004). To identify a possible signal peptide targeting the protein for the export to the periplasm, the SignalP 4.0 algorithm (Petersen *et al.*, 2011) was used. An N-terminal signal peptide with a cut-off site between amino acids 32 and 33 was predicted. In Gram-negative bacteria, periplasmic solute binding proteins are held back by the outer membrane. Since the latter is missing in Gram-positive bacteria, the loss of periplasmic proteins to the

surrounding has to be prevented otherwise. Cysteine acylation commonly tethers these proteins to the membrane (Nielsen & Lampen, 1982). Using the LipoP1.0 algorithm (Juncker *et al.*, 2003), a signal sequence typical for lipoproteins with a cleavage site between amino acids 25 and 26 was identified, resulting in an N-terminal cysteine residue that could be modified by acylation in the mature protein.

Next, the function of the *cg0834* gene product was tested experimentally. *cg0834* and a truncated version lacking the first 25 codons from the N-terminus were cloned by PCR and overexpressed in *E. coli* BL21 (DE3). Both proteins, carrying a C-terminal His_6-tag, were then purified in two steps via IMAC and SEC. For SEC, a 20 mM K_2HPO_4/KH_2PO_4 buffer pH 7.5 plus 150 mM NaCl was used. When purified via SEC, full length TusE eluted in the void volume of the column probably due to aggregation of the protein. It was thus not examined further. Under the same conditions, the truncated protein was purified to apparent homogeneity as shown by SDS-PAGE (Figure 28 A) and its identity was confirmed by Western-blot analysis using anti-His_6 antibody (Figure 28 B).

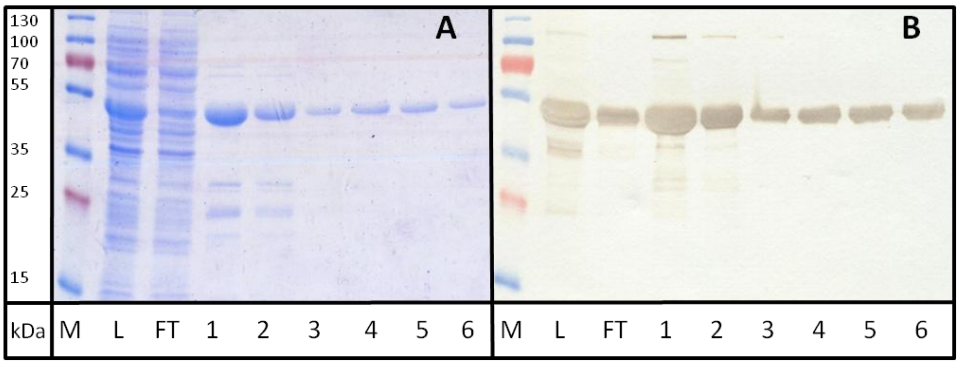

Figure 28: Purification of TusEΔN25-His_6 by IMAC and SEC. A: SDS-PAGE analysis; **B**: Western-Blot analysis using anti-His_6 antibody. **M:** Protein marker; **L**: Cell lysate; **FT**: Flow-through of unbound protein; **1 – 3**: IMAC elution fractions; **4– 6**: SEC elution fractions.

To examine trehalose binding to the protein, the change of fluorescence intensity of the protein upon trehalose addition was tested (Figure 29). The experiment showed the binding of trehalose with a dissociation constant of 0.42 ± 0.02 µM. The addition of buffer as a negative control did not lead to a change of the fluorescence intensity (not shown).

These studies confirm that *cg0834* encodes a trehalose binding protein with high substrate affinity (TusE in the following). The first 25 amino acids of TusE are not necessary for trehalose binding and probably target the protein for the export to the periplasm and for acylation.

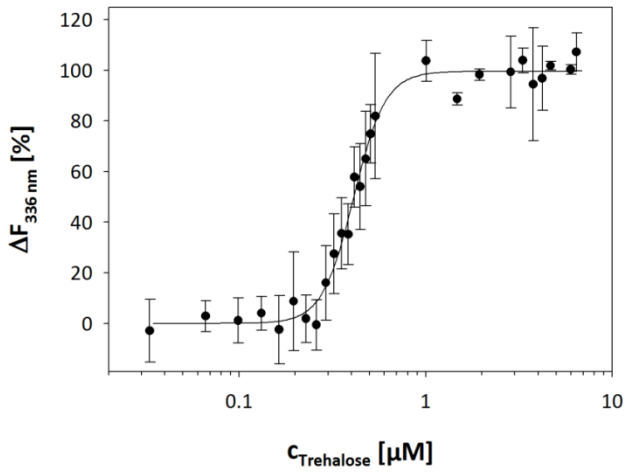

Figure 29: Change of the intrinsic fluorescence of TusEΔN25-His6 after trehalose addition. ΔF_{336nm} represents the relative difference of the fluorescence intensity at 336 nm (289 nm excitation).

3.3.3 Development of a trehalose nanosensor

Periplasmic solute binding proteins have been used to construct a number of metabolite sensors based on the proteins conformational change upon ligand binding. Coupled to two fluorescent proteins constituting a FRET-pair, ligand binding is translated into a change of FRET-efficiency. TusE was shown to bind trehalose with high affinity (see section 3.3.2) and it was thus chosen to construct a genetically encoded trehalose sensor (TreSen). Enhanced cyan and yellow fluorescent proteins (ECFP, EYFP) are commonly used as FRET pair for the construction of nanosensors (Fehr *et al.*, 2002; Kaper *et al.*, 2008; Imamura *et al.*, 2009) and were also applied here.

For the construction of a trehalose sensor, a *tusE* PCR product was used to exchange the maltose binding protein encoding *malE* gene of a maltose sensor (Fehr *et al.*, 2002) using *Kpn*I restriction sites. This resulted in a construct encoding TusE N- and C-terminally fused to ECFP and EYFP, respectively, by two linkers consisting of six amino acids (compare Figure 30). This construct was then ligated to the pET29b vector and overexpressed in *E. coli* BL21 (DE3). Cell lysates were prepared and titrated with a trehalose stock solution.

After excitation at 435 nm, the fluorescence intensities at 480 nm and 525 nm, corresponding to the emission maxima of ECFP and EYFP, respectively, were recorded in a microplate reader. FRET-efficiencies were calculated by division of the latter value by the former. Features of all sensor constructs described in the following are summarised in Table 6. Oligonucleotides used for the construction are given in Table 3 in the methods section.

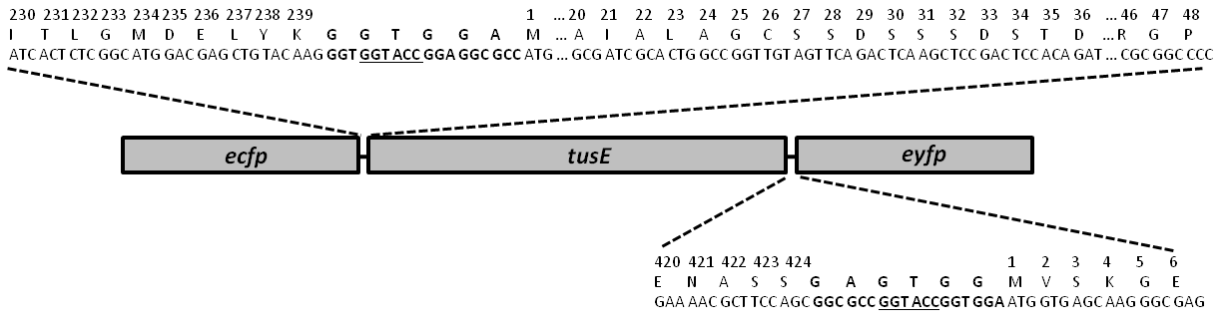

Figure 30: Schematic representation of the trehalose nanosensor TreSen1. For construction, a full length *tusE* PCR product was ligated in between *ecfp* and *eyfp* using *Kpn*I restriction sites (underlined). Linker regions are shown in bold letters. Amino acids are numbered according to their position in the original proteins.

For construction of TreSen1, the full length *tusE* gene was used. The FRET-efficiency of this construct, however, remained unchanged after the addition of trehalose (Figure 31). Using a truncated version of TusE lacking the first 32 N-terminal amino acids (TusEΔN32) resulted in a functional sensor (TreSen2 in Figure 31). The FRET-efficiency increased from 1.19 (R_0) in the absence of trehalose to a maximum of 1.22 in the presence of trehalose (R_{max}) resulting in a maximum change of FRET-efficiency (ΔR_{max}) of 0.03. The dissociation constant for trehalose was 0.80 µM. Removal the 47 N-terminal amino acids from TusE resulted in a non-functional construct (TreSen3 in Figure 31).

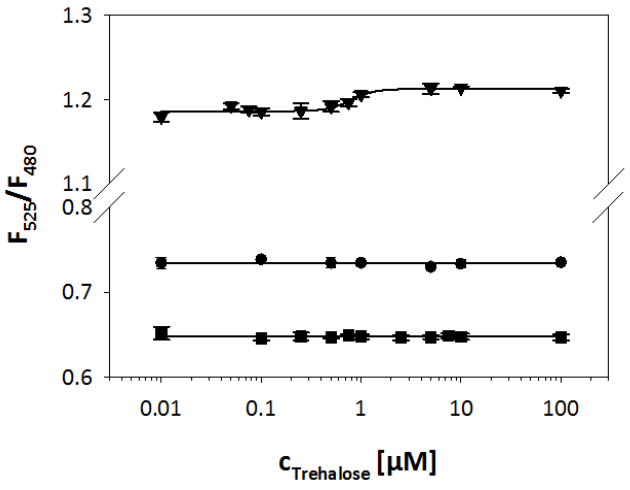

Figure 31: Construction of a trehalose nanosensor. ● TreSen1; ▼ TreSen2; ■ TreSen3. The FRET-efficiency F_{525}/F_{480} was calculated by division of the yellow by the cyan fluorescence intensity.

3.3.4 Improving the sensor response by linker modifications

The response of FRET-nanosensors is based on a spatial reorientation of the two fluorescent proteins due to conformational changes of the solute binding protein upon ligand binding. Therefore, this conformational change has to be transmitted efficiently to the fluorescent proteins by the linker sequences. The latter are thus one target for the optimisation of FRET-nanosensors (Deuschle *et al.*, 2005; Takanaga *et al.*, 2008).

TreSen4 - 6 were constructed from TreSen1 - 3 by removal of 3 amino acids from the first (GGTGGA → GGT) and two amino acids from the second linker (GAGTGG → GGTG, see Figure 30) via PCR. While the constructs containing full length TusE (TreSen4) and TusEΔN47 (TreSen6) remained non-functional, ΔR_{max} for TreSen5 (TusEΔN32) was improved to 0.07 (K_d = 1.22 µM, Figure 32) compared to 0.03 for the parental construct (TreSen2). Additionally, TreSen7 was constructed using TusEΔN25 and the same truncated linker sequences. The maximum signal change was in the same range as for TreSen2 and 5 (ΔR_{max} = 0.04). Further truncation of the linker between TusEΔN25 and EYFP in TreSen7 by two amino acids (GTGG → GT), resulting in TreSen14, hardly improved the maximum signal change of the sensor (ΔR_{max} = 0.05, Table 6). Next, EYFP in TreSen14 was replaced by mVenus, a yellow fluorescent protein reported to be brighter and less susceptible to acidic pH and chlorine ions than EYFP (Kremers *et al.*, 2006). While the FRET-efficiency in the apo-state remained constant (1.14), ΔR_{max} slightly increased to 0.07 for the resulting construct (TreSen15) (Table 6).

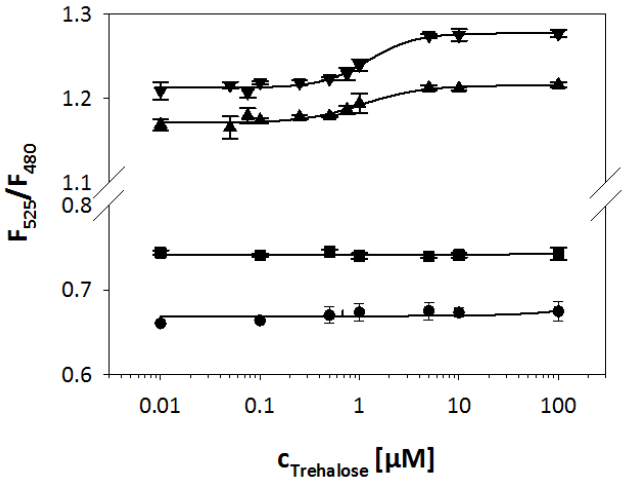

Figure 32: Sensor optimisation by linker modification. ● TreSen4; ▼TreSen5; ■ TreSen6; ▲ TreSen7. For sensor properties see text and Table 6. The FRET-efficiency F_{525}/F_{480} was calculated by division of the yellow by the cyan fluorescence intensity.

Truncation of both linker sequences only slightly improved the sensor response so far. The actual peptide linkers of the fused proteins are not limited to the synthetic linkers introduced by cloning. In fact, the terminal amino acids of TusE and the two fluorescent proteins also have to be considered. Since the terminal amino acids of GFP are not necessary for the fluorescence of the protein (Li *et al.*, 1997), ten amino acids from the C-terminus of ECFP, one glycine residue from the linker between ECFP and TusE, and six amino acids from the N-terminus of mVenus were removed by standard PCR methods. Compared to the parental sensor construct (TreSen15), the resulting sensor (TreSen24) showed a significant improvement of ΔR_{max} from 0.07 to 0.33. Additional N-terminal truncations of TusE, TusEΔN28 – TusEΔN35, were also tested in this sensor background (Table 6). Among the so constructed sensors, TreSen28 (TusEΔN32) performed best with a maximum signal change of 0.39 (Figure 33). The K_d values of these sensors varied between 0.09 µM (TreSen34) and 0.26 µM (TreSen24).

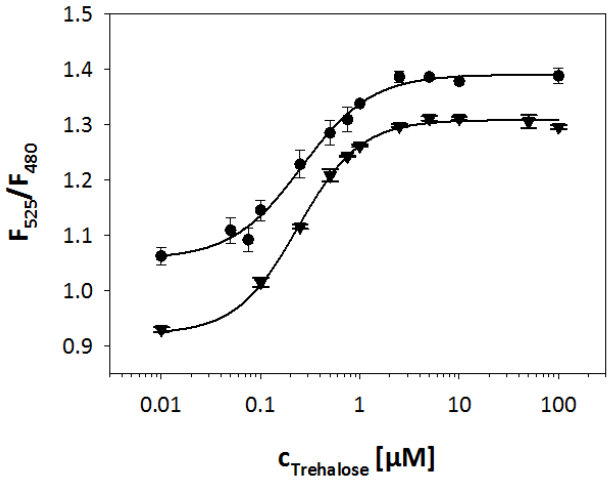

Figure 33: Sensor optimisation by truncation of the terminal regions of ECFP and mVenus. ● TreSen24; ▼ TreSen28. For sensor properties see text and Table 6. The FRET-efficiency F_{525}/F_{480} was calculated by division of the yellow by the cyan fluorescence intensity.

In conclusion, a set of genetically encoded trehalose nanosensors was successfully constructed. As expected from previous experiments with TusE, the affinities of these sensors were in the nanomolar range. The sensor response upon trehalose binding was optimised by systematic linker truncations and the best sensor, TreSen28, showed a maximum signal change of 0.39.

Table 6: Trehalose nanosensors constructed in this work. Linker sequences are shown in bold.

Construct	Features	K_d [µM]	R_0	ΔR_{max}
TreSen1	ECFP-**GGTGGA**-TusE-**GAGTGG**-EYFP	-	0.73	-
TreSen2	ECFP-**GGTGGA**-TusEΔN32-**GAGTGG**-EYFP	0.80	1.19	0.03
TreSen3	ECFP-**GGTGGA**-TusEΔN47-**GAGTGG**-EYFP	-	0.64	-
TreSen4	ECFP-**GGT**-TusE-**GTGG**-EYFP	0.21	0.66	0.02
TreSen5	ECFP-**GGT**-TusE ΔN32-**GTGG**-EYFP	1.22	1.22	0.07
TreSen6	ECFP-**GGT**-TusEΔN47-**GTGG**-EYFP	-	0.74	-
TreSen7	ECFP-**GGT**-TusEΔN25-**GTGG**-EYFP	1.08	1.17	0.04
TreSen14	ECFP-**GGT**-TusEΔN25-**GT**-EYFP	0.56	1.06	0.05
TreSen15	ECFP-**GGT**-TusEΔN25-**GT**-mVenus	0.70	1.14	0.07
TreSen24	ECFPΔC10-**GT**-TusEΔN25-**GT**-mVenusΔN6	0.26	1.06	0.33
TreSen25	ECFPΔC10-**GT**-TusEΔN28-**GT**-mVenusΔN6	0.19	1.15	0.31
TreSen26	ECFPΔC10-**GT**-TusEΔN29-**GT**-mVenusΔN6	0.13	1.21	0.34
TreSen21	ECFPΔC10-**GT**-TusEΔN31-**GT**-mVenusΔN6	0.17	1.09	0.35
TreSen28	ECFPΔC10-**GT**-TusEΔN32-**GT**-mVenusΔN6	0.24	0.92	0.39
TreSen32	ECFPΔC10-**GT**-TusEΔN33-**GT**-mVenusΔN6	0.06	1.26	0.38
TreSen33	ECFPΔC10-**GT**-TusEΔN34-**GT**-mVenusΔN6	0.15	1.19	0.27
TreSen34	ECFPΔC10-**GT**-TusEΔN35-**GT**-mVenusΔN6	0.09	1.08	0.33

3.3.5 Trehalose quantification with FRET-sensors

TreSen28 performed best among the constructed set of genetically encoded trehalose sensors. It was applied next for the determination of trehalose concentrations in trehalose containing culture supernatants of *C. glutamicum* Δ*malQ* Δ*treX* Δ*tus*. In parallel, the samples were also measured using an enzymatic assay and the results are compared in Figure 34.

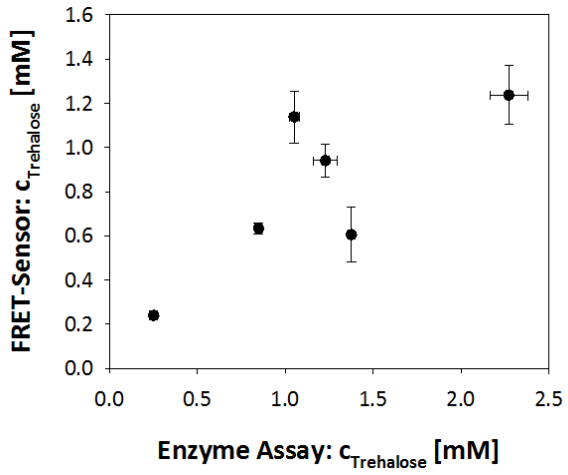

Figure 34: Comparison of enzymatic trehalose quantification and FRET-sensor measurement. Supernatants of *C. glutamicum* Δ*malQ* Δ*treX* Δ*tus* were analysed with both methods. For trehalose detection using a FRET-sensor, TreSen28 was titrated with a series of dilutions of each sample.

The trehalose concentrations determined for all samples were in the low millimolar range with both techniques. Although the absolute values were slightly different, a good correlation was obtained for most samples, showing that TreSen28 can be used for the quantitative determination of trehalose concentrations in culture supernatants.

3.3.6 Development of affinity mutants

Trehalose concentrations in *C. glutamicum* have been reported to reside in the millimolar range under various conditions (Wolf *et al.*, 2003). As a consequence, the affinity of a trehalose nanosensor has to be in the same order of magnitude for experiments *in vivo*. The K_d-value of TreSen28, the sensor with the highest signal change described in section 3.3.4, was 0.24 µM. To alter its affinity, a rational approach was chosen. Based on a structural homology model, the predicted substrate binding site of TusE was redesigned by the introduction of point mutations to create sensors with altered affinity for trehalose.

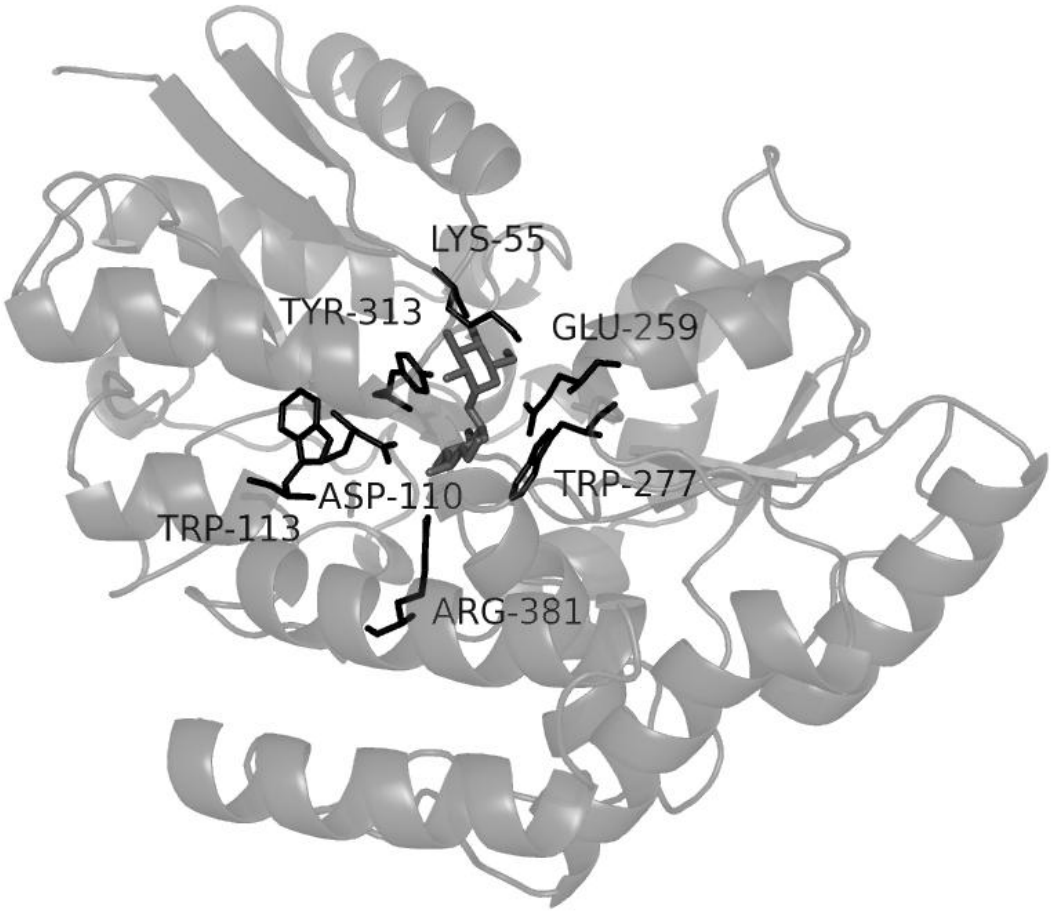

Figure 35: Structural homology model of TusE. Amino acids mutated in this work are represented as sticks. A trehalose molecule is shown in the centre of the protein model. The image was generated with the PyMOL molecular graphics system.

A structural homology model for TusE was constructed using the SWISS-MODEL web server in the automatic mode (Arnold *et al.*, 2006). As template for modelling, the structure of the *T. litoralis* trehalose/maltose binding protein, which was resolved by X-ray crystallography (1.85 Å resolution) in the presence of trehalose (Diez *et al.*, 2001), was used. Significant homology of both proteins (score 163 bits, E-value 2^{-40}) was found for amino acids 47 – 411 of TusE although the sequence identity of both proteins is only 30%. The homology model comprises amino acids 45 to 423 of TusE. The Qmean4 (Benkert *et al.*, 2008) score of the modelled structure is 0.56, the Z-score (Benkert *et al.*, 2011) is -3.4. The structural model was used to identify amino acids possibly contributing to trehalose binding (Figure 35).

Seven amino acids, K55, D110, W113, E259, W277, Y313, and R381 were then exchanged in TreSen28 for alanine by site-directed mutagenesis. TreSen28^{D110A}, TreSen28^{W113A}, TreSen28^{E259A}, TreSen28^{W277A}, and TreSen28^{R381A} were no longer functional. TreSen28^{K55A} and TreSen28^{Y313A}, however, remained functional and were also altered in their affinity for trehalose. The dissociation constants were 0.56 µM for TreSen28^{K55A} and 1.11 µM for TreSen28^{Y313A}, compared to 0.24 µM for the parental sensor (Figure 36).

W277 and Y313 were also mutated to phenylalanine to test the exchange of these amino acids for ones with higher structural similarity than alanine. While TreSen28^{W277F} was non-functional, TreSen28^{Y313F} bound trehalose with a K_d-value of 2.04 µM (Figure 36). Further, the positively charged lysine at position 55 was exchanged for the negatively charged glutamate. The resulting sensor, TreSen28^{K55E}, bound trehalose with a K_d-value of 1.34 µM.

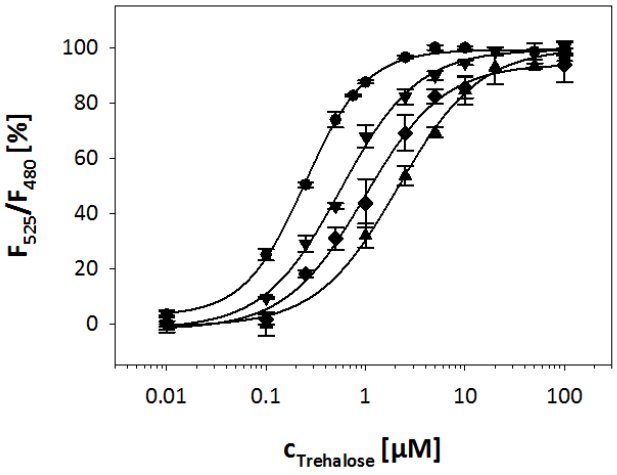

Figure 36: Construction of trehalose nanosensors with altered trehalose affinity. ● TreSen28; ▼ TreSen28^{K55A}; ◆ TreSen28^{Y313A}; ▲ TreSen28^{Y313F}. The FRET-efficiency F_{525}/F_{480} was calculated by division of the yellow by the cyan fluorescence intensity.

In conclusion, amino acids of TusE putatively contributing to ligand binding were identified with the help of homology modelling and mutated to construct a series of trehalose nanosensors with different dissociation constants, ranging from 0.24 µM to 2.04 µM. However, the affinity for trehalose still has to be reduced significantly to apply these sensors for intracellular trehalose detection in *C. glutamicum*.

3.4 Synthesis and transport of mycolic acids in *C. glutamicum*

A second, outer permeability barrier present in the cell envelope of Corynebacterineae is one reason for the high resistance of these bacteria against antibiotic compounds. Besides its function as a carbon source for *C. glutamicum*, trehalose is an important building block for TMM and TDM, which are the main constituents of this layer in *C. glutamicum* (Tropis *et al.*, 2005). While lethal in mycobacteria, viable mutants of *C. glutamicum* with impaired trehalose glycolipid metabolism have been constructed (Gande *et al.*, 2004; Portevin *et al.*, 2004; Gebhardt, 2005; Varela *et al.*, 2012). A common phenotype of such mutants is the agglutination of cells in liquid medium due to altered physical properties of the cell envelope (Portevin *et al.*, 2004; Tropis *et al.*, 2005). For example, the inability to synthesise trehalose renders *C. glutamicum* Δ*otsA* Δ*treS* Δ*treY* unable to form trehalose glycolipids. Since the addition of trehalose to the medium complemented this phenotype, it has been concluded that the incorporation of trehalose into glycolipids must take place in the periplasmic space rather than the cytosol (Tropis *et al.*, 2005). The recent discovery of a trehalose uptake system in *C. glutamicum* (Henrich, 2011) questioned this hypothesis. Because the addition of trehalose also restored TMM and TDM synthesis in *C. glutamicum* Δ*otsA* Δ*treS* Δ*treY* Δ*tus*, in which the genes encoding the trehalose uptake system are also deleted, the trehalose export hypothesis still remained valid (Henrich, 2011). One major prerequisite for this model is the export of trehalose to the periplasm and thus the presence of a trehalose export system in *C. glutamicum.*

Cytosolic reactions of mycolic acid synthesis have been studied in detail in *M. tuberculosis* and *C. glutamicum*. However, proteins catalysing the transport of precursors to the periplasm were not known at the beginning of this work. Within the last two years, targeting of MmpL3, a transport protein of the RND family, by several antibiotic compounds in different mycobacteria was shown to cause the accumulation of TMM in cell extracts and MmpL3 was thus assumed to export TMM to the periplasm (Grzegorzewicz *et al.*, 2012; Tahlan *et al.*, 2012; Varela *et al.*, 2012). In contrast, the only of these compounds tested in *C. glutamicum* was completely inactive (Grzegorzewicz *et al.*, 2012). Further, only the successive disruption of two *mmpL*-genes in *C. glutamicum* caused the phenotype observed for MmpL3-inhibition in mycobacteria and no accumulation of TMM as a potential transport substrate was seen in this strain (Varela *et al.*, 2012). The function of MmpL proteins in *C. glutamicum* is thus not fully understood yet and was investigated here.

3.4.1 Trehalose uptake is not required to restore mycolic acid synthesis

For the synthesis of TMM and TDM in *C. glutamicum*, trehalose is required as a precursor. Strains deficient in trehalose synthesis and uptake have been shown to incorporate trehalose into cell wall glycolipids and this step is thus thought to take place in the periplasm (Henrich, 2011). This hypothesis was further investigated in this work.

C. glutamicum Δ*otsA* Δ*treS* Δ*treY* is not able to form trehalose since all three pathways known to exist in *C. glutamicum* are inactive in this strain. In addition, *C. glutamicum* Δ*otsA* Δ*treS* Δ*treY* Δ*tus* is unable to import external trehalose. Both strains were cultivated in minimal medium containing fructose or fructose plus trehalose as carbon sources and lipids were extracted and analysed via TLC. *C. glutamicum* was used as a positive control. As already reported earlier (Henrich, 2011), *C. glutamicum* Δ*otsA* Δ*treS* Δ*treY* and *C. glutamicum* Δ*otsA* Δ*treS* Δ*treY* Δ*tus* formed both TMM and TDM only in the presence of trehalose while TDM was also detected in extracts of *C. glutamicum* grown without trehalose (Figure 37).

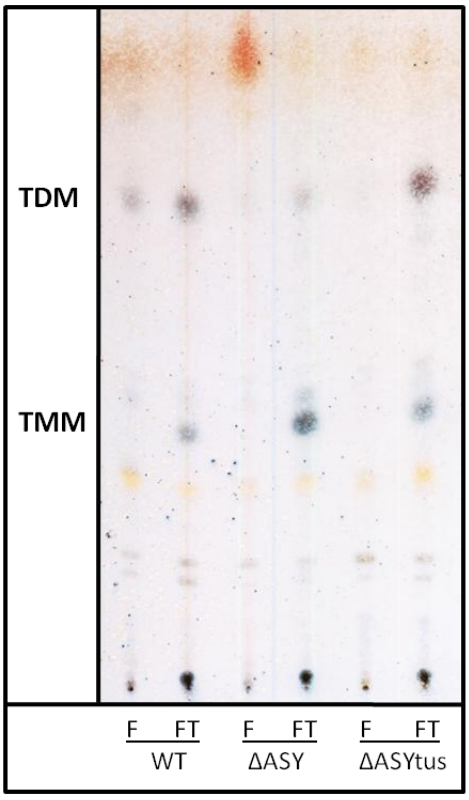

Figure 37: TLC analysis of lipid extracts. WT: *C. glutamicum*; **ΔASY**: *C. glutamicum* Δ*otsA* Δ*treS* Δ*treY*; **ΔASYtus**: *C. glutamicum* Δ*otsA* Δ*treS* Δ*treY* Δ*tus*. Cells were grown in CgC minimal medium with fructose (**F**) or fructose plus trehalose (**FT**). Glycolipids are stained blue, phospholipids orange.

Earlier experiments showed that the permeability of the cell envelope is increased in *C. glutamicum* Δ*otsA* Δ*treS* Δ*treY* (Gebhardt, 2005). To test whether this is also true for *C. glutamicum* Δ*otsA* Δ*treS* Δ*treY* Δ*tus*, growth of this strain in the presence of ethambutol or carbenicillin was examined in this study. While ethambutol interferes with arabinose metabolism in the cytosol, carbenicillin is an inhibitor of the cross-linkage of cell wall peptides in the periplasm. Both antibiotics have to pass the mycolic acid layer to act on their targets.

Different dilutions of cell suspensions were spotted on agar plates containing either 1 µg/ml ethambutol or 1 µg/ml carbenicillin. The plates were incubated for two days at 30°C. The presence of trehalose in the medium did not alter the growth of *C. glutamicum* on agar plates containing either antibiotic (Figure 38). Growth of *C. glutamicum* Δ*otsA* Δ*treS* Δ*treY* and *C. glutamicum* Δ*otsA* Δ*treS* Δ*treY* Δ*tus*, however, was improved by the addition of trehalose under both conditions. Surprisingly, *C. glutamicum* Δ*otsA* Δ*treS* Δ*treY* Δ*tus* grew better compared to *C. glutamicum* Δ*otsA* Δ*treS* Δ*treY* under all conditions. On agar plates containing carbenicillin, growth of *C. glutamicum* Δ*otsA* Δ*treS* Δ*treY* Δ*tus* was fully restored to the level of *C. glutamicum* by the addition of trehalose. This was not the case on agar plates containing ethambutol, where growth of the former strain remained impaired.

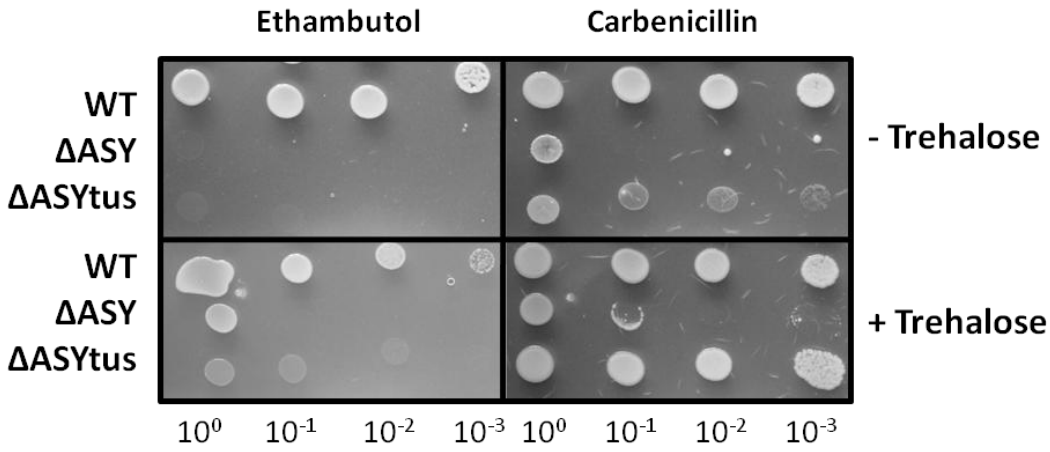

Figure 38: Test of antibiotic sensitivity. WT: *C. glutamicum;* **ΔASY:** *C. glutamicum* Δ*otsA* Δ*treS* Δ*treY*; **ΔASYtus***: C. glutamicum* Δ*otsA* Δ*treS* Δ*treY* Δ*tus.* Cells were grown on CgC minimal agar plates containing fructose or fructose plus trehalose. 1 µg/ml ethambutol or carbenicillin was added. Precultures were diluted to OD_{600} = 1.0 and 2 µl of a series of dilutions (1×10^{-0} - 1×10^{-3}) were spotted on the plates.

In conclusion, the addition of trehalose to cells unable to form or to import trehalose not only restored the formation of TMM and TDM but also improved the growth of these strains in the presence of carbenicillin or ethambutol. These results further strengthen the model of extracellular trehalose incorporation into cell wall glycolipids.

3.4.2 Trehalose export is independent of mycolic acid synthesis

A prerequisite for the model of periplasmic incorporation of trehalose into glycolipids is the export of trehalose from the cytosol to the periplasm. The experiments described in section 3.2 prove that this prerequisite is indeed fulfilled in *C. glutamicum*. Nevertheless, the formation of TDM involves the transfer of the mycolic acid moiety from one molecule of TMM to another. In this periplasmic reaction, one molecule of trehalose is released per reaction cycle. TDM synthesis could thus contribute to the accumulation of trehalose in the medium and the interconnection of trehalose export and glycolipid synthesis was investigated here.

A mutant devoid of mycolic acid synthesis was constructed. *cg3178*, encoding a polyketide synthase essential for mycolic acid synthesis, was deleted in *C. glutamicum* Δ*malQ* Δ*treX* Δ*tus* resulting in *C. glutamicum* Δ*malQ* Δ*treX* Δ*tus* Δ*pks*. Trehalose export by this strain was examined in growth experiments using 2% glucose and 1% maltose as substrates for growth and trehalose production, respectively, as already described (see section 3.2.4).

Growth of *C. glutamicum* Δ*malQ* Δ*treX* Δ*tus* Δ*pks* on glucose was severely impaired (Figure 39). The OD_{600} increased to 13.9 ± 1.1 after 81 h with a growth rate of only 0.03 ± 0.00 h^{-1}. Cells aggregated during cultivation and no synthesis of TMM or TDM was detectable (compare Figure 41). After the addition of maltose as substrate for trehalose production, the OD_{600} further increased to 16.2 ± 0.7 and remained steady at this level. Simultaneously, trehalose accumulated in the culture broth with a constant rate of 0.16 ± 0.01 nmol × mg^{-1} cdw × min^{-1} and a yield of 0.16 ± 0.02 mol × mol^{-1} maltose.

These results show that trehalose accumulation in the culture broth was hardly decreased in the absence of trehalose mycolate synthesis and the trehalose excretion observed here was therefore independent of glycolipid synthesis in *C. glutamicum*. To prove the significance of trehalose export for glycolipid synthesis, the identification of the trehalose export system is inevitable.

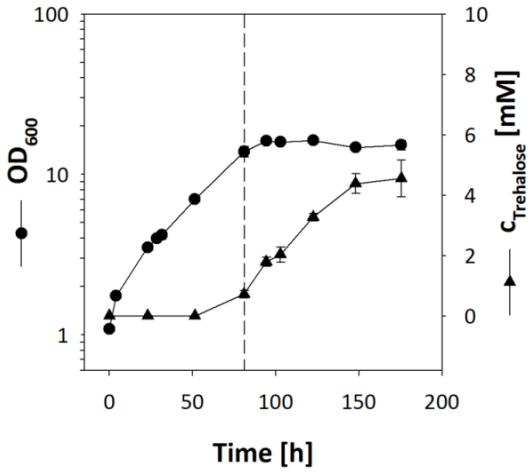

Figure 39: Trehalose export is independent of trehalose mycolate synthesis. *C. glutamicum* Δ*malQ* Δ*treX* Δ*tus* Δ*pks* was cultivated in minimal medium with 100 mM glucose. The dashed line indicates the addition of 29 mM maltose as substrate for trehalose production after 81 h.

3.4.3 Two RND-type proteins are involved in mycolic acid metabolism of *C. glutamicum*

Two MmpL proteins were recently described to be involved in mycolic acid transport in *C. glutamicum* (Varela *et al.*, 2012). To validate these observations in our *C. glutamicum* laboratory strain, the two corresponding *mmpL*-genes were inactivated, resulting in *C. glutamicum* Δ*cg0284* Δ*cg3174*. Noteworthy, both genes could be deleted in this work while this was not possible in a recent study (Varela *et al.*, 2012).

C. glutamicum Δ*cg0284* Δ*cg3174* was cultivated in CgC minimal medium plus glucose. *C. glutamicum* and a strain deficient in mycolic acid synthesis due to the deletion of the polyketide synthase gene, *C. glutamicum* Δ*malQ* Δ*treX* Δ*tus* Δ*pks*, were used as reference strains (Figure 40 A). As described above (see section 3.4.2), the latter strain hardly grew at all (OD_{600} = 1.8 after 24 h). *C. glutamicum* Δ*cg0284* Δ*cg3174* reached a final OD_{600} of 7.8 after 24 h with a growth rate of 0.12 h^{-1} compared to a growth rate of 0.39 h^{-1} and a final OD_{600} of 21.1 for *C. glutamicum*. Both mutants, *C. glutamicum* Δ*cg0284* Δ*cg3174* and *C. glutamicum* Δ*malQ* Δ*treX* Δ*tus* Δ*pks*, formed cell aggregates and adhered to the glass wall of the shaking flask (Figure 40 B). To analyse the influence of the deletion of *cg0284* and *cg3174* on cell wall glycolipid synthesis, these were extracted from cells grown in minimal medium with fructose or fructose plus trehalose and analysed via TLC (Figure 41). For *C. glutamicum* grown on fructose the major glycolipid detected was TDM, TMM was detected only when trehalose was added to the medium. Both *C. glutamicum* Δ*cg0284* Δ*cg3174* and *C. glutamicum* Δ*malQ* Δ*treX* Δ*tus* Δ*pks* did neither form TDM nor TMM while the chromatographic lipid pattern was

unaltered in other respects. Single mutants of *cg0284* and *cg3174* were also constructed but they did not show a growth phenotype or an altered glycolipid composition (Figure 41).

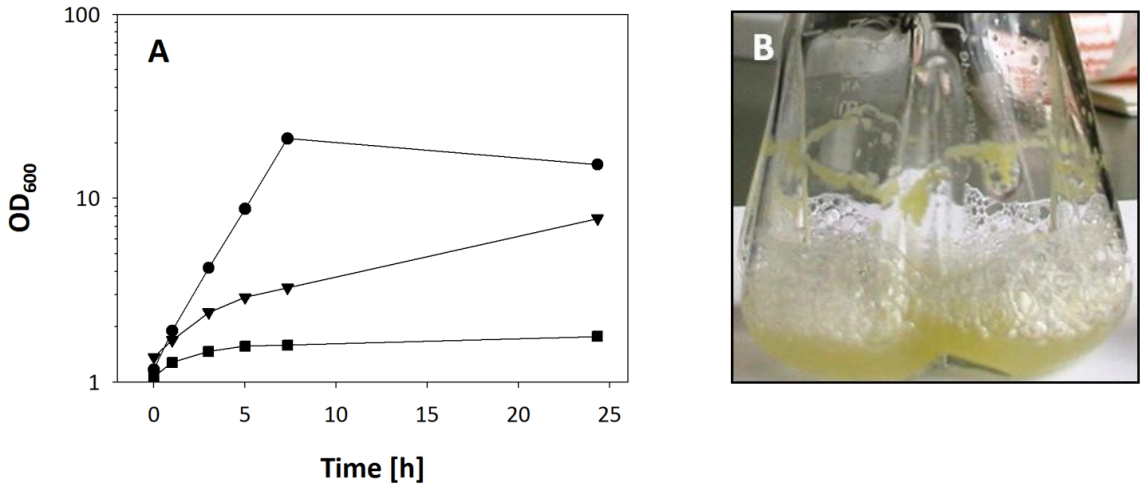

Figure 40: Growth of *C. glutamicum* (●), *C. glutamicum* Δ*cg3174* Δ*cg0284* (▼), and *C. glutamicum* Δ*malQ* Δ*treX* Δ*tus* Δ*pks* (■) in minimal medium with 1% glucose (A). *C. glutamicum* Δ*cg3174* Δ*cg0284* cells aggregated in liquid culture and adhered to the glass wall of the shaking flask **(B).**

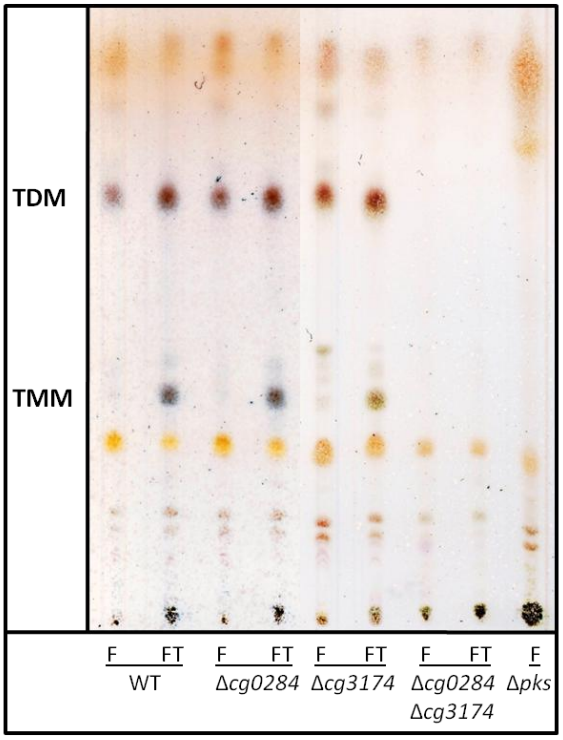

Figure 41: TLC analysis of lipid extracts. WT: *C. glutamicum;* **Δ*cg0284*:** *C. glutamicum* Δ*cg0284*; **Δ*cg3174*:***C. glutamicum* Δ*cg3174;* **Δ*cg0284* Δ*cg3174*:** *C. glutamicum* Δ*cg0284* Δ*cg3174:* **Δ*pks*:** *C. glutamicum* Δ*malQ* Δ*treX* Δ*tus* Δ*pks*. Cells were grown in minimal medium with fructose (**F**) or fructose plus trehalose (**FT**). Glycolipids are stained blue, phospholipids orange.

3.4.4 Inactivation of *cg2893* leads to altered cell envelope composition

In the screening for gene(s) encoding a trehalose export system, disruption of *cg2893* was found to cause a growth phenotype reminiscent of *C. glutamicum* strains with impaired glycolipid metabolism. The growth rate in *C. glutamicum* Δ*malQ* Δ*treX* Δ*tus* IM*cg2893* was reduced drastically compared to *C. glutamicum* and the cells adhered to the glass wall of the shaking flask.

The gene *cg2893* encodes a MFS transporter and homologous genes are found throughout the bacterial kingdom. Cg2893 has been identified as the exporter of diaminopentane in an engineered *C. glutamicum* diaminopentane overproducing strain (Kind *et al.*, 2011). However, since *C. glutamicum* does not naturally produce diaminopentane, the original substrate of this exporter remained unknown. To further investigate the function of the *cg2893* gene product, *cg2893* was inactivated in *C. glutamicum* wild type. When cultivated in minimal medium plus glucose or glucose plus trehalose, no growth of *C. glutamicum* IM*cg2893* was observed (Figure 42).

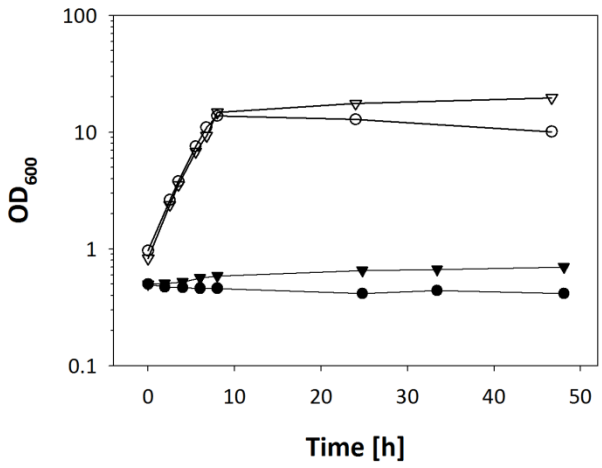

Figure 42: Cultivation of *C. glutamicum* (open symbols) and *C. glutamicum* IM*cg2893* (closed symbols) in minimal medium with glucose (●) or glucose plus trehalose (▼).

To analyse cell wall glycolipids in *C. glutamicum* IM*cg2893*, the strain was cultivated in 2TY medium and incubated in minimal medium with glucose or glucose plus trehalose for 24 h before lipid extraction. As shown in Figure 43, the chromatographic pattern of the extracted lipids was dramatically altered in this strain. While for *C. glutamicum* several spots stained as glycolipids or phospholipids were found under both conditions, only three spots staining as unknown glycolipids were present in extracts of the mutant. TMM and TDM were not

detected. After overexpression of *cg2893* the only difference to the wild type was the absence of TMM when grown on glucose plus trehalose (Figure 43). Thus, the role of Cg2893 in cell wall synthesis remains unclear.

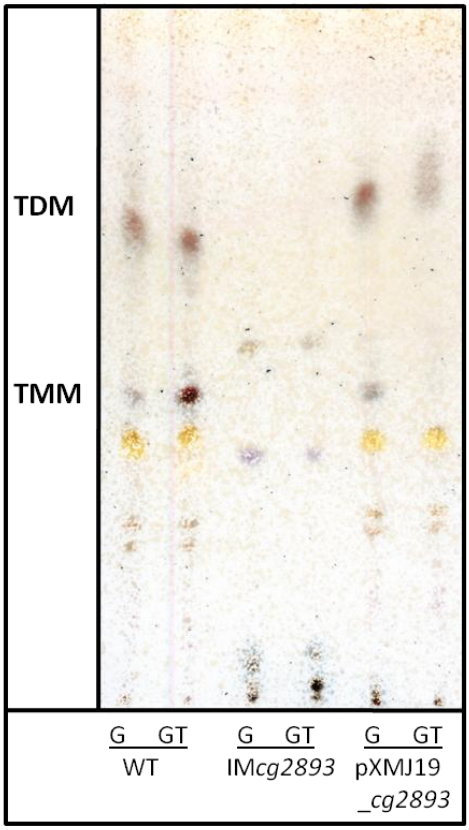

Figure 43: TLC analysis of cell wall glycolipids. WT: *C. glutamicum*; **IM*cg2893***: *C. glutamicum* IM*cg2893*; **pXMJ19*_cg2893***: *C. glutamicum* (pXMJ19*_cg2893*); **G**: glucose, **T**: trehalose. Glycolipids are stained blue, phospholipids orange.

4 Discussion

4.1 Trehalose export in *C. glutamicum*

For more than 50 years, *C. glutamicum* has been known as an amino acid producer. During bioreactor cultivation of this bacterium, the accumulation of trehalose is a common observation and the identification of the mechanism leading to trehalose excretion could be valuable for further optimisation of bioprocesses.

C. glutamicum also serves as a model organism for the investigation of mycolic acid synthesis within the Corynebacterineae. Trehalose containing mycolic acids contribute to the high resistance of these bacteria against different antibiotic compounds, for example. Earlier studies suggested the export of trehalose in *C. glutamicum* prior to its incorporation into trehalose containing mycolic acids, defining the necessity of a trehalose export system in this bacterium. However, trehalose export has neither been shown biochemically in *C. glutamicum* nor has an export system been identified or characterised so far. The recent linkage of MmpL transporters to the export of TMM challenged the hypothesis of trehalose export for glycolipid synthesis. Trehalose export was thus investigated in this study to validate this model and to examine the reason for trehalose accumulation in *C. glutamicum* cultures.

4.1.1 Qualitative and quantitative analysis of trehalose export

Trehalose accumulation is usually not observed during shake flask cultivation of *C. glutamicum*, probably due to the low rate of excretion and trehalose recycling by the trehalose uptake system. To study trehalose export in *C. glutamicum* biochemically, a set-up was thus chosen that has been suggested earlier (Henrich, 2011). Maltose was used as a substrate for TreS-mediated trehalose production and excretion in the test strain *C. glutamicum* Δ*malQ* Δ*treX* Δ*tus*. As a negative control, the strain *C. glutamicum* Δ*malQ* Δ*treX* Δ*treS* was used. For *C. glutamicum* Δ*malQ* Δ*treX* Δ*tus*, but not for the control strain, trehalose accumulated in the supernatant with a constant rate of 0.19 nmol × mg^{-1} cdw × min^{-1} and with a yield of 0.19 mol × mol^{-1} after the addition of maltose (Figure 17). Using [^{14}C]-maltose as substrate, trehalose excretion was investigated in more detail in both strains (Figure 11). *C. glutamicum* Δ*malQ* Δ*treX* Δ*tus* and *C. glutamicum* Δ*malQ* Δ*treX* Δ*treS* imported all substrate within 50 min. As expected, conversion of maltose to trehalose in the

cytosol and export of the latter were only observed for *C. glutamicum* Δ*malQ* Δ*treX* Δ*tus*. Trehalose accumulation was also not observed for *C. glutamicum* Δ*mus*, ruling out an extracellular conversion of maltose to trehalose.

In the test strain, the intracellular amount of labelled substrate decreased with a rate of 1.23 nmol × mg^{-1} cdw × min^{-1}. However, this rate is only an approximation of the actual export rate since the total radioactivity in the assay decreased at the same time. This suggests the active metabolization of labelled maltose and the release of [^{14}C]-CO_2. Hydrolytic activity in addition to its transglucosylation activity has been described for purified TreS from *C. glutamicum* (Kim *et al.*, 2010a) as well as for TreS -enzymes from other organisms (Chen *et al.*, 2006; Wang *et al.*, 2007; Zhang *et al.*, 2011). Purified TreS from *C. glutamicum* produced 0.51 mol trehalose and 0.24 mol glucose per mol maltose (Kim *et al.*, 2010a). The decrease of the total radioactivity in the experiment was thus probably caused by the TreS-catalysed release of glucose during the interconversion of maltose and trehalose. Glucose could then be phosphorylated by one of several glucokinases present in *C. glutamicum* (Park *et al.*, 2000; Lindner *et al.*, 2010) and enter central carbon metabolism. This is also consistent with the increase of the OD_{600} observed for *C. glutamicum* Δ*malQ* Δ*treX* Δ*tus* after the addition of maltose to cells precultivated with glucose (Figure 17). Nevertheless, these experiments prove that cytosolic trehalose is excreted to the culture broth in *C. glutamicum*.

Trehalose excretion has also been observed in other bacteria. After heterologous over-expression of *otsB*, *Lactococcus lactis* accumulated 170 mM trehalose in the cytosol but at least 67% of the total product was found in the supernatant (Carvalho *et al.*, 2011). Mechanosensitive channels were proposed to catalyse trehalose excretion in this case. Trehalose reuptake and its concomitant phosphorylation by a phosphotransferase system could then allow the degradation of trehalose in this bacterium (Carvalho *et al.*, 2011).

Similarly, *E. coli* is also known to release trehalose, although this is only detectable in strains without periplasmic trehalase activity (Styrvold & Strom, 1991). Under hyperosmotic conditions, trehalose is synthesised as an osmoprotectant in *E. coli*. Its excretion from the cytosol via mechanosensitive channels allows the fine-tuning of its cytosolic concentration (Berrier *et al.*, 1992; Schleyer *et al.*, 1993). In the periplasm trehalose can be hydrolysed to glucose, which is re-imported and metabolised further (Styrvold & Strom, 1991).

A similar cycle of export of accumulated trehalose, periplasmic hydrolysis, and import of released glucose was shown to be involved in trehalose mobilisation in *Saccharomyces*

cerevisiae at the entry into the stationary growth phase but the trehalose exporter is unknown in this organism (Jules *et al.*, 2008).

In contrast, *C. glutamicum* does not possess a periplasmic trehalase and trehalose uptake is catalysed by an ABC transport system (Henrich, 2011), which does not phosphorylate trehalose during its transport. Cytosolic trehalose can be directly metabolised without the need to create a futile cycle of export and re-import and mechanosensitive channels did not contribute to trehalose excretion. Trehalose is thus not likely to be exported to adjust the osmotic strength of the cytosol in *C. glutamicum* so that another reason for its export must be assumed.

The trehalose export rate determined is very low and less than 10% of the maximum trehalose uptake rate. It is in good agreement with the trehalose accumulation rate in bioreactor cultivations of *C. glutamicum* DM1729 (pXMJ19) (see section 3.1.1), where 4.7 mM accumulated within 24 h (0.08 nmol × mg^{-1} cdw × min^{-1}). However, the export rate determined for *C. glutamicum* Δ*treS* Δ*tus* (pXMJ19_$otsBA_{E.\ coli}$), which produces trehalose during the growth phase opposed to production with stationary cells of *C. glutamicum* Δ*malQ* Δ*treX* Δ*tus*, was markedly higher (0.44 nmol × mg^{-1} cdw × min^{-1}). This indicates that the expression of the trehalose export system could be regulated in dependence of the growth phase, supporting its assumed function in cell envelope synthesis. Notably, even higher trehalose production rates (2.97 nmol × mg^{-1} cdw × min^{-1}) have been reported in the literature for a *C. glutamicum* strain overexpressing *galU* and the *otsBA*-operon from *E. coli* (Carpinelli *et al.*, 2006).

As a prerequisite for its assumed function in the periplasmic synthesis of glycolipids, trehalose export has to be fast enough to sustain the synthesis of TMM during growth of *C. glutamicum* and this question is assessed next. The cell envelope composition of *C. glutamicum* grown in minimal medium plus acetate has been determined quantitatively in a recent study (Bansal-Mutalik & Nikaido, 2011). The main glycolipid is TDM (0.5% cdw), while amounts of TMM and mycolic acids covalently bound to arabinogalactan were negligible (Bansal-Mutalik & Nikaido, 2011). Taking into consideration that two molecules of TMM are needed for the synthesis of one molecule of TDM, the minimum trehalose export rate needed to sustain growth with a specific rate of 0.35 h^{-1} is 0.05 nmol × mg^{-1} cdw × min^{-1}. The export rate determined in this work is in the same order of magnitude and sufficient to maintain periplasmic glycolipid synthesis, further supporting this assumption.

4.1.2 Trehalose export is catalysed by an unknown carrier

To characterise the nature of trehalose excretion, possible mechanisms are discussed in the following section. The observed trehalose release by *C. glutamicum* Δ*malQ* Δ*treX* Δ*tus* rules out simple diffusion of trehalose through the plasma membrane since no excretion of maltose was seen in the control strain, although the gradient of intra- to extracellular maltose was even higher than for trehalose after complete substrate uptake. In addition, the excretion rate did not depend on the intracellular trehalose concentration in this strain. Simple diffusion contributes to the excretion of some hydrophobic amino acids like L-isoleucine (Zittrich & Krämer, 1994), L-leucine (Driessen *et al.*, 1987), and L-proline (Rancourt *et al.*, 1984), for example. However, this was expected for neither trehalose nor maltose due to the hydrophilicity of both sugars.

Although transport via ABC uptake systems is generally accepted as an irreversible reaction, substrate export has been suggested for the L-histidine uptake system from *Salmonella* Typhimurium and two amino acid import systems from *Rhizobium leguminosarum* (Hosie *et al.*, 2001). However, trehalose excretion in the experiments described here was not caused by a reversal of the uptake system since the sole trehalose uptake system of *C. glutamicum* was deleted in the test strain.

The experiments discussed so far do not finally prove the presence of a trehalose export system in *C. glutamicum*. For example, the accumulation of trehalose in the supernatant could be caused by the release of trehalose during the synthesis of TDM from TMM in the periplasm. This has been described in the case of *M. tuberculosis*, where trehalose accumulation in the culture broth was detectable after the deletion of the trehalose uptake system (Kalscheuer *et al.*, 2010). To test this possibility, a strain deficient in mycolic acid synthesis was constructed by deletion of *cg3178* in the trehalose exporting test strain *C. glutamicum* Δ*malQ* Δ*treX* Δ*tus*. This gene encodes a polyketide synthase that is required for one of the last steps in mycolic acid synthesis, the condensation of two activated fatty acid precursors, forming a β-ketoacyl intermediate of TMM synthesis (Portevin *et al.*, 2004). Growth of the resulting strain in minimal medium was severely impaired and TMM and TDM were not detectable in cell extracts of this mutant. Trehalose accumulation was still observed with a rate of 0.16 nmol × mg^{-1} cdw × min^{-1}. Thus, trehalose excretion is independent of mycolic acid synthesis in *C. glutamicum*. Nevertheless, the reduction in the accumulation rate compared to the parental strain could indicate a minor contribution of

this reaction to trehalose release. Besides TMM and TDM, no other trehalose containing compounds are known to be present in the cell envelope of *C. glutamicum* so that no further trehalose releasing reactions have to be considered as potential sources for periplasmic trehalose formation. Taken together, these data prove the presence of a trehalose export system in *C. glutamicum* since neither passive diffusion across the plasma membrane, nor reversal of the import mechanism nor a periplasmic reaction releasing trehalose were responsible for trehalose accumulation in the medium.

Still, the export of trehalose could be caused by an unspecific export system like mechanosensitive channels. These are widely distributed among bacteria and have an important function in the adaptation to hypoosmotic conditions. Activated by the membrane stretch after passive water influx in response to sudden osmotic downshifts, they have been shown to release small ions and metabolites like ATP, lactose, L-glutamate, and trehalose in *E. coli* to readjust the osmotic strength of the cytosol to the surrounding (Berrier *et al.*, 1992; Schleyer *et al.*, 1993). In *C. glutamicum*, two mechanosensitive channels were identified and characterised, MscCG and MscS (Ruffert *et al.*, 1999), and the presence of further stretch activated channels has been suggested (Nottebrock *et al.*, 2003). In contrast to *E. coli*, a preferential excretion of glycine betaine and L-proline after hypoosmotic shocks was observed in *C. glutamicum* (Ruffert *et al.*, 1997). Nevertheless, the efflux of trehalose via stretch activated channels was tested in *C. glutamicum* Δ*malQ* Δ*treX* Δ*tus* after loading with [^{14}C]-maltose and performing hypoosmotic shocks. Neither maltose nor trehalose was released while the excretion of glycine betaine in a parallel experiment demonstrated the opening of mechanosensitive channels under the applied conditions (Figure 18). The formation of trehalose from maltose in the cytosol has been shown in another experiment under similar conditions (Figure 12). Thus, although assumed for *E. coli* (Berrier *et al.*, 1992; Schleyer *et al.*, 1993) and *L. Lactis* (Carvalho *et al.*, 2011), mechanosensitive channels do not contribute to trehalose export in *C. glutamicum.* Therefore, the presence of a transport system dedicated to the export of trehalose can be assumed.

Albeit trehalose export needed for cell envelope synthesis is expected to depend on the constitutive expression of (a) gene(s), additional export systems could be responsible for the transport of trehalose in the presence of high intracellular trehalose concentrations. The upregulation of genes encoding amino acid export systems in *C. glutamicum* has been observed in situations of high internal amino acid concentrations but limited catabolism. For

example, expression of *brnF*, encoding a subunit of the branched chain amino acid exporter of *C. glutamicum*, was upregulated in the presence of high intracellular L-methionine concentrations (Trötschel *et al.*, 2005). Similarly, the synthesis of the L-lysine/L-arginine exporter LysE was induced in the presence of 30 – 40 mM L-lysine (Bellmann *et al.*, 2001) and a gene encoding a diaminopentane efflux permease was upregulated in a diamino-pentane producing *C. glutamicum* strain (Kind *et al.*, 2011). Induction of export only at high concentrations prevents a futile cycle of export and import of the corresponding metabolite when present at low concentrations and this could also be the case for trehalose export. To test for a possible transcriptional regulation of trehalose export, export experiments with *C. glutamicum* Δ*malQ* Δ*treX* Δ*tus* were carried out in the presence of chloramphenicol to block *de novo* protein synthesis. Surprisingly, the trehalose efflux rate was even increased in the presence of chloramphenicol compared to the control without inhibitor. While the intracellular trehalose concentration increased to more than 150 mM, the export rate remained nearly constant during the experiment. This implies that no further export system was activated in the presence of high intracellular trehalose concentrations. Taking into consideration the low transport velocity measured, this points to a carrier-mediated export under substrate saturating conditions rather than a channel.

In *E. coli*, members of the sugar efflux transporter (SET) subfamily of the MFS permeases have been shown to catalyse the export of sugars like glucose and lactose and various glucosides and galactosides (Liu *et al.*, 1999a; Liu *et al.*, 1999b). A multitude of putative arabinose exporters has also been identified in this organism (Koita & Rao, 2012). Their physiological role is not yet clear but they have been suggested to serve as emergency valves to prevent the accumulation of toxic sugar phosphates under conditions that lead to high sugar concentrations in the cell (Sun & Vanderpool, 2011; Koita & Rao, 2012).

To assess a possible contribution of proteins homologous to known sugar exporters to the export of trehalose in *C. glutamicum*, a set of 23 genes was inactivated in the trehalose exporting test strain *C. glutamicum* Δ*malQ* Δ*treX* Δ*tus*. The sole gene that attracted attention in this screening was *cg2893* (Figure 19). Its gene product has been reported to export diaminopentane in *C. glutamicum* since the deletion of *cg2893* caused a 90% reduction of diaminopentane excretion and the product yield increased by 20% after its overexpression (Kind *et al.*, 2011). Diaminopentane is not naturally produced by *C. glutamicum* and thus the natural substrate of this permease remains unknown. However, it is not likely that trehalose

is its substrate for several reasons. First, although trehalose accumulation was no longer observed after the inactivation of this gene, the poor growth and maltose import of this strain compared to the parental strain do not allow the interpretation of these results as a lack of export. Second, in comparison to other *C. glutamicum* strains defective in mycolic acid synthesis like *C. glutamicum* Δ*cg0284* Δ*cg3174* or *C. glutamicum* Δ*otsA* Δ*treS* Δ*treY* Δ*tus*, the poor growth of *C. glutamicum* IM*cg2893* in minimal medium and the dramatically altered composition of lipid extracts (Figure 43) was also unexpected and points to a more general defect in this strain with the observed missing of TMM and TDM as a secondary effect. Third, neither the poor growth nor the altered lipid composition was restored after the addition of trehalose to the medium, which was expected in the case that this gene encoded the sole trehalose exporter in *C. glutamicum*. However, Cg2893 could also be important for the formation of a protein complex at the plasma membrane which could be needed for the biosynthesis and/or transport of further precursors for cell wall synthesis. The absence of Cg2893 could then not be compensated for by the addition of trehalose to the medium. Coupling of biosynthesis and export has been reported earlier. For example, the interaction of the phthiocerol dimycocerosate (PDIM) transporter MmpL7 and PpsE, a polyketide synthase involved in PDIM synthesis, has been shown in *M. tuberculosis* (Jain & Cox, 2005). Fourth, the trehalose export rate was not increased by the overexpression of *cg2893* in *C. glutamicum*. Finally, a BLAST search showed that *cg2893* is conserved throughout the bacterial kingdom but mycolic acid synthesis, for which trehalose export is assumed to be necessary, is limited to the Corynebacterineae subgroup of the Actinobacteria. To fully characterise the effect of *cg2893* inactivation in *C. glutamicum*, further examination of the composition of the cell envelope, including the plasma membrane, the peptidoglycan, arabinogalactan, and mycolic acid layers are necessary.

An overview of the mechanisms investigated for trehalose export in this work is shown in Figure 44. Simple diffusion of trehalose through the plasma membrane was excluded as well as an unspecific excretion via mechanosensitive channels, a reversal of trehalose import, and the dependence of trehalose export on glycolipid synthesis. Analysis of the export mechanism indicated a carrier mediated export of trehalose. The export rate determined here was very low but sufficient to sustain glycolipid synthesis in the periplasm during growth. These observations indicate the dedication of trehalose export for this purpose and further support the model of periplasmic TMM synthesis in *C. glutamicum*.

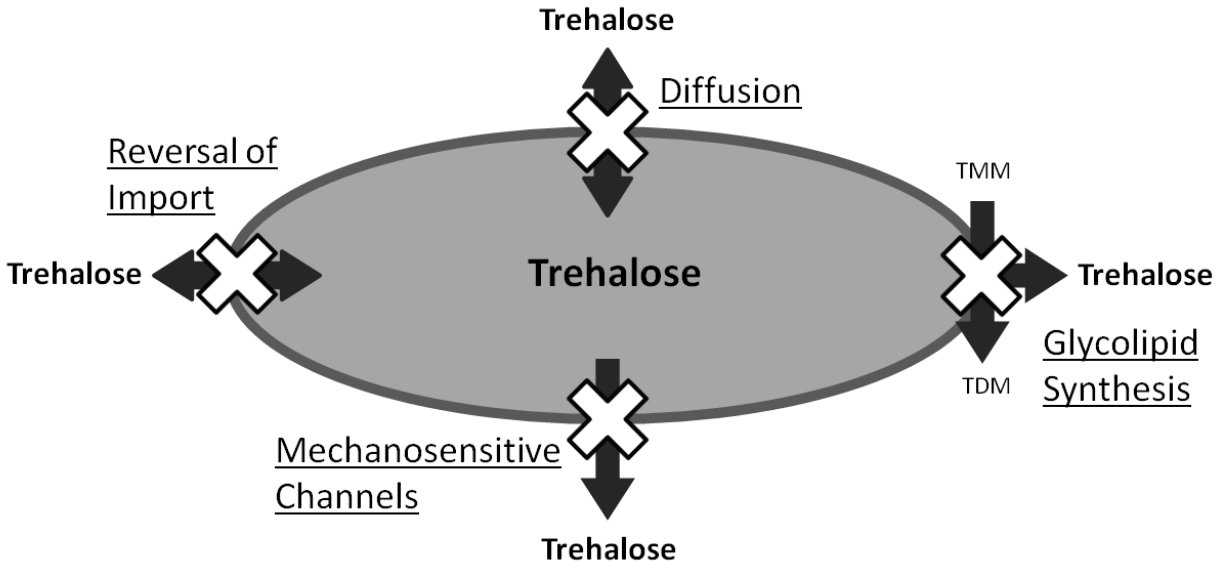

Figure 44: Mechanisms for trehalose excretion investigated and excluded in this work.

4.2 Glycolipid metabolism in *C. glutamicum*

The model of periplasmic TMM synthesis in *C. glutamicum* was challenged by the recent assignment of TMM export from the cytosol to the periplasm by MmpL transporters in *M. tuberculosis, M. smegmatis*, and *C. glutamicum*. TMM accumulation was observed in *M. tuberculosis* and *M. smegmatis* extracts after inhibition of MmpL3 and this was explained by the inability to export TMM from the cytosol (Grzegorzewicz *et al.*, 2012; Tahlan *et al.*, 2012; Varela *et al.*, 2012). Although this was not observed in *C. glutamicum* after the inactivation of *cg0284* and *cg3174*, two *mmpL*-genes encoding proteins with apparent redundant function, the resulting mutants were unable to form TMM and TDM (Varela *et al.*, 2012). This phenotype was also confirmed in this work. Notably, the deletion of both *mmpL*-genes was possible while this was not achieved in the above cited study and was also not possible for *mmpL3*, the corresponding gene in *M. tuberculosis* and *M. smegmatis* (Grzegorzewicz *et al.*, 2012). This again shows that mycolic acid synthesis is not essential in *C. glutamicum*.

The model of periplasmic TMM synthesis is mainly based on the incorporation of external trehalose into TMM in *C. glutamicum* Δ*otsA* Δ*treS* Δ*treY* Δ*tus* (Henrich, 2011). It is also supported by the improved resistance of this strain against carbenicillin and ethambutol after the addition of trehalose to the medium, indicating a reduced permeability of the cell envelope due to the restoration of mycolic acid synthesis in the presence of external

trehalose (Figure 37 and 38). Still, the observed accumulation of TMM in *M. tuberculosis* and *M. smegmatis* does not contradict the extracellular incorporation of trehalose into glycolipids in *C. glutamicum*. No evidence was given in these studies that TMM accumulated in the cytosol and the accumulation of TMM in the periplasmic leaflet of the plasma membrane could still be possible. Further, no accumulation of TMM was seen under similar conditions in *C. glutamicum* (see Figure 41 and Varela *et al.* (2012)), which indicates either differences in the mechanism or the regulation of TMM synthesis between these bacteria.

MmpL transporters belong to the RND transporter family. In Gram-negative bacteria, these proteins are typically associated with at least two other proteins to span the periplasm, a so called membrane fusion protein and a channel forming outer membrane protein. Well known examples are AcrB-AcrA-TolC from *E. coli*, which exports β-lactam antibiotics, fluoroquinolones, free fatty acids, and other substrates (Sulavik *et al.*, 2001), and MexB-MexA-OprM from *Pseudomonas aeruginosa*, which transports a broad range of antibiotics and other substances (Poole *et al.*, 1993). Importantly, based on structural studies, the export of periplasmic substrates by RND transporters has been suggested in some cases (Murakami *et al.*, 2002; Symmons *et al.*, 2009).

In the following, a possible role of MmpL transporters in the synthesis and transport of mycolic acids in *C. glutamicum* is presented, which - besides the transport of mycolic acids over the plasma membrane - also considers its transport through the periplasmic space (Figure 45). Since TMM synthesis does not depend on activated trehalose as a precursor (Tzvetkov *et al.*, 2003; Woodruff *et al.*, 2004), the activation of a mycolic acid precursor (Myc-X) must be assumed to energise the formation of a covalent bond to trehalose. The uptake of external trehalose is also not required for TMM synthesis (Henrich, 2011) and in addition, the export of trehalose could be shown in this study. Thus, the hypothetical linkage of trehalose and Myc-X, resulting in TMM formation, could occur on the periplasmic side of the membrane after the export of Myc-X by an unknown transporter. A mannosylphosphopolyprenol-bound mycolic acid has indeed been identified in *M. smegmatis* (Besra *et al.*, 1994) and this could serve both as the carrier and the activated precursor for the periplasmic synthesis of TMM. In *C. matruchotii*, an ABC transporter was linked to the export of short chain mycolic acids from the cytosol, which was concluded from an altered lipid composition of the mycolic acid layer in the absence of this transporter (Wang *et al.*, 2006). ABC transporters could thus flip Myc-X to the periplasmic leaflet of the plasma membrane.

LipidA, for example, which is the main constituent of the outer membrane in Gram-negative bacteria, is flipped from the cytosolic leaflet of the plasma membrane to the periplasmic site by a homodimer of MsbA, a protein belonging to the ABC superfamily (Polissi & Georgopoulos, 1996; Zhou *et al.*, 1998).

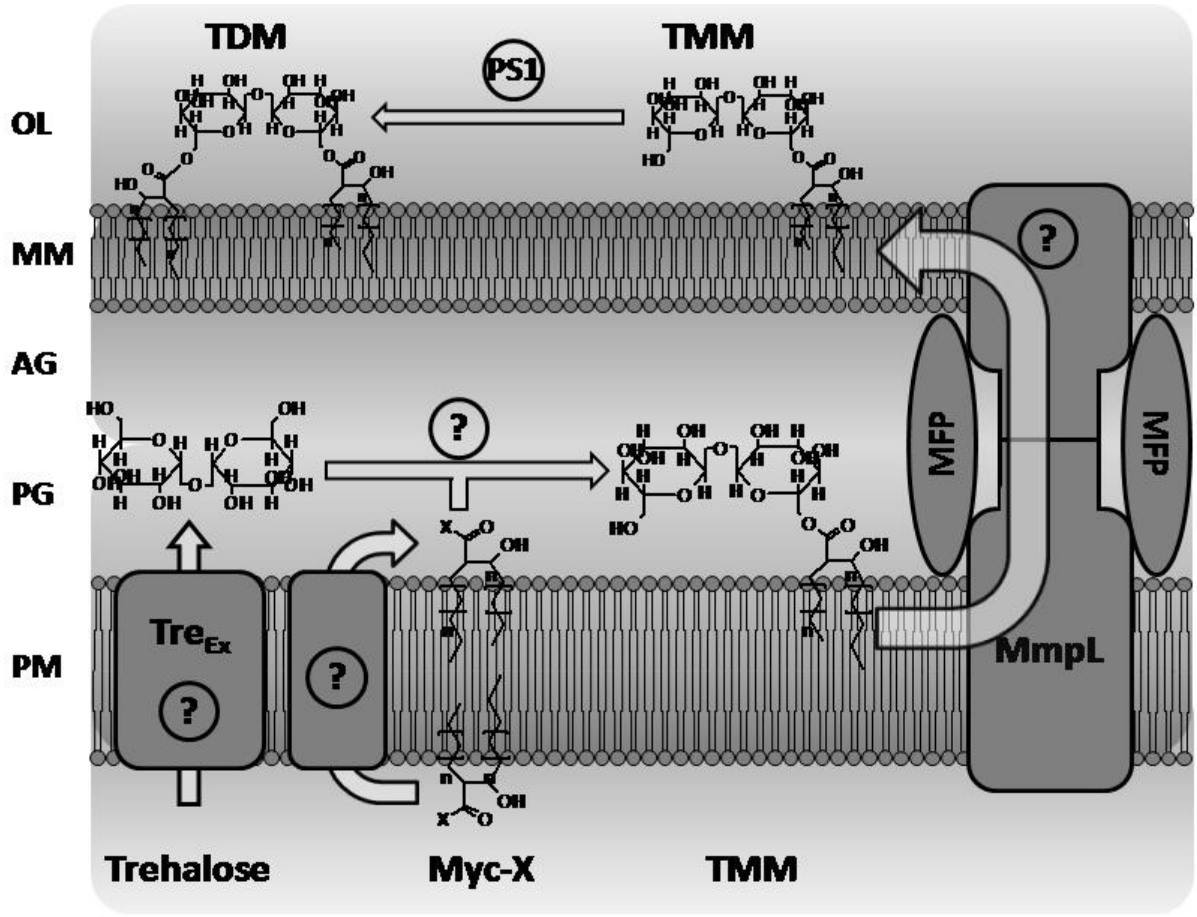

Figure 45: Hypothetical model for the synthesis and transport of TMM in *C. glutamicum*. OL: outer layer; **MM**: mycolic acid membrane; **AG**: arabinogalactan layer; **PG**: Peptidoglycan layer; **PM**: plasma membrane; **TMM**: trehalose monomycolate; **TDM**: trehalose dimycolate; **Myc-X**: unknown activated mycolic acid precursor; **PS1**: mycolyltransferase (6 isoenzymes present); **MFP**: membrane fusion protein; **MmpL**: mycobacterial membrane protein large (2 proteins with redundant function).

In *M. tuberculosis*, the gene *rv3802* was speculated to encode an enzyme that could catalyse the transfer of mycolic acids from a carrier to trehalose (Gande *et al.*, 2004). This gene clusters with genes encoding proteins involved in trehalose glycolipid synthesis. This cluster is conserved in all Corynebacterineae (two mycolyltransferases, a polyketide synthase, an acyl-AMP ligase, and an acyl-CoA carboxylase; compare Figure 4) and *rv3802* is essential in *M. tuberculosis* (Sassetti *et al.*, 2003). The encoded protein contains a serine esterase motif

that could catalyse the formation of an ester bond between trehalose and a mycolic acid and it is predicted to be localised in the periplasm and to be anchored in the plasma membrane. This gene is thus an interesting candidate for further analysis of TMM synthesis.

In agreement with periplasmic substrate recognition of RND transporters (see above), TMM formed in this hypothetical pathway could then be transported from the periplasmic side of the plasma membrane to the mycolic acid layer by a tripartite complex consisting of either of two redundant MmpL proteins (Varela *et al.*, 2012), an unidentified membrane fusion protein, and an also unidentified protein in the mycolic acid layer, where TMM serves as mycolic acid donor for the formation of TDM (Puech *et al.*, 2000) and the mycolylation of arabinogalactan and of several proteins (Brand *et al.*, 2003; Huc *et al.*, 2010; Huc *et al.*, 2013). A putative membrane fusion protein was found in the *C. glutamicum* genome (*cg3322*) that shows significant sequence identity to the membrane fusion protein HlyD involved in haemolysin export in different bacteria. Although the annotated protein is markedly bigger than AcrA from *E. coli* (620 and 397 amino acids), both are predicted periplasmic proteins with an N-terminal transmembrane helix, tethering the protein to the membrane. Unfortunately, attempts to delete *cg3322* in this study were not successful. The genome of *M. tuberculosis* contains 5 *mmpS* genes (mycobacterial membrane proteins small), which all except for one cluster with *mmpL* genes and which all encode periplasmic proteins with putative N-terminal transmembrane helices. Consequently, MmpS4 and MmpS5 have been shown to participate in siderophore and glycopeptidolipid export via MmpL4 and MmpL5 and were suggested to function as membrane fusion proteins in *M. tuberculosis* (Deshayes *et al.*, 2010; Wells *et al.*, 2013).

This model integrates both the assumption of periplasmic TMM formation and the recent linkage of MmpL proteins with mycolic acid transport. Nevertheless, further experimental confirmation is needed to evaluate this model. To finally prove the significance of trehalose export for TMM synthesis in *C. glutamicum*, the trehalose export system has to be identified.

4.3 Characterisation of TusE and trehalose nanosensor construction

Since a trehalose export system in *C. glutamicum* could not be identified by a rational approach, the screening of a library of *C. glutamicum* mutants was targeted next. As a screening tool to display altered intracellular trehalose concentrations, a genetically encoded FRET-nanosensor for trehalose was constructed. Such sensors have been described

for a number of different metabolites in the literature and they allow the non-disruptive real-time analysis of metabolite dynamics in living cells (Fehr *et al.*, 2004; Takanaga *et al.*, 2008). Periplasmic solute binding proteins have been successfully applied as metabolite sensing domains in nanosensors and the putative trehalose binding protein of *C. glutamicum* was characterised in this study and subsequently used for sensor construction.

4.3.1 The gene *cg0834* encodes the binding protein of the ABC trehalose uptake system

Trehalose uptake and metabolisation were recently described in *C. glutamicum* (Henrich, 2011). While deletion and episomal overexpression of *cg0830* – *cg0835* confirmed that this gene cluster encodes a trehalose uptake system (Henrich, 2011), the functions of the individual gene products have not been investigated experimentally yet. Since the putative periplasmic trehalose binding protein should be used to construct a genetically encoded trehalose nanosensor, the function of the *cg0834* gene product was assessed in this study. The encoded protein was overproduced in *E. coli* BL21 (DE3) without the putative N-terminal signal peptide and purified via IMAC and SEC. When analysed for trehalose binding by fluorescence detection, the high affinity binding of trehalose to the protein could be shown (Figure 29). This confirms the function of TusE as the sugar binding protein of the trehalose ABC uptake system and shows that the 25 N-terminal amino acids are not required for trehalose binding. The dissociation constant (0.42 µM) is slightly higher than the Michaelis-constant (0.16 µM) determined in transport assays (Henrich, 2011). A possible explanation could be a transport model which only allows the interaction of substrate loaded binding proteins with the permease domains of the transporter (Horlacher *et al.*, 1998). Further, acylation of TusE could alter its substrate affinity *in vivo*.

Periplasmic binding proteins are responsible for the high substrate affinity of ABC uptake systems and the dissociation constants reported for other periplasmic sugar binding proteins are in a similar range as for TusE. The trehalose/maltose binding protein of *T. litoralis*, for example, binds trehalose and maltose both with a dissociation constant of 0.16 µM (Horlacher *et al.*, 1998). For the binding of maltose and maltotriose to the periplasmic maltose binding protein of *E. coli*, dissociation constants of 1 µM and 0.16 µM, respectively, were reported, while the Michaelis-constants for the two substrates determined in transport measurements were 1 µM and 2 µM, respectively (Szmelcman *et al.*, 1976).

TusE carries an N-terminal signal peptide typical for lipoproteins. Acylation is a common

modification of substrate binding proteins of Gram-positive bacteria to anchor these proteins in the plasma membrane to prevent their loss to the surrounding (Gilson *et al.*, 1988). The lipobox sequence of TusE formed by amino acids 22 to 27, A-L-A-G-C-S, matches well with the consensus sequence (L/V/A)-L-(S/A)-(A/G)-C-(S/G) (Sutcliffe & Russell, 1995), where C denotes the first amino acid of the mature protein and is also the residue that is thioacylated. However, acylation of TusE has not been shown experimentally. This could be achieved by labelling of the protein with [^{14}C]-fatty acids during growth, for example. Interestingly, TusE was identified in extraction fractions containing proteins inserted into or associated with the peptidoglycan-arabinogalactan-mycolate-complex (Marchand *et al.*, 2012), verifying its periplasmic localisation *in vivo*.

4.3.2 Construction of a genetically encoded trehalose nanosensor

TusE was applied for the construction of a genetically encoded FRET-nanosensor. Therefore, *tusE* was terminally fused to *ecfp* and *eyfp*. Constructs using full length TusE or TusEΔN47, which lacks the predicted N-terminal PepSY domain probably not needed for trehalose binding, did not show a change of the FRET-efficiency upon trehalose addition. A functional sensor could be constructed using TusEΔN32 (TreSen2, Figure 31). However, the signal change of TreSen2 was only very low (0.03). A high signal change upon ligand binding is needed for reliable metabolite detection. Further, the maximum signal change of a sensor can be significantly reduced *in vivo* as in the case of one of the ATP-sensors tested in this study.

The sensor was thus optimised by systematic linker truncations taking into consideration not only the artificial amino acid linkers introduced between the binding protein and the two fluorescent proteins but also the terminal regions of the proteins. Rigid linkers are thought to translate the conformational change of the binding protein more efficiently into an altered distance and/or orientation of the two fluorescent proteins than long and flexible linkers, leading to an altered FRET-efficiency (Deuschle *et al.*, 2005; Lager *et al.*, 2006). In the sensor with the highest signal change upon trehalose addition, TreSen28, both linkers were truncated from 2 × 6 to 2 × 2 amino acids, and 10, 6, and 32 amino acids were removed from the C-terminus of ECFP, the N-terminus of mVenus (which replaced EYFP), and from the N-terminus of TusE, respectively. The maximum signal change of 0.39 for TreSen28 is in the same order of magnitude as reported for different other FRET-sensors. For example, a set of

maltose sensors with signal changes between 0.15 and 0.30 (Fehr *et al.*, 2002), ATP sensors with signal changes between 0.3 – 1.9 (Imamura *et al.*, 2009) and glucose sensors with signal changes from 0.15 – 0.7 were described (Deuschle *et al.*, 2005).

The K_d-values of trehalose sensors containing different N-terminal truncations of TusE varied between 0.06 µM and 1.22 µM. Since variations of the K_d–value for different constructs using the same truncation, TusEΔN25, were also measured (0.26 µM – 1.08 µM), these values likely not represent altered affinities of these constructs but were rather due to differences in sample preparation and analysis at different time points. Further, truncation of the N-terminal PepSY domain should not alter the affinity of the protein since this domain is not likely to be needed for substrate binding.

Although FRET-sensors have been used successfully for a variety of applications described in the literature, some drawbacks were observed in this study. For example, using the ECFP-EYFP FRET-pair, the blue light used for excitation was phototoxic for *C. glutamicum* cells when exposed repeatedly. Formation of the chromophore of GFP and derivatives thereof needs oxygen and causes a time-dependent change of the fluorescent properties of the protein (Nagai *et al.*, 2002). Although the analyte is not altered chemically by this kind of detection, high-level expression of FRET-sensors could decrease the concentration of free ligand in the cell and thereby indirectly influence metabolite concentrations. Constitutive expression of ATP-sensors was highly unstable in *C. glutamicum* opposed to an inducible expression, for example, indicating detrimental effects of these sensors for the cell. Signal changes of a FRET-sensor rely on a conformational change of the binding protein and this could also be triggered by conditions other than ligand binding. Sensors with K_d-values far below or above the prevailing ligand concentration are thus valuable controls to exclude unspecific sensor responses and have been constructed in many cases by the introduction of point mutations in the ligand binding site (Deuschle *et al.*, 2006; Imamura *et al.*, 2009).

4.3.3 Engineering the trehalose binding site of TusE

For the use of a FRET-sensor *in vivo*, its K_d-value has to be in the same range as the intracellular ligand concentration. In *C. glutamicum*, trehalose concentrations in the millimolar range were reported under different conditions (Tzvetkov *et al.*, 2003; Wolf *et al.*, 2003). In *C. glutamicum* Δ*malQ* Δ*treX* Δ*tus* the intracellular trehalose concentration was around 4 mM even in the stationary growth phase and exceeded 100 mM several hours after

the addition of maltose. To use a trehalose sensor for the screening of a *C. glutamicum* mutant library, the affinity of TreSen28 should be reduced by a rational approach. Based on a structural homology model of TusE, amino acids putatively involved in trehalose binding were mutated in TreSen28. However, the affinity of four resulting constructs was only slightly altered compared to TreSen28 (0.24 µM) with the lowest affinity being 2.04 µM for TreSen28^{Y313F}. Most mutations in TusE tested here led to sensors no longer responding to trehalose addition but it cannot be told whether trehalose binding or the translation of binding to an altered FRET-efficiency was impeded by these mutations.

Several FRET-sensors described in the literature have been changed in their affinity using site-directed mutagenesis. For example, the sucrose binding protein from *Agrobacterium tumefaciens* was used to construct a sucrose sensor and its K_d-value could be increased from 4 µM to 46 mM by replacing only one tryptophan residue by alanine (Lager *et al.*, 2006). Similarly, the K_d-value of a maltose sensor was changed from 2 µM to 226 µM also by mutation of one tryptophan residue to alanine (Fehr *et al.*, 2002).

The inability to markedly change the sensors affinity for trehalose suggests that the binding site might not have been predicted correctly. For the construction of a structural homology model of TusE, the crystal structure of the trehalose/maltose binding protein from *T. litoralis* served as a template. This has been resolved at 1.85 Å resolution in the presence of trehalose, which is bound in the sugar binding site forming van der Waals contacts and hydrogen bonds with a total of 16 amino acids (Diez *et al.*, 2001). The amino acid identity of both proteins is only 30%, which is very low for the construction of an accurate structural model. At low sequence identity, alignment errors can lead to the false prediction of the entire structure of a protein (Baker & Sali, 2001). However, the structures of periplasmic solute binding proteins are usually similar despite their low sequence identity (Quiocho & Ledvina, 1996). The quality of a homology model can be described with the help of the Qmean4- and the Z-score. The former is a combination of structural descriptors for distances, torsion angles, and solvation using statistical potentials (Benkert *et al.*, 2008). The Z-score evaluates the model by comparison of its structural features to experimentally determined structures (Benkert *et al.*, 2011). Both values (0.56 and -3.4, respectively) indicate that the overall quality of the structural prediction for TusE is rather low. Analysis of the local scores of the model shows that this is mainly caused by regions of undefined secondary structure (loops) in TusE while structural elements like α-helices and β-sheets

including the central region of TusE containing the putative sugar binding pocket show good local scores. Thus, the quality of the TusE model should be acceptable in the regions essential for substrate binding. The amino acids exerting trehalose binding are probably not conserved between TusE and the *T. litoralis* trehalose/maltose binding protein and were thus not identified correctly in this approach.

4.4 Manipulation of trehalose uptake leads to optimised production strains

C. glutamicum is one of the industrial workhorses for the production of amino acids. The economic viability of a production process for a bulk product is largely determined by the substrate costs and therefore the product yield of a bioprocess is an important parameter. The maximum theoretical yield is determined by the topology of the metabolic network and the substrate used, but is often not achieved in reality. One reason can be the redirection of the carbon flux from product synthesis to the formation of one or more byproducts. Besides their influence on the product yield, the latter can also hamper the purification of the product. The reduction of byproduct synthesis is thus important for several reasons. Typical byproducts accumulating during the cultivation of *C. glutamicum* are pyruvate, acetate, lactate, L-alanine, L-valine, L-glutamate, α-ketoglutarate, and trehalose (Vallino & Stephanopoulos, 1993; Wittmann & Heinzle, 2001; Kind *et al.*, 2011). In this work, the accumulation of trehalose in the culture broth of *C. glutamicum* during bioreactor cultivation was investigated to clarify the apparent contradiction of trehalose accumulation in spite of the presence of a high-affinity trehalose uptake system in *C. glutamicum* and the observed utilisation of trehalose as substrate for growth during shake flask cultivation (Henrich, 2011). During bioreactor cultivation of *C. glutamicum* DM1729 (pXMJ19), 4.7 ± 2.1 mM trehalose was detected in the supernatant, corresponding to 2.1% of the amount of carbon used as substrate. This could be reduced to only 0.57 ± 0.2 mM (0.3%) by the homologous over-expression of the *tus*-genes in *C. glutamicum* DM1729 (pXMJ19_*tus*).

Expression of the *tus*-genes was examined in both strains to investigate the reason for trehalose accumulation. While *tusK* transcripts were hardly detected at any time in *C. glutamicum* DM1729 (pXMJ19), *tusFG* and *tusE* transcripts were detectable at the beginning of the fermentation but decreased rapidly (Figure 7). Correspondingly, trehalose accumulated during the second half of the fermentation.

Since the function of TusK can be partially taken over by the ATPase of the maltose uptake

system in *C. glutamicum* (Schulte, 2011), the absence of *tusK* transcripts does not necessarily abolish trehalose import. Further, *tusK* transcripts were also detected comparatively weakly in *C. glutamicum* DM1729 (pXMJ19_*tus*) and thus there might have been a problem with the probe used for detection. The permeases TusF and TusG, on the other hand, are essential constituents of the uptake system (Henrich, 2011; Rehorst, 2013) as well as the trehalose binding protein TusE (Schulte, 2011). Summing up, the rapid decrease of *tus*-gene expression was responsible for trehalose accumulation during fermenter cultivations of *C. glutamicum* DM1729 (pXMJ19).

The transcriptional organisation and regulation of these genes has been investigated in several studies. Binding sites for the global transcriptional regulator AtlR were identified upstream of *tusE* and *tusG* and AtlR has been shown to activate the transcription of both genes (Laslo *et al.*, 2012; Rehorst, 2013). As an effector molecule of this regulator, an intermediate of arabitol metabolism has been suggested but could not be identified so far (Laslo *et al.*, 2012). The global regulator RamA was also identified as a transcriptional activator for *tusE* expression during growth on glucose (Auchter *et al.*, 2010). RamB regulates the expression of *tusG* (Schulte, 2011) and cAMP dependent binding of the global regulator GlxR to a binding site upstream of *tusK* was shown (Jungwirth *et al.*, 2013). Since cAMP levels are high in *C. glutamicum* during growth on glucose (Kim *et al.*, 2004) and GlxR acts as transcriptional activator of *tusK* (Toyoda *et al.*, 2011), the decrease of *tusK* expression during bioreactor cultivation with glucose cannot be explained. In spite of the knowledge gained on their transcriptional regulation, it is not understood why *tus*-gene expression decreased during the fermenter cultivation of *C. glutamicum* DM1729 (pXMJ19) and to the contrary, trehalose serves as carbon source for *C. glutamicum* during shake flask cultivation.

While beneficial for byproduct reduction, trehalose reuptake could be detrimental for trehalose overproduction in *C. glutamicum*. This could lead to enhanced product degradation and further, increased intracellular product concentrations can exert negative regulatory effects on biosynthetic pathways. For example, L-tryptophan production was enhanced by 10% to 20% in a *C. glutamicum* strain with a lower level of L-tryptophan uptake (Ikeda & Katsumata, 1995).

The *tus*-gene cluster was therefore deleted in *C. glutamicum* Δ*treS* (pXMJ19_$otsBA_{E.\ coli}$), which has been reported to produce trehalose (Padilla *et al.*, 2004a). Compared to the parental strain, the trehalose yield increased by 40% for *C. glutamicum* Δ*treS* Δ*tus*

(pXMJ19_*otsBA*$_{E.\ coli}$) while the amount of external trehalose even increased by 80%. The higher rate of trehalose accumulation in the medium for the latter strain can be explained by the lack of trehalose reuptake, which thus effects trehalose production significantly. The trehalose export rate in *C. glutamicum* Δ*treS* Δ*tus* (pXMJ19_*otsBA*$_{E.\ coli}$) did not depend on the internal trehalose concentration, showing that trehalose production is limited by its export. In contrast, overexpression of *galU* has been reported to further increase the trehalose production rate in *C. glutamicum* Δ*treS* (pXMJ19_*otsBA*) by improving the supply of UDP-glucose, which was reported to be limiting in this strain (Padilla *et al.*, 2004b). To test whether trehalose synthesis or its export is limiting, the overexpression of *galU* in *C. glutamicum* Δ*treS* Δ*tus* (pXMJ19_*otsBA*$_{E.\ coli}$) would be interesting.

At the entry to the stationary phase, the intracellular trehalose concentrations increased in both strains tested here. This could result from an enhanced rate of trehalose synthesis caused by the degradation of glycogen. Glycogen accumulates in *C. glutamicum* during the growth phase and is degraded afterwards via the debranching enzyme GlgX, producing linear maltodextrines, which serve as precursors for trehalose synthesis via the TreYZ pathway (Seibold & Eikmanns, 2007). Trehalose overproduction via the TreYZ-pathway has already been shown in *C. glutamicum* strains (Padilla *et al.*, 2004b) and likely contributed to trehalose production in the experiments described in this work.

Concluding, deletion of the *tus*-genes improved trehalose production in *C. glutamicum* Δ*treS* Δ*tus* (pXMJ19_*otsBA*$_{E.\ coli}$). On the other hand, the overproduction of the trehalose uptake system resulted in a significant reduction of byproduct accumulation in L-lysine producing strains. Engineering trehalose uptake is thus an interesting target for the optimisation of production strains.

5 References

Abe, S., Takayama, K. I. & Kinoshita, S. (1967). Taxonomical studies on glutamic acid-producing bacteria. *J Gen Appl Microbiol* **13**, 279-301.

Altschul, S. F., Madden, T. L., Schaffer, A. A., Zhang, J., Zhang, Z., Miller, W. & Lipman, D. J. (1997). Gapped BLAST and PSI-BLAST: A new generation of protein database search programs. *Nucleic Acids Res* **25**, 3389-3402.

Arguelles, J. C. (2000). Physiological role of trehalose in bacteria and yeasts: a comparative analysis. *Arch Microbiol* **174**, 217-224.

Arndt, A. & Eikmanns, B. J. (2008). Regulation of carbon metabolism in *Corynebacterium glutamicum*. In *Corynebacteria: genomics and molecular biology*, pp. 155-182. Edited by A. Burkovski. Norfolk: Caister Academic.

Arnold, K., Bordoli, L., Kopp, J. & Schwede, T. (2006). The SWISS-MODEL workspace: A web-based environment for protein structure homology modelling. *Bioinformatics* **22**, 195-201.

Auchter, M., Cramer, A., Huser, A. *et al.* (2010). RamA and RamB are global transcriptional regulators in *Corynebacterium glutamicum* and control genes for enzymes of the central metabolism. *J Biotechnol*.

Baker, D. & Sali, A. (2001). Protein structure prediction and structural genomics. *Science* **294**, 93-96.

Bansal-Mutalik, R. & Nikaido, H. (2011). Quantitative lipid composition of cell envelopes of *Corynebacterium glutamicum* elucidated through reverse micelle extraction. *Proc Natl Acad Sci U S A* **108**, 15360-15365.

Barbas, J. P. & Mascarenhas, R. D. (2009). Cryopreservation of domestic animal sperm cells. *Cell Tissue Bank* **10**, 49-62.

Becker, J. & Wittmann, C. (2012). Systems and synthetic metabolic engineering for amino acid production - the heartbeat of industrial strain development. *Curr Opin Biotechnol* **23**, 718-726.

Bellmann, A., Vrljic, M., Patek, M., Sahm, H., Krämer, R. & Eggeling, L. (2001). Expression control and specificity of the basic amino acid exporter LysE of *Corynebacterium glutamicum*. *Microbiology* **147**, 1765-1774.

Benkert, P., Tosatto, S. C. E. & Schomburg, D. (2008). QMEAN: A comprehensive scoring function for model quality assessment. *Proteins: Structure, Function, and Bioinformatics* **71**, 261-277.

Benkert, P., Biasini, M. & Schwede, T. (2011). Toward the estimation of the absolute quality of individual protein structure models. *Bioinformatics* **27**, 343-350.

Berrier, C., Coulombe, A., Szabo, I., Zoratti, M. & Ghazi, A. (1992). Gadolinium ion inhibits loss of metabolites induced by osmotic shock and large stretch-activated channels in bacteria. *Eur J Biochem* **206**, 559-565.

Besra, G. S., Sievert, T., Lee, R. E., Slayden, R. A., Brennan, P. J. & Takayama, K. (1994). Identification of the apparent carrier in mycolic acid synthesis. *Proc Natl Acad Sci U S A* **91**, 12735-12739.

Bideaux, C., Alfenore, S., Cameleyre, X., Molina-Jouve, C., Uribelarrea, J. L. & Guillouet, S. E. (2006). Minimization of glycerol production during the high-performance fed-batch ethanolic fermentation process in *Saccharomyces cerevisiae*, using a metabolic model as a prediction tool. *Appl Environ Microbiol* **72**, 2134-2140.

Bloch, K. (1977). Control mechanisms for fatty acid synthesis in *Mycobacterium smegmatis*. *Adv Enzmol RAMB* **45**, 1-84.

Blombach, B., Riester, T., Wieschalka, S., Ziert, C., Youn, J. W., Wendisch, V. F. & Eikmanns, B. J. (2011). *Corynebacterium glutamicum* tailored for efficient isobutanol production. *Appl Environ Microbiol* **77**, 3300-3310.

Botzenhardt, J. (2004). Regulation des Betaintransporters BetP aus *Corynebacterium glutamicum* während der Anpassung an hyperosmotischen Stress. Inaugural-Dissertation, Mathematisch-Naturwissenschaftliche Fakultät, Universität zu Köln.

Brand, S., Niehaus, K., Pühler, A. & Kalinowski, J. (2003). Identification and functional analysis of six mycolyltransferase genes of *Corynebacterium glutamicum* ATCC 13032: the genes *cop1*, *cmt1*, and *cmt2* can replace each other in the synthesis of trehalose dicorynomycolate, a component of the mycolic acid layer of the cell envelope. *Arch Microbiol* **180**, 33-44.

Brennan, P. J. & Nikaido, H. (1995). The Envelope of Mycobacteria. *Annu Rev Biochem* **64**, 29-63.

Burkovski, A. & Krämer, R. (2002). Bacterial amino acid transport proteins: occurrence, functions, and significance for biotechnological applications. *Appl Microbiol Biotechnol* **58**, 265-274.

Camacho, L. R., Constant, P., Raynaud, C., Lanéelle, M. A., Triccas, J. A., Gicquel, B., Daffé, M. & Guilhot, C. (2001). Analysis of the phthiocerol dimycocerosate locus of *Mycobacterium tuberculosis*. Evidence that this lipid is involved in the cell wall permeability barrier. *J Biol Chem* **276**, 19845-19854.

Carolé, S., Pichoff, S. & Bouch, J. P. (1999). *Escherichia coli* gene *ydeA* encodes a major facilitator pump which exports L-arabinose and isopropyl-beta-D-thiogalactopyranoside. *J Bacteriol* **181**, 5123-5125.

Carpenter, J. F., Crowe, L. M. & Crowe, J. H. (1987). Stabilization of phosphofructokinase with sugars during freeze-drying: characterization of enhanced protection in the presence of divalent cations. *Biochim Biophys Acta* **923**, 109-115.

Carpinelli, J., Krämer, R. & Agosin, E. (2006). Metabolic engineering of *Corynebacterium glutamicum* for trehalose overproduction: role of the TreYZ trehalose biosynthetic pathway. *Appl Environ Microbiol* **72**, 1949-1955.

Carvalho, A. L., Cardoso, F. S., Bohn, A., Neves, A. R. & Santos, H. (2011). Engineering trehalose synthesis in *Lactococcus lactis* for improved stress tolerance. *Appl Environ Microbiol* **77**, 4189-4199.

Chami, M., Bayan, N., Dedieu, J. C., Leblon, G., Shechter, E. & Gulikkrzywicki, T. (1995). Organization of the outer layers of the cell-envelope of *Corynebacterium glutamicum* - a combined freeze-etch electron-microscopy and biochemical-study. *Biol Cell* **83**, 219-229.

Chen, L. Q., Qu, X. Q., Hou, B. H., Sosso, D., Osorio, S., Fernie, A. R. & Frommer, W. B. (2012). Sucrose efflux mediated by SWEET proteins as a key step for phloem transport. *Science* **335**, 207-211.

Chen, Y. S., Lee, G. C. & Shaw, J. F. (2006). Gene cloning, expression, and biochemical characterization of a recombinant trehalose synthase from *Picrophilus torridus* in *Escherichia coli*. *J Agric Food Chem* **54**, 7098-7104.

Converse, S. E., Mougous, J. D., Leavell, M. D., Leary, J. A., Bertozzi, C. R. & Cox, J. S. (2003). MmpL8 is required for sulfolipid-1 biosynthesis and *Mycobacterium tuberculosis* virulence. *Proc Natl Acad Sci U S A* **100**, 6121-6126.

Crowe, J. H., Carpenter, J. F. & Crowe, L. M. (1998). The role of vitrification in anhydrobiosis. *Annu Rev Physiol* **60**, 73-103.

De Smet, K. A., Weston, A., Brown, I. N., Young, D. B. & Robertson, B. D. (2000). Three pathways for trehalose biosynthesis in mycobacteria. *Microbiology* **146 (Pt 1)**, 199-208.

De Sousa-D'Auria, C., Kacem, R., Puech, V., Tropis, M., Leblon, G., Houssin, C. & Daffé, M. (2003). New insights into the biogenesis of the cell envelope of corynebacteria: identification and functional characterization of five new mycoloyltransferase genes in *Corynebacterium glutamicum*. *FEMS Microbiol Lett* **224**, 35-44.

Delaunay, S., Gourdon, P., Lapujade, P., Mailly, E., Oriol, E., Engasser, J. M., Lindley, N. D. & Goergen, J. L. (1999). An improved temperature-triggered process for glutamate production with *Corynebacterium glutamicum*. *Enzyme Microb Tech* **25**, 762-768.

Demain, A. L., Jackson, M., Vitali, R. A., Hendlin, D. & Jacob, T. A. (1966). Production of guanosine-5'-monophosphate and inosine-5'-monophosphate by fermentation. *Appl Microbiol* **14**, 821-825.

Deshayes, C., Bach, H., Euphrasie, D. *et al.* (2010). MmpS4 promotes glycopeptidolipids biosynthesis and export in *Mycobacterium smegmatis*. *Mol Microbiol* **78**, 989-1003.

Deuschle, K., Okumoto, S., Fehr, M., Looger, L. L., Kozhukh, L. & Frommer, W. B. (2005). Construction and optimization of a family of genetically encoded metabolite sensors by semirational protein engineering. *Protein Sci* **14**, 2304-2314.

Deuschle, K., Chaudhuri, B., Okumoto, S., Lager, I., Lalonde, S. & Frommer, W. B. (2006). Rapid metabolism of glucose detected with FRET glucose nanosensors in epidermal cells and intact roots of *Arabidopsis* RNA-silencing mutants. *Plant Cell* **18**, 2314-2325.

Diez, J., Diederichs, K., Greller, G., Horlacher, R., Boos, W. & Welte, W. (2001). The crystal structure of a liganded trehalose/maltose-binding protein from the hyperthermophilic archaeon *Thermococcus litoralis* at 1.85 A. *J Mol Biol* **305**, 905-915.

Domenech, P., Reed, M. B., Dowd, C. S., Manca, C., Kaplan, G. & Barry, C. E. (2004). The role of MmpL8 in sulfatide biogenesis and virulence of *Mycobacterium tuberculosis*. *J Biol Chem* **279**, 21257-21265.

Driessen, A. J. M., Dejong, S. & Konings, W. N. (1987). Transport of branched-chain amino-acids in membrane-vesicles of *Streptococcus cremoris*. *J Bacteriol* **169**, 5193-5200.

Dwyer, M. A. & Hellinga, H. W. (2004). Periplasmic binding proteins: a versatile superfamily for protein engineering. *Curr Opin Struct Biol* **14**, 495-504.

Dye, C. (2006). Global epidemiology of tuberculosis. *Lancet* **367**, 938-940.

Eroglu, A., Toner, M. & Toth, T. L. (2002). Beneficial effect of microinjected trehalose on the cryosurvival of human oocytes. *Fertil Steril* **77**, 152-158.

Fehr, M., Frommer, W. B. & Lalonde, S. (2002). Visualization of maltose uptake in living yeast cells by fluorescent nanosensors. *Proc Natl Acad Sci U S A* **99**, 9846-9851.

Fehr, M., Lalonde, S., Lager, I., Wolff, M. W. & Frommer, W. B. (2003). *In vivo* imaging of the dynamics of glucose uptake in the cytosol of COS-7 cells by fluorescent nanosensors. *J Biol Chem* **278**, 19127-19133.

Fehr, M., Lalonde, S., Ehrhardt, D. W. & Frommer, W. B. (2004). Live imaging of glucose homeostasis in nuclei of COS-7 cells. *J Fluoresc* **14**, 603-609.

Fehr, M., Takanaga, H., Ehrhardt, D. W. & Frommer, W. B. (2005). Evidence for high-capacity bidirectional glucose transport across the endoplasmic reticulum membrane by genetically encoded fluorescence resonance energy transfer nanosensors. *Mol Cell Biol* **25**, 11102-11112.

Gande, R., Gibson, K. J., Brown, A. K. *et al.* (2004). Acyl-CoA carboxylases (*accD2* and *accD3*), together with a unique polyketide synthase (*Cg-pks*), are key to mycolic acid biosynthesis in *Corynebacterianeae* such as *Corynebacterium glutamicum* and *Mycobacterium tuberculosis*. *J Biol Chem* **279**, 44847-44857.

Gande, R., Dover, L. G., Krumbach, K., Besra, G. S., Sahm, H., Oikawa, T. & Eggeling, L. (2007). The two carboxylases of *Corynebacterium glutamicum* essential for fatty acid and mycolic acid synthesis. *J Bacteriol* **189**, 5257-5264.

Gebhardt, H. (2005). Impact of trehalose and mycolate biosynthesis on the cell envelope of a *Corynebacterium glutamicum* L-lysine production strain. Dissertation, Mathematisch-Naturwissenschaftliche Fakultät, Universität zu Köln.

Gebhardt, H., Meniche, X., Tropis, M., Krämer, R., Daffé, M. & Morbach, S. (2007). The key role of the mycolic acid content in the functionality of the cell wall permeability barrier in *Corynebacterineae*. *Microbiology* **153**, 1424-1434.

Georgi, T., Rittmann, D. & Wendisch, V. F. (2005). Lysine and glutamate production by *Corynebacterium glutamicum* on glucose, fructose and sucrose: roles of malic enzyme and fructose-1,6-bisphosphatase. *Metab Eng* **7**, 291-301.

Gilson, E., Alloing, G., Schmidt, T., Claverys, J. P., Dudler, R. & Hofnung, M. (1988). Evidence for high affinity binding-protein dependent transport systems in gram-positive bacteria and in *Mycoplasma*. *EMBO J* **7**, 3971-3974.

Gourdon, P. & Lindley, N. D. (1999). Metabolic analysis of glutamate production by *Corynebacterium glutamicum*. *Metab Eng* **1**, 224-231.

Grant, S. G., Jessee, J., Bloom, F. R. & Hanahan, D. (1990). Differential plasmid rescue from transgenic mouse DNAs into *Escherichia coli* methylation-restriction mutants. *Proc Natl Acad Sci U S A* **87**, 4645-4649.

Grzegorzewicz, A. E., Pham, H., Gundi, V. A. *et al.* (2012). Inhibition of mycolic acid transport across the *Mycobacterium tuberculosis* plasma membrane. *Nat Chem Biol* **8**, 334-341.

Gu, H., Lalonde, S., Okumoto, S., Looger, L. L., Scharff-Poulsen, A. M., Grossman, A. R., Kossmann, J., Jakobsen, I. & Frommer, W. B. (2006). A novel analytical method for *in vivo* phosphate tracking. *FEBS Lett* **580**, 5885-5893.

Henrich, A. (2011). Characterization of maltose and trehalose transport in *Corynebacterium glutamicum*. Dissertation, Mathematisch-Naturwissenschaftliche Fakultät, Universität zu Köln.

Henrich, A., Kuhlmann, N., Eck, A. W., Krämer, R. & Seibold, G. M. (2013). Maltose uptake by the novel ABC transport system MusEFGK2I causes increased expression of *ptsG* in *Corynebacterium glutamicum*. *J Bacteriol* **195**, 2573-2584.

Horlacher, R., Xavier, K. B., Santos, H., DiRuggiero, J., Kossmann, M. & Boos, W. (1998). Archaeal binding protein-dependent ABC transporter: molecular and biochemical analysis of the trehalose/maltose transport system of the hyperthermophilic archaeon *Thermococcus litoralis*. *J Bacteriol* **180**, 680-689.

Hosie, A. H. F., Allaway, D., Jones, M. A., Walshaw, D. L., Johnston, A. W. B. & Poole, P. S. (2001). Solute-binding protein-dependent ABC transporters are responsible for solute efflux in addition to solute uptake. *Mol Microbiol* **40**, 1449-1459.

Huc, E., Meniche, X., Benz, R., Bayan, N., Ghazi, A., Tropis, M. & Daffe, M. (2010). O-mycoloylated proteins from *Corynebacterium*: an unprecedented post-translational modification in bacteria. *J Biol Chem* **285**, 21908-21912.

Huc, E., De Sousa-D'Auria, C., de la Sierra-Gallay, I., Salmeron, C., van Tilbeurgh, H., Bayan, N., Houssin, C., Daffé, M. & Tropis, M. (2013). Identification of a mycoloyl transferase selectively involved in O-acylation of polypeptides in *Corynebacteriales*. *J Bacteriol* **195**, 4121-4128.

Ikeda, M., Nakanishi, K., Kino, K. & Katsumata, R. (1994). Fermentative production of tryptophan by a stable recombinant strain of *Corynebacterium glutamicum* with a modified serine-biosynthetic pathway. *Biosci Biotechnol Biochem* **58**, 674-678.

Ikeda, M. & Katsumata, R. (1995). Tryptophane production by transport mutants of *Corynebacterium glutamicum*. *Biosci Biotech Biochem* **90**, 1600-1602.

Imamura, H., Nhat, K. P., Togawa, H., Saito, K., Iino, R., Kato-Yamada, Y., Nagai, T. & Noji, H. (2009). Visualization of ATP levels inside single living cells with fluorescence resonance energy transfer-based genetically encoded indicators. *Proc Natl Acad Sci U S A* **106**, 15651-15656.

Inoue, H., Nojima, H. & Okayama, H. (1990). High efficiency transformation of *Escherichia coli* with plasmids. *Gene* **96**, 23-28.

Inui, M., Kawaguchi, H., Murakami, S., Vertes, A. A. & Yukawa, H. (2004). Metabolic engineering of *Corynebacterium glutamicum* for fuel ethanol production under oxygen-deprivation conditions. *J Mol Microbiol Biotechnol* **8**, 243-254.

Jackson, M., Raynaud, C., Lanéelle, M. A., Guilhot, C., Laurent-Winter, C., Ensergueix, D., Gicquel, B. & Daffé, M. (1999). Inactivation of the antigen 85C gene profoundly affects the mycolate content and alters the permeability of the *Mycobacterium tuberculosis* cell envelope. *Mol Microbiol* **31**, 1573-1587.

Jain, M. & Cox, J. S. (2005). Interaction between polyketide synthase and transporter suggests coupled synthesis and export of virulence lipid in *M. tuberculosis*. *PLoS Pathog* **1**, e2.

Jakoby, M., Ngouoto-Nkili, C.-E. & Burkovski, A. (1999). Construction and application of new *Corynebacterium glutamicum* vectors. *Biotechnol Tech* **13**, 437-441.

Jeffery, C. J. (2010). Engineering periplasmic ligand binding proteins as glucose nanosensors. *Nano Reviews* **2**, 5743-5747.

Jorge, C. D., Sampaio, M. M., Hreggvidsson, G. O., Kristjanson, J. K. & Santos, H. (2007). A highly thermostable trehalase from the thermophilic bacterium *Rhodothermus marinus*. *Extremophiles* **11**, 115-122.

Jules, M., Beltran, G., Francois, J. & Parrou, J. L. (2008). New insights into trehalose metabolism by *Saccharomyces cerevisiae*: NTH2 encodes a functional cytosolic trehalase, and deletion of TPS1 reveals Ath1p-dependent trehalose mobilization. *Appl Environ Microbiol* **74**, 605-614.

Juncker, A. S., Willenbrock, H., Von Heijne, G., Brunak, S., Nielsen, H. & Krogh, A. (2003). Prediction of lipoprotein signal peptides in Gram-negative bacteria. *Protein Sci* **12**, 1652-1662.

Jungwirth, B., Sala, C., Kohl, T. A., Uplekar, S., Baumbach, J., Cole, S. T., Pühler, A. & Tauch, A. (2013). High-resolution detection of DNA binding sites of the global transcriptional regulator GlxR in *Corynebacterium glutamicum*. *Microbiology* **159**, 12-22.

Kalinowski, J., Bathe, B., Bartels, D. *et al.* (2003). The complete *Corynebacterium glutamicum* ATCC 13032 genome sequence and its impact on the production of L-aspartate-derived amino acids and vitamins. *J Biotechnol* **104**, 5-25.

Kalscheuer, R., Weinrick, B., Veeraraghavan, U., Besra, G. S. & Jacobs, W. R., Jr. (2010). Trehalose-recycling ABC transporter LpqY-SugA-SugB-SugC is essential for virulence of *Mycobacterium tuberculosis*. *Proc Natl Acad Sci U S A* **107**, 21761-21766.

Kanehisa, M. & Goto, S. (2000). KEGG: kyoto encyclopedia of genes and genomes. *Nucleic Acids Res* **28**, 27-30.

Kaper, T., Lager, I., Looger, L. L., Chermak, D. & Frommer, W. B. (2008). Fluorescence resonance energy transfer sensors for quantitative monitoring of pentose and disaccharide accumulation in bacteria. *Biotechnol Biofuels* **1**, 11.

Kazarinova, L. A., Livshits, V. A., Preobrazhenskaya, E. S. & Starovoytova, I. M. (2002). Method for producing uridine-5'-monophosphate by fermentation using mutant strains of coryneform bacteria. Ajinomoto Co., Inc. Japan *U. S. Patent* US 6344344 B1.

Kim, H. J., Kim, T. H., Kim, Y. & Lee, H. S. (2004). Identification and characterization of *glxR*, a gene involved in regulation of glyoxylate bypass in *Corynebacterium glutamicum*. *J Bacteriol* **186**, 3453-3460.

Kim, T. K., Jang, J. H., Cho, H. Y., Lee, H. S. & Kim, Y. W. (2010a). Gene cloning and characterization of a trehalose synthase from *Corynebacterium glutamicum* ATCC13032. *Food Sci Biotechnol* **19**, 565-569.

Kim, Y. C., Quan, F. S., Song, J. M., Vunnava, A., Yoo, D. G., Park, K. M., Compans, R. W., Kang, S. M. & Prausnitz, M. R. (2010b). Influenza immunization with trehalose-stabilized virus-like particle vaccine using microneedles. *Procedia Vaccinol* **2**, 15-19.

Kind, S., Kreye, S. & Wittmann, C. (2011). Metabolic engineering of cellular transport for overproduction of the platform chemical 1,5-diaminopentane in *Corynebacterium glutamicum*. *Metab Eng* **13**, 617-627.

Kinoshita, S., Udaka, S. & Shimono, M. (1957). Studies on the amino acid fermentation. Part 1. Production of L-glutamic acid by various microorganisms. *J Gen Appl Microbiol* **3**, 193-205.

Koh, S., Shin, H. J., Kim, J. S., Lee, D. S. & Lee, S. Y. (1998). Trehalose synthesis from maltose by a thermostable trehalose synthase from *Thermos caldophilus*. *Biotechnol Lett* **20**, 757-761.

Koita, K. & Rao, C. V. (2012). Identification and analysis of the putative pentose sugar efflux transporters in *Escherichia coli*. *PLoS One* **7**, e43700.

Krause, F. S., Henrich, A., Blombach, B., Krämer, R., Eikmanns, B. J. & Seibold, G. M. (2010). Increased glucose utilization in *Corynebacterium glutamicum* by use of maltose, and its application for the improvement of L-valine productivity. *Appl Environ Microbiol* **76**, 370-374.

Kremers, G. J., Goedhart, J., van Munster, E. B. & Gadella, T. W., Jr. (2006). Cyan and yellow super fluorescent proteins with improved brightness, protein folding, and FRET Förster radius. *Biochemistry* **45**, 6570-6580.

Kyhse-Andersen, J. (1984). Electroblotting of multiple gels: a simple apparatus without buffer tank for rapid transfer of proteins from polyacrylamide to nitrocellulose. *J Biochem Biophys Methods* **10**, 203-209.

La Rosa, V., Poce, G., Canseco, J. O. *et al.* (2012). MmpL3 is the cellular target of the antitubercular pyrrole derivative BM212. *Antimicrob Agents Chemother* **56**, 324-331.

Laemmli, U. K. (1970). Cleavage of structural proteins during the assembly of the head of bacteriophage T4. *Nature* **227**, 680-685.

Lager, I., Looger, L. L., Hilpert, M., Lalonde, S. & Frommer, W. B. (2006). Conversion of a putative *Agrobacterium* sugar-binding protein into a FRET sensor with high selectivity for sucrose. *J Biol Chem* **281**, 30875-30883.

Laslo, T., von Zaluskowski, P., Gabris, C. *et al.* (2012). Arabitol metabolism of *Corynebacterium glutamicum* and its regulation by AtlR. *J Bacteriol* **194**, 941-955.

Lea-Smith, D. J., Pyke, J. S., Tull, D., McConville, M. J., Coppel, R. L. & Crellin, P. K. (2007). The reductase that catalyzes mycolic motif synthesis is required for efficient attachment of mycolic acids to arabinogalactan. *J Biol Chem* **282**, 11000-11008.

Lee, P. C., Lee, W. G., Lee, S. Y. & Chang, H. N. (2001). Succinic acid production with reduced by-product formation in the fermentation of *Anaerobiospirillum succiniciproducens* using glycerol as a carbon source. *Biotechnol Bioeng* **72**, 41-48.

Li, X., Zhang, G., Ngo, N., Zhao, X., Kain, S. R. & Huang, C. C. (1997). Deletions of the *Aequorea victoria* green fluorescent protein define the minimal domain required for fluorescence. *J Biol Chem* **272**, 28545-28549.

Liebl, W. (2005). *Corynebacterium* taxonomy. In *Handbook of Corynebacterium glutamicum*, pp. 9-34. Edited by L. Eggeling & M. Bott. Boca Raton: CRC Press.

Lindner, S. N., Knebel, S., Pallerla, S. R., Schoberth, S. M. & Wendisch, V. F. (2010). *cg2091* encodes a polyphosphate/ATP-dependent glucokinase of *Corynebacterium glutamicum*. *Appl Microbiol Biotechnol* **87**, 703-713.

Liu, J., Barry, C. E., 3rd, Besra, G. S. & Nikaido, H. (1996). Mycolic acid structure determines the fluidity of the mycobacterial cell wall. *J Biol Chem* **271**, 29545-29551.

Liu, J. Y., Miller, P. F., Gosink, M. & Olson, E. R. (1999a). The identification of a new family of sugar efflux pumps in *Escherichia coli*. *Mol Microbiol* **31**, 1845-1851.

Liu, J. Y., Miller, P. F., Willard, J. & Olson, E. R. (1999b). Functional and biochemical characterization of *Escherichia coli* sugar efflux transporters. *J Biol Chem* **274**, 22977-22984.

Luzardo, M. D., Amalfa, F., Nunez, A. M., Diaz, S., de Lopez, A. C. B. & Disalvo, E. A. (2000). Effect of trehalose and sucrose on the hydration and dipole potential of lipid bilayers. *Biophys J* **78**, 2452-2458.

Marchand, C. H., Salmeron, C., Raad, R. B. *et al.* (2012). Biochemical Disclosure of the Mycolate Outer Membrane of *Corynebacterium glutamicum*. *J Bacteriol* **194**, 587-597.

Marrero, J., Rhee, K. Y., Schnappinger, D., Pethe, K. & Ehrt, S. (2010). Gluconeogenic carbon flow of tricarboxylic acid cycle intermediates is critical for *Mycobacterium tuberculosis* to establish and maintain infection. *Proc Natl Acad Sci U S A* **107**, 9819-9824.

Martinac, B., Buechner, M., Delcour, A. H., Adler, J. & Kung, C. (1987). Pressure-sensitive ion channel in *Escherichia coli*. *Proc Natl Acad Sci U S A* **84**, 2297-2301.

Maruta, K., Mukai, K., Yamashita, H., Kubota, M., Chaen, H., Fukuda, S. & Kurimoto, M. (2002). Gene encoding a trehalose phosphorylase from *Thermoanaerobacter brockii* ATCC 35047. *Biosci Biotechnol Biochem* **66**, 1976-1980.

Miah, F., Koliwer-Brandl, H., Rejzek, M., Field, R. A., Kalscheuer, R. & Bornemann, S. (2013). Flux through trehalose synthase flows from trehalose to the alpha anomer of maltose in mycobacteria. *Chem Biol* **20**, 487-493.

Mimitsuka, T., Sawai, H., Hatsu, M. & Yamada, K. (2007). Metabolic engineering of *Corynebacterium glutamicum* for cadaverine fermentation. *Biosci Biotechnol Biochem* **71**, 2130-2135.

Mohsin, M., Abdin, M. Z., Nischal, L., Kardam, H. & Ahmad, A. (2013). Genetically encoded FRET-based nanosensor for *in vivo* measurement of leucine. *Biosens Bioelectron* **50**, 72-77.

Möker, N., Brocker, M., Schaffer, S., Krämer, R., Morbach, S. & Bott, M. (2004). Deletion of the genes encoding the MtrA-MtrB two-component system of *Corynebacterium glutamicum* has a strong influence on cell morphology, antibiotics susceptibility and expression of genes involved in osmoprotection. *Mol Microbiol* **54**, 420-438.

Mullis, K., Faloona, F., Scharf, S., Saiki, R., Horn, G. & Erlich, H. (1986). Specific enzymatic amplification of DNA *in vitro*: the polymerase chain reaction. *Cold Spring Harb Symp Quant Biol* **51 Pt 1**, 263-273.

Murakami, S., Nakashima, R., Yamashita, E. & Yamaguchi, A. (2002). Crystal structure of bacterial multidrug efflux transporter AcrB. *Nature* **419**, 587-593.

Murphy, H. N., Stewart, G. R., Mischenko, V. V., Apt, A. S., Harris, R., McAlister, M. S. B., Driscoll, P. C., Young, D. B. & Robertson, B. D. (2005). The OtsAB pathway is essential for trehalose biosynthesis in *Mycobacterium tuberculosis*. *J Biol Chem* **280**, 14524-14529.

Nagai, T., Ibata, K., Park, E. S., Kubota, M., Mikoshiba, K. & Miyawaki, A. (2002). A variant of yellow fluorescent protein with fast and efficient maturation for cell-biological applications. *Nat Biotechnol* **20**, 87-90.

Nakai, J., Ohkura, M. & Imoto, K. (2001). A high signal-to-noise Ca(2+) probe composed of a single green fluorescent protein. *Nat Biotechnol* **19**, 137-141.

Nakamura, J., Hirano, S., Ito, H. & Wachi, M. (2007). Mutations of the *Corynebacterium glutamicum NCgl1221* gene, encoding a mechanosensitive channel homolog, induce L-glutamic acid production. *Appl Environ Microbiol* **73**, 4491-4498.

Nara, T., Kinoshita, S. & Samejima, H. (1964). Effect of penicillin on amino acid fermentation. *Agr Biol Chem Tokyo* **28**, 120-124.

Nielsen, J. B. & Lampen, J. O. (1982). Glyceride-cysteine lipoproteins and secretion by Gram-positive bacteria. *J Bacteriol* **152**, 315-322.

Nottebrock, D., Meyer, U., Krämer, R. & Morbach, S. (2003). Molecular and biochemical characterization of mechanosensitive channels in *Corynebacterium glutamicum*. *FEMS Microbiol Lett* **218**, 305-309.

Okino, S., Inui, M. & Yukawa, H. (2005). Production of organic acids by *Corynebacterium glutamicum* under oxygen deprivation. *Appl Microbiol Biotechnol* **68**, 475-480.

Okumoto, S., Looger, L. L., Micheva, K. D., Reimer, R. J., Smith, S. J. & Frommer, W. B. (2005). Detection of glutamate release from neurons by genetically encoded surface-displayed FRET nanosensors. *Proc Natl Acad Sci U S A* **102**, 8740-8745.

Padilla, L., Krämer, R., Stephanopoulos, G. & Agosin, E. (2004a). Overproduction of trehalose: heterologous expression of *Escherichia coli* trehalose-6-phosphate synthase and trehalose-6-phosphate phosphatase in *Corynebacterium glutamicum*. *Appl Environ Microbiol* **70**, 370-376.

Padilla, L., Morbach, S., Krämer, R. & Agosin, E. (2004b). Impact of heterologous expression of *Escherichia coli* UDP-glucose pyrophosphorylase on trehalose and glycogen synthesis in *Corynebacterium glutamicum*. *Appl Environ Microbiol* **70**, 3845-3854.

Pan, Y. T., Koroth Edavana, V., Jourdian, W. J., Edmondson, R., Carroll, J. D., Pastuszak, I. & Elbein, A. D. (2004). Trehalose synthase of *Mycobacterium smegmatis*: purification, cloning, expression, and properties of the enzyme. *Eur J Biochem* **271**, 4259-4269.

Park, S. Y., Kim, H. K., Yoo, S. K., Oh, T. K. & Lee, J. K. (2000). Characterization of *glk*, a gene coding for glucose kinase of *Corynebacterium glutamicum*. *FEMS Microbiol Lett* **188**, 209-215.

Patist, A. & Zoerb, H. (2005). Preservation mechanisms of trehalose in food and biosystems. *Colloids Surf B Biointerfaces* **40**, 107-113.

Petersen, T. N., Brunak, S., von Heijne, G. & Nielsen, H. (2011). SignalP 4.0: discriminating signal peptides from transmembrane regions. *Nat Methods* **8**, 785-786.

Polissi, A. & Georgopoulos, C. (1996). Mutational analysis and properties of the *msbA* gene of *Escherichia coli*, coding for an essential ABC family transporter. *Mol Microbiol* **20**, 1221-1233.

Poole, K., Krebes, K., McNally, C. & Neshat, S. (1993). Multiple antibiotic resistance in *Pseudomonas aeruginosa*: evidence for involvement of an efflux operon. *J Bacteriol* **175**, 7363-7372.

Portevin, D., De Sousa-D'Auria, C., Houssin, C., Grimaldi, C., Chami, M., Daffé, M. & Guilhot, C. (2004). A polyketide synthase catalyzes the last condensation step of mycolic acid biosynthesis in mycobacteria and related organisms. *Proc Natl Acad Sci U S A* **101**, 314-319.

Portevin, D., de Sousa-D'Auria, C., Montrozier, H., Houssin, C., Stella, A., Lanéelle, M. A., Bardou, F., Guilhot, C. & Daffé, M. (2005). The acyl-AMP ligase FadD32 and AccD4-containing acyl-CoA carboxylase are required for the synthesis of mycolic acids and essential for mycobacterial growth: identification of the carboxylation product and determination of the acyl-CoA carboxylase components. *J Biol Chem* **280**, 8862-8874.

Puech, V., Bayan, N., Salim, K., Leblon, G. & Daffé, M. (2000). Characterization of the *in vivo* acceptors of the mycoloyl residues transferred by the corynebacterial PS1 and the related mycobacterial antigens 85. *Mol Microbiol* **35**, 1026-1041.

Puech, V., Chami, M., Lemassu, A., Lanéelle, M. A., Schiffler, B., Gounon, P., Bayan, N., Benz, R. & Daffé, M. (2001). Structure of the cell envelope of *Corynebacteria*: importance of the non-covalently bound lipids in the formation of the cell wall permeability barrier and fracture plane. *Microbiology* **147**, 1365-1382.

Qu, Q., Lee, S. J. & Boos, W. (2004). TreT, a novel trehalose glycosyltransferring synthase of the hyperthermophilic archaeon *Thermococcus litoralis*. *J Biol Chem* **279**, 47890-47897.

Quiocho, F. A. & Ledvina, P. S. (1996). Atomic structure and specificity of bacterial periplasmic receptors for active transport and chemotaxis: variation of common themes. *Mol Microbiol* **20**, 17-25.

Radmacher, E., Alderwick, L. J., Besra, G. S., Brown, A. K., Gibson, K. J. C., Sahm, H. & Eggeling, L. (2005a). Two functional FAS-I type fatty acid synthases in *Corynebacterium glutamicum*. *Microbiol-Sgm* **151**, 2421-2427.

Radmacher, E., Stansen, K. C., Besra, G. S., Alderwick, L. J., Maughan, W. N., Hollweg, G., Sahm, H., Wendisch, V. F. & Eggeling, L. (2005b). Ethambutol, a cell wall inhibitor of *Mycobacterium tuberculosis*, elicits L-glutamate efflux of *Corynebacterium glutamicum*. *Microbiol-Sgm* **151**, 1359-1368.

Rancourt, D. E., Stephenson, J. T., Vickell, G. A. & Wood, J. M. (1984). Proline excretion by *Escherichia coli* K12. *Biotechnol Bioeng* **26**, 74-80.

Rath, P., Saurel, O., Czaplicki, G., Tropis, M., Daffé, M., Ghazi, A., Demange, P. & Milon, A. (2013). Cord factor (trehalose 6,6'-dimycolate) forms fully stable and non-permeable lipid bilayers required for a functional outer membrane. *Biochim Biophys Acta* **1828**, 2173-2181.

Rehorst, W. (2013). Untersuchung der Kontrolle der Genexpression des TusFGK$_2$-E Trehaloseaufnahmesystems in *Corynebacterium glutamicum*. Mathematisch-Naturwissenschaftliche Fakultät, Universität zu Köln.

Ruffert, S., Lambert, C., Peter, H., Wendisch, V. F. & Krämer, R. (1997). Efflux of compatible solutes in *Corynebacterium glutamicum* mediated by osmoregulated channel activity. *Eur J Biochem* **247**, 572-580.

Ruffert, S., Berrier, C., Krämer, R. & Ghazi, A. (1999). Identification of mechanosensitive ion channels in the cytoplasmic membrane of *Corynebacterium glutamicum*. *J Bacteriol* **181**, 1673-1676.

Sahm, H. & Eggeling, L. (1999). D-Pantothenate synthesis in *Corynebacterium glutamicum* and use of *panBC* and genes encoding L-valine synthesis for D-pantothenate overproduction. *Appl Environ Microbiol* **65**, 1973-1979.

Sakurai, M., Furuki, T., Akao, K., Tanaka, D., Nakahara, Y., Kikawada, T., Watanabe, M. & Okuda, T. (2008). Vitrification is essential for anhydrobiosis in an African chironomid, *Polypedilum vanderplanki*. *Proc Natl Acad Sci U S A* **105**, 5093-5098.

Sambrook, J. & Russel, D. W. (2001). Molecular cloning: a laboratory manual. Cold Spring Harbor, NY: Cold Spring Harbor Laboratory Press.

Sassetti, C. M., Boyd, D. H. & Rubin, E. J. (2003). Genes required for mycobacterial growth defined by high density mutagenesis. *Mol Microbiol* **48**, 77-84.

Schäfer, A., Tauch, A., Jäger, W., Kalinowski, J., Thierbach, G. & Pühler, A. (1994). Small mobilizable multi-purpose cloning vectors derived from the *Escherichia coli* plasmids pK18 and pK19: selection of defined deletions in the chromosome of *Corynebacterium glutamicum*. *Gene* **145**, 69-73.

Schleyer, M., Schmid, R. & Bakker, E. P. (1993). Transient, specific and extremely rapid release of osmolytes from growing cells of *Escherichia coli* K-12 exposed to hypoosmotic shock. *Arch Microbiol* **160**, 424-431.

Schulte, J. (2011). Characterization of the trehalose uptake system of *Cornynebacterium glutamicum*. Master Thesis, Mathematisch-Naturwissenschaftliche Fakultät, Universität zu Köln.

Seibold, G. M. & Eikmanns, B. J. (2007). The *glgX* gene product of *Corynebacterium glutamicum* is required for glycogen degradation and for fast adaptation to hyperosmotic stress. *Microbiology* **153**, 2212-2220.

Shiio, I., Otsuka, S. I. & Takahashi, M. (1962). Effect of biotin on the bacterial formation of glutamic acid. I. Glutamate formation and cellular premeability of amino acids. *J Biochem* **51**, 56-62.

Shimakata, T. & Minatogawa, Y. (2000). Essential role of trehalose in the synthesis and subsequent metabolism of corynomycolic acid in *Corynebacterium matruchotii*. *Arch Biochem Biophys* **380**, 331-338.

Smith, K. M., Cho, K. M. & Liao, J. C. (2010). Engineering *Corynebacterium glutamicum* for isobutanol production. *Appl Microbiol Biotechnol* **87**, 1045-1055.

Soual-Hoebeke, E., de Sousa-D'Auria, C., Chami, M., Baucher, M. F., Guyonvarch, A., Bayan, N., Salim, K. & Leblon, G. (1999). S-layer protein production by *Corynebacterium* strains is dependent on the carbon source. *Microbiol-Uk* **145**, 3399-3408.

Strom, A. R. & Kaasen, I. (1993). Trehalose metabolism in *Escherichia coli* - stress protection and stress regulation of gene-expression. *Mol Microbiol* **8**, 205-210.

Studier, F. W. & Moffatt, B. A. (1986). Use of bacteriophage T7 RNA polymerase to direct selective high-level expression of cloned genes. *J Mol Biol* **189**, 113-130.

Styrvold, O. B. & Strom, A. R. (1991). Synthesis, accumulation, and excretion of trehalose in osmotically stressed *Escherichia coli*-K-12 strains - influence of amber suppressors and function of the periplasmic trehalase. *J Bacteriol* **173**, 1187-1192.

Sugiyama, Y., Kitano, K. & Kanzaki, T. (1973). Purification of cytochrome a of an L-glutamate-producing microorganism, *Brevibacterium thiogenitalis*. *Agric Biol Chem* **37**, 1607 - 1612.

Sulavik, M. C., Houseweart, C., Cramer, C. *et al.* (2001). Antibiotic susceptibility profiles of *Escherichia coli* strains lacking multidrug efflux pump genes. *Antimicrob Agents Chemother* **45**, 1126-1136.

Sun, Y. & Vanderpool, C. K. (2011). Regulation and function of *Escherichia coli* sugar efflux transporter A (SetA) during glucose-phosphate stress. *J Bacteriol* **193**, 143-153.

Sutcliffe, I. C. & Russell, R. R. (1995). Lipoproteins of Gram-positive bacteria. *J Bacteriol* **177**, 1123-1128.

Symmons, M. F., Bokma, E., Koronakis, E., Hughes, C. & Koronakis, V. (2009). The assembled structure of a complete tripartite bacterial multidrug efflux pump. *Proc Natl Acad Sci U S A* **106**, 7173-7178.

Szmelcman, S., Schwartz, M., Silhavy, T. J. & Boos, W. (1976). Maltose transport in *Escherichia coli K12*. A comparison of transport kinetics in wild-type and lambda-resistant mutants with the dissociation constants of the maltose-binding protein as measured by fluorescence quenching. *Eur J Biochem* **65**, 13-19.

Tahlan, K., Wilson, R., Kastrinsky, D. B. *et al.* (2012). SQ109 targets MmpL3, a membrane transporter of trehalose monomycolate involved in mycolic acid donation to the cell wall core of *Mycobacterium tuberculosis*. *Antimicrob Agents Chemother* **56**, 1797-1809.

Takanaga, H., Chaudhuri, B. & Frommer, W. B. (2008). GLUT1 and GLUT9 as major contributors to glucose influx in HepG2 cells identified by a high sensitivity intramolecular FRET glucose sensor. *Biochim Biophys Acta* **1778**, 1091-1099.

Takayama, K., Wang, C. & Besra, G. S. (2005). Pathway to synthesis and processing of mycolic acids in *Mycobacterium tuberculosis*. *Clin Microbiol Rev* **18**, 81-101.

Takinami, K., Okada, H. & Tsunoda, T. (1964). Biochemical effects of fatty acid and its derivatives on L-glutamic acid fermentation part II. Effective chemical structure of fatty acid derivatives on the accummlation of L-glutamic acid in biotin sufficient medium. *Agric Biol Chem* **28**, 114-119.

Tam, R. & Saier, M. H., Jr. (1993). Structural, functional, and evolutionary relationships among extracellular solute-binding receptors of bacteria. *Microbiol Rev* **57**, 320-346.

Toyoda, K., Teramoto, H., Inui, M. & Yukawa, H. (2011). Genome-wide identification of in vivo binding sites of GlxR, a cyclic AMP receptor protein-type regulator in *Corynebacterium glutamicum*. *J Bacteriol* **193**, 4123-4133.

Trivedi, O. A., Arora, P., Sridharan, V., Tickoo, R., Mohanty, D. & Gokhale, R. S. (2004). Enzymic activation and transfer of fatty acids as acyl-adenylates in mycobacteria. *Nature* **428**, 441-445.

Tropis, M., Meniche, X., Wolf, A. *et al.* (2005). The crucial role of trehalose and structurally related oligosaccharides in the biosynthesis and transfer of mycolic acids in *Corynebacterineae*. *J Biol Chem* **280**, 26573-26585.

Trötschel, C., Deutenberg, D., Bathe, B., Burkovski, A. & Krämer, R. (2005). Characterization of methionine export in *Corynebacterium glutamicum*. *J Bacteriol* **187**, 3786-3794.

Tzvetkov, M., Klopprogge, C., Zelder, O. & Liebl, W. (2003). Genetic dissection of trehalose biosynthesis in *Corynebacterium glutamicum*: inactivation of trehalose production leads to impaired growth and an altered cell wall lipid composition. *Microbiol-Sgm* **149**, 1659-1673.

Vallino, J. J. & Stephanopoulos, G. (1993). Metabolic flux distributions in *Corynebacterium glutamicum* during growth and lysine overproduction. *Biotechnol Bioeng* **41**, 633-646.

van der Rest, M. E., Lange, C. & Molenaar, D. (1999). A heat shock following electroporation induces highly efficient transformation of *Corynebacterium glutamicum* with xenogeneic plasmid DNA. *Appl Microbiol Biotechnol* **52**, 541-545.

Varela, C., Rittmann, D., Singh, A., Krumbach, K., Bhatt, K., Eggeling, L., Besra, G. S. & Bhatt, A. (2012). *MmpL* genes are associated with mycolic acid metabolism in *Mycobacteria* and *Corynebacteria*. *Chem Biol* **19**, 498-506.

Wang, C., Hayes, B., Vestling, M. M. & Takayama, K. (2006). Transposome mutagenesis of an integral membrane transporter in *Corynebacterium matruchotii*. *Biochem Biophys Res Commun* **340**, 953-960.

Wang, J. H., Tsai, M. Y., Chen, J. J., Lee, G. C. & Shaw, J. F. (2007). Role of the C-terminal domain of *Thermus thermophilus* trehalose synthase in the thermophilicity, thermostability, and efficient production of trehalose. *J Agric Food Chem* **55**, 3435-3443.

Wells, R. M., Jones, C. M., Xi, Z. *et al.* (2013). Discovery of a siderophore export system essential for virulence of *Mycobacterium tuberculosis*. *PLoS Pathog* **9**, e1003120.

Wittmann, C. & Heinzle, E. (2001). Modeling and experimental design for metabolic flux analysis of lysine-producing *Corynebacteria* by mass spectrometry. *Metab Eng* **3**, 173-191.

Wolf, A., Krämer, R. & Morbach, S. (2003). Three pathways for trehalose metabolism in *Corynebacterium glutamicum* ATCC13032 and their significance in response to osmotic stress. *Mol Microbiol* **49**, 1119-1134.

Woodruff, P. J., Carlson, B. L., Siridechadilok, B., Pratt, M. R., Senaratne, R. H., Mougous, J. D., Riley, L. W., Williams, S. J. & Bertozzi, C. R. (2004). Trehalose is required for growth of *Mycobacterium smegmatis*. *J Biol Chem* **279**, 28835-28843.

Yanisch-Perron, C., Vieira, J. & Messing, J. (1985). Improved M13 phage cloning vectors and host strains: nucleotide sequences of the M13mp18 and pUC19 vectors. *Gene* **33**, 103-119.

Yeats, C., Rawlings, N. D. & Bateman, A. (2004). The PepSY domain: a regulator of peptidase activity in the microbial environment? *Trends Biochem Sci* **29**, 169-172.

Yu, E. W., Aires, J. R., McDermott, G. & Nikaido, H. (2005). A periplasmic drug-binding site of the AcrB multidrug efflux pump: a crystallographic and site-directed mutagenesis study. *J Bacteriol* **187**, 6804-6815.

Zhang, R., Pan, Y. T., He, S., Lam, M., Brayer, G. D., Elbein, A. D. & Withers, S. G. (2011). Mechanistic analysis of trehalose synthase from *Mycobacterium smegmatis*. *J Biol Chem* **286**, 35601-35609.

Zhou, Z., White, K. A., Polissi, A., Georgopoulos, C. & Raetz, C. R. H. (1998). Function of *Escherichia coli* MsbA, an essential ABC family transporter, in lipid A and phospholipid biosynthesis. *Faseb Journal* **12**, A1284-A1284.

Zittrich, S. & Krämer, R. (1994). Quantitative discrimination of carrier-mediated excretion of isoleucine from uptake and diffusion in *Corynebacterium glutamicum*. *J Bacteriol* **176**, 6892-6899.

Danksagung

Herrn Prof. Dr. Reinhardt Krämer danke ich für die freundliche Aufnahme in seine Arbeitsgruppe, für die stete Unterstützung sowie für die zahlreichen Events abseits des Forschungsalltags, die für mich immer interessant und lehrreich waren.

Frau Prof. Dr. Karin Schnetz danke ich herzlich für die Übernahme des Zweitgutachtens.

Ein besonderer Dank gilt Dr. Gerd Seibold für seine Betreuung, Geduld und Kaffee.

Ohne die Unterstützung durch meine Kollegen wäre vieles schwieriger gewesen. Ich danke euch allen für die gute Zusammenarbeit und vor allem auch für die Ablenkung von der Arbeit bei allen Gelegenheiten. Danke Andi, Anja, Anna, Benni, Boris, Cat, Caro, Dimi, Eva, Gaby, Judith, Julia, Jury, Katja, Lina, Markus, Michael, Natalie, Nora, Oli, Stan, Ute.

Meiner Familie und meinen Freunden danke ich für die Unterstützung während der letzten Jahre und während meines gesamten Studiums. Euch gehört das größte Stück vom Kuchen.

Erklärung

Ich versichere, dass ich die von mir vorgelegte Dissertation selbständig angefertigt, die benutzten Quellen und Hilfsmittel vollständig angegeben und die Stellen der Arbeit − einschließlich Tabellen, Karten und Abbildungen −, die anderen Werken im Wortlaut oder dem Sinn nach entnommen sind, in jedem Einzelfall als Entlehnung kenntlich gemacht habe; dass diese Dissertation noch keiner anderen Fakultät oder Universität zur Prüfung vorgelegen hat; dass sie − abgesehen von unten angegebenen Teilpublikationen − noch nicht veröffentlicht worden ist sowie, dass ich eine solche Veröffentlichung vor Abschluss des Promotionsverfahrens nicht vornehmen werde. Die Bestimmungen der Promotionsordnung sind mir bekannt. Die von mir vorgelegte Dissertation ist von Prof. Dr. Reinhard Krämer betreut worden.

Teilpublikationen liegen nicht vor.

Köln, den 16.06.2014

Unterschrift